Joint Uplink/Downlink Radio Resource Allocation in 5G HetNets

Bachir Lahad

Thèse de doctorat

NNT: 2020UPASG057

Joint Uplink / Downlink Radio Resource Allocation in 5G HetNets

Thèse de doctorat de l'Université Paris-Saclay et de l'Université Saint-Joseph de Beyrouth

École doctorale n° 580, Sciences et technologies de l'information et de la communication (STIC)

Spécialité de doctorat: Informatique

Unité de recherche: Université Paris-Saclay, CNRS, Laboratoire de recherche en informatique, 91405, Orsay, France

Référent: Faculté des sciences d'Orsay

Thèse présentée et soutenue à Paris-Saclay, le 10 Décembre 2020, par

Bachir LAHAD

Composition du jury:

Véronique Vèque Professeur, Université Paris-Saclay	Président
Abed Ellatif Samhat Professeur, Université Libanaise	Rapporteur
Xavier Lagrange Professeur, IMT Atlantique	Rapporteur
Marwen Abdennebi Professeur associé, Université Sorbonne Paris Nord	Examinateur
Stefano Secci Professeur, CNAM	Examinateur
Steven Martin Professeur, Université Paris-Saclay	Directeur
Marc Ibrahim Professeur, USJ	Codirecteur
Kinda Khawam Professeur associée, UVSQ	Co-encadrante et examinatrice
Samer Lahoud Professeur, USJ	Coencadrant, Invité
Salah Eddine Elayoubi Professeur associé, Centrale Supélec	Invité

To my parents.
The reason of what I become Today.
Thanks for your great support and continuous care.

To the most loving person i know my partner Hiba.

Yesterday is gone. Tomorrow has not yet come. We have only today. Let us begin.

Mother Teresa.

Acknowledgments

The success and final outcome of this thesis required a lot of guidance and assistance from many people and I am extremely privileged to have got this all along the completion of my project. As I struggled with writing this document, I pictured all the hardworking members of the team who dedicated months to this effort holding me accountable, challenging me to create a final manuscript that met their standards, worthy of their support and contribution.
First, I would like to express my sincere gratitude to my advisor Kinda Khawam for the continuous support during my PhD studies and related researches, for her motivation and constant follow up. Her guidance helped me in all the time of research and writing of this thesis. I respect and thank my advisor Samer Lahoud for his support, guidance and suggestions during this project work.
My sincere thanks also goes to my thesis directors Marc Ibrahim and Steven Martin, who provided me an opportunity to join their research team, and who gave me access to the laboratory and research facilities. Without their precious support in administrative tasks, it would not be possible to conduct this research. I would like to take the opportunity to thank Marc Ibrahim for enlightening me the first glance of research.
Second, i am particularly indebted to the rest of my thesis committee for their insightful comments and feedback which incented me to widen my research from various perspectives. In particular, I am grateful for Prof. Xavier Lagrange for his constructive comments given during my mid-term follow up that helped me to strengthen and further improve my thesis scope of work. I am particularly indebted to a large numbers of critical readers and reviewers who invested hours in reading my published manuscripts and feeding me the brutal facts about what needed to be improved.
Thanks go out to the USJ research council and Sada (Echo) committee. This work would not have been possible without their financial support and granted awards.
Also, I would like to thank my parents and my family for their love and support. My parents raised me to believe that I could achieve anything I set my mind to.
Finally, I am deeply thankful to my partner Hiba Massoudy, not only she is my most helpful critic but she is also my deepest and most enduring support.

Abstract (Fr)

La croissance rapide du trafic de données sans fil et des services intensifs en bande passante (voix sur IP, streaming vidéo, live streaming, etc.) nécessite de trouver des solutions viables pour améliorer la qualité de service et maximiser les performances du réseau. Pour s'adapter à ces applications intensives en bande passante, les réseaux cellulaires hétérogènes (HetNets) ont été introduits dans le 3GPP comme l'une des principales caractéristiques pour répondre à ces exigences avancées. Les opérateurs ont adopté des solutions HetNet pour décharger le trafic d'une station de base macro (BS) vers une petite cellule BS. Maintenant, en raison de la différence de charges de trafic de liaison montante (UL) et de liaison descendante (DL) attendues dans les prochaines générations HetNets, il devient essentiel d'ajuster dynamiquement les ressources UL/DL. Pour soutenir cette nouvelle approche, le duplexage temporel (TDD) dynamique a été proposé. Plusieurs mesures de performance de réseau peuvent être étudiés et modélisés statistiquement pour analyser un HetNet basé sur TDD. Le facteur métrique important et le facteur performance clé dans les réseaux cellulaires est l'interférence intercellulaire (ICI). La modélisation statistique de l'ICI joue un rôle impératif dans l'évaluation des mesures de performance du système et le développement des techniques efficaces d'atténuation des interférences pour les réseaux 5G. Dans ce travail, l'interférence subie à un niveau (petite cellule de référence) résultant de l'autre niveau (macro-cellule) est appelée interférence cross-tier. Il convient également de mentionner que, puisque plusieurs petites cellules sont déployées dans des scénarios réels en superposition à la macro-cellule, la modélisation de l'interférence subie au niveau de la petite cellule de référence résultant d'autres petites cellules devient indispensable pour évaluer les performances globales du système. Dans cette étude, ce type d'interférence est appelé interférence co-tier. Néanmoins, l'importance d'UL se pose avec l'évolution des réseaux sociaux et des solutions cloud. Par conséquent, il est très intéressant d'introduire de nouvelles techniques qui atténuent les interférences de l'UL, améliorent les débits UL et DL et permettent également une meilleure utilisation des ressources radio en fournissant un équilibrage de charge adéquat entre UL et DL. Une telle caractéristique supplémentaire est le découplage accès UL/DL. Afin d'aborder les défis susmentionnés, un changement impératif des HetNets classiques aux HetNets de nouvelle génération (5G) émerge dans le but d'améliorer globalement la performance du système.

Dans les HetNets de nouvelle génération, la dérivation d'expressions de forme fermée pour les cross-tier/co-tier et la capacité des utilisateurs dans TDD HetNets aident à la conception et l'optimisation des techniques avancées d'amélioration, y compris, mais sans s'y limiter, la technique d'accès découplé. La dérivation de ces expressions réduit également le besoin d'utiliser des simulations Monte-Carlo qui prennent assez du temps, en particulier dans le cas du déploiement de plusieurs petites cellules où le temps requis pour exécuter des simulations Monte-Carlo augmente considérablement.

Dans notre travail, nous développons d'abord un modèle TDD dans HetNets. Dans ce modèle, nous dérivons des expressions analytiques pour la distribution de l'emplacement du brouilleur considérant tous les scénarios d'interférences possibles qui pourraient se produire dans les réseaux basés sur TDD, tout en tenant compte de l'impact nocif de cette interférence. Basé sur ce dernier résultat, nous dérivons la fonction de distribution et de génération de moment (MGF) de l'interférence intercellulaire montante et descendante considérant un réseau composé d'une macro-cellule et d'une petite cellule. Nous nous appuyons sur les expressions dérivées pour analyser la capacité moyenne de la cellule de référence dans les transmissions en liaison montante et en liaison descendante. Deuxièmement, nous développons un modèle statistique conjoint TDD/découplage pour mettre en évidence les avantages que le mode d'accès de découplage peut apporter à un système basé sur HetNet TDD, en termes d'efficacité spectrale UL et DL. Cette étude était basée sur une approche de probabilité géométrique. L'introduction du mode de découplage nécessite une analyse approfondie de l'étude de comparaison avec le mode d'accès couplé UL/DL conventionnel. Par conséquent, nous dérivons les statistiques du signal d'interférence et du signal d'intérêt des deux modes, puis analysons leur impact sur le performance du système.

Ce travail a été étendu pour inclure le déploiement de plusieurs petites cellules, où des aperçus supplémentaires sur les avantages du mode de découplage sont fournies en termes de gains de découplage UL et DL. Nous nous

appuyons sur les expressions de capacité dérivées dans le mode couplé et le mode découplé pour calculer le gain de découplage et ainsi identifier l'emplacement de la petite cellule interférente, où le mode découplé maintient un gain plus élevé à la fois en DL et en UL. Suite à la mise en œuvre du modèle développé, il est démontré que le cas de découplage apporte de plus grands avantages dans la liaison montante et maintient la même amélioration dans la liaison descendante pour diverses valeurs de décalage et, ainsi, améliore les performances globales du système lorsqu'il est associé avec une technologie TDD dynamique. Il est en outre démontré que notre réseau modélisé peut être optimisé en adoptant la combinaison optimale à la fois du facteur de décalage des petites cellules et de la distance entre les petites cellules.

D'un autre côté, l'évaluation des avantages d'un TDD adaptatif et du découplage dans un système basé sur HetNet en fonction des charges de trafic variant dans le temps, nécessite de trouver un simulateur de niveau système où nous pouvons présenter le motif derrière l' adoption de découplage et de TDD dynamique et évaluer avec précision le rôle de ces techniques dans le problème d'optimisation UL / DL. Il convient de mentionner que le modèle proposé joue un rôle impératif dans l'évaluation des mesures de performance du système telles que l'efficacité spectrale, le gain de découplage et la consommation électrique moyenne. Cependant, ce modèle évalue la capacité moyenne d'un utilisateur seulement et sans relever les défis d'adaptation du trafic et d'allocation dynamique des ressources. En outre, il ne prend pas en compte un fading variable. Pour cette raison, nous proposons un simulateur de niveau système 5G HetNet qui complète un simulateur LTE existant. Cette combinaison permet une simulation détaillée des techniques TDD dynamique et de découplage et d'étudier leur impact dans des scénarios de cas réels. Nous créons un environnement de simulation approprié qui est relatif à des scénarios réels, c'est-à-dire des simulations où plusieurs petites cellules sont déployées dans un système HetNet lourdement chargé et sous diverses charges de trafic. Ces scénarios de simulation prennent en compte la distribution aléatoire des utilisateurs avec des décisions d'allocation de ressources dans les directions montante et descendante. Dans ce contexte, nous considérons une stratégie d'association d'utilisateurs couplée UL/DL conventionnelle et deux types de stratégies d'association de liaison découplées UL/DL. Notre objectif est de trouver la combinaison optimale entre les configurations TDD macro et petites cellules d'un côté et la stratégie de découplage avec ses différents paramètres de l'autre côté, et ceci en fonction de tout changement dans le système, notamment dans le rapport de trafic UL/DL. À partir des scénarios de simulation mise en œuvre, il est observé que l'algorithme adaptatif proposé (TDD dynamique avec stratégies de découplage) apporte des améliorations de performances significatives dans le débit UL et DL par rapport à un certain nombre de schémas conventionnels, principalement dans le déploiement HetNet dense et dans les systèmes fortement chargés.

Abstract

The rapid growth in wireless data traffic and bandwidth intensive services (voice over IP, video streaming, live streaming, etc.) necessitates finding viable solutions to improve service quality and maximize the network performance. To accommodate these bandwidth intensive applications, heterogeneous cellular networks (HetNets) were introduced in 3GPP as one of the main features to meet these advanced requirements. Operators have adopted HetNet solutions to offload traffic from a macro base station (BS) to a small cell BS. Yet, because of the difference in uplink (UL) and downlink (DL) traffic loads expected in the next HetNets generation, it becomes essential to dynamically adjust UL/DL resources. To support this new approach, dynamic time-division duplexing (TDD) has been proposed. Several network performance metrics can be studied and statistically modeled to analyze a TDD based HetNet. One important metric and key performance factor in cellular networks is the Inter-Cell Interference (ICI). Statistical modeling of ICI plays an imperative role in evaluating the system performance metrics and developing efficient interference mitigation techniques for 5G networks. In this work, the interference incurred at one tier (reference small cell) arising from the other tier (macro cell) is referred to as cross-tier interference. It may also be worth mentioning that, since multiple small cells are being deployed in real scenarios as an overlay to the macro cell, the modeling of the interference incurred at the reference small cell arising from other small cells is becoming essential to evaluate the overall system performance. In this study, this type of interference is referred to as co-tier interference. Nevertheless, the importance of UL arises along with the evolution of social networking and cloud solutions. Therefore, it is of great interest to introduce novel techniques that mitigate UL interferences, improve UL and DL throughputs and allow as well, a better use of radio resources by providing adequate load balancing among UL and DL. Such an additional feature is the decoupled UL/DL access. In order to address the aforementioned challenges, an important shift from classical HetNets to next-generation HetNets (5G) is emerging in the aim of improving overall system performance.

In the next-generation HetNets, deriving closed-form expressions for cross-tier/co-tier interference and average user capacity in TDD HetNets helps in designing and optimizing advanced enhancement techniques, including but not limited to the decoupled access technique. Deriving these expressions reduces as well the need for time consuming Monte-Carlo simulations, especially in the case of multiple small cells deployment where the time required to run Monte-Carlo simulations significantly increases.

In our work, we first develop a TDD model in HetNets. Under this model,we derive analytical expressions for the distribution of the interferer location considering all possible interference scenarios that could occur in TDD-based networks, while taking into account the harmful impact of interference. Based on the latter result, we derive the distribution and moment generating function (MGF) of the uplink and downlink inter-cell interference considering a network consisting of one macro cell and one small cell. We build on the derived expressions to analyze the average capacity of the reference cell in both uplink and downlink transmissions.

Second, we develop a joint TDD/decoupling statistical model to highlight the benefits that the decoupling access mode can bring to a HetNet TDD based system, in terms of UL and DL spectral efficiencies and throughputs. This study was based on a geometric probability approach. Introducing the decoupling mode necessitates a thorough comparison study with the conventional coupled UL/DL access mode. Therefore, we derive the statistics of the interference signal and the signal of interest of both modes and then analyze their impact on the system performance. This work was extended to include multiple small cells deployment, where more insight into the benefits of decoupling mode is provided in terms of UL and DL decoupling gains. We build on the derived capacity expressions in the coupled and decoupled modes to calculate the decoupling gain and thus, identify the location of the interferer small cell where the decoupled mode maintains a higher gain in both DL and UL. Further to the implementation of the developed model, it is shown that the decoupling case brings greater benefits in the uplink and maintains the same improvement in the downlink for various offset values and thus, improves the overall system performance when being combined with a dynamic TDD technology. It is further shown that our modeled network can be optimized by adopting the optimal combination of both the small cell offset factor and the distance between small cells.

On the other hand, evaluating the benefits of an adaptive TDD and decoupling in a HetNet based system according to time-variant traffic loads, necessitates finding a system level simulator where we can present the motivation and accurately assess the role of both decoupling and dynamic TDD techniques in the UL/DL optimization problem. It is worth mentioning that the proposed model plays an imperative role in evaluating the system performance metrics such as spectral efficiency, decoupling gain and average power consumption. However, this model evaluates the average capacity of only one user and without addressing the traffic adaptation and dynamic resource allocation challenges. Also, it doesn't consider a variable slow and fast fading. For this reason, we propose a 5G HetNet system level simulator that supplements an existing LTE simulator. This combination allows for detailed simulation of both dynamic TDD and decoupling techniques and to study their impact in real case scenarios. We create appropriate simulation environment that is relative to real scenarios i.e. simulations where multiple small cells are deployed in a heavy loaded HetNet system and under various traffic loads. These simulation scenarios consider random users distribution with scheduling decisions in both the uplink and the downlink directions. In this context, we consider one conventional UL/DL coupled user association policy and two types of decoupled UL/DL link association policies. Our objective is to find the optimal combination between both the macro cell and the small cells TDD configurations from one side and the decoupling association with its various parameters from the other side, and this with respect to any change in the system, especially in the UL/DL traffic ratio. From the applied simulation scenarios, it is observed that the proposed adaptive algorithm (dynamic TDD with decoupling policies) yields significant performance improvements in UL and DL throughput compared to a number of conventional schemes, mainly in dense HetNet deployment and in highly loaded systems.

Acronymes

3G	Third Generation
3GPP	Third Generation Partnership Project
4G	Fourth Generation
5G	Fifth Generation
ABS	Almost Blank Subframe
AMC	Adaptive Modulation and Coding
BBU	BBU Baseband Unit
BS	Base Station
C-RAN	Cloud-Radio Access Networks
CA	Carrier Aggregation
CAPEX	Capital Expenditures
CoMP	Coordinated MultiPoint
CoUD	Coupled UL/DL Access
CQI	Channel Quality Indicator
CRE	Cell Range Expansion
CRS	Cell Specific Reference Signals
CSI	Channel State Information
D2D	Device to Device
DL	Downlink
DeUD	Decoupled UL/DL Access
E-UTRAN	Evolved Universal Terrestrial Radio Access
eNB	evolved Node B
EPS	Evolved Packet System
FDD	Frequency Division Duplexing
GW	Gateway
HOs	Handovers
ICI	Inter-Cell Interference
KPI	Key Performance Indicator
LTE	Long Term Evolution

M2M	Machine-to-Machine
MGF	Moment Generating Function
MIMO	Multiple-Input Multiple-Output
MME	Mobility Management Entity
MNOs	Mobile Network Operators
MTC	Machine Type Communications
MU-MIMO	Multi-User Multiple-Input Multiple-Output
MWC	Mobile World Congress
NOMA	Non-Orthogonal Multiple Access
OFDMA	Orthogonal Frequency Division Multiple Access
OMA	Orthogonal Multiple Access
OPEX	Operational Expenditures
PC	Power Control
PDF	Probability Density Function
PL	Path Loss
QoS	Quality of Service
RBs	Resource Blocks
RF	Radio Frequency
RRH	Remote Radio Head
RSRP	Reference Signal Received Power
SE	Spectral Efficiency
SIM	Simulator
SINR	Signal-To-Interference Noise Ratio
SLS	System Level Simulator
TCOs	Total Cost of Ownerships
TDD	Time Division Duplex
TTI	Transmit Time Interval
UE	User Equipment
UL	Uplink
VoIP	Voice Over IP
WCDMA	Wideband Code Division Multiple Access

Contents

List of Tables

List of Figures

Chapter 1

Introduction

In this chapter, we first describe the challenges faced in mobile networks nowadays and the way to address them. Second, we present the key techniques in next generation HetNets compared to classical HetNets. Further, the motivation behind adopting dynamic TDD and decoupling techniques in next generation 5G HetNets is also presented. Finally, we explain the goals and research objectives of this study.

1.1 Challenges in Mobile Networks

Over the past few years, the demand for mobile traffic has been largely increasing. According to [1], the global mobile data will reach 77 exabytes per month by 2022. Recent reports show that more than 600 million (*i.e*, 648 million) mobile devices were added in 2017. By 2022, there will be 8.4 billion personal mobile-ready devices, and 3.9 billion Machine-to-Machine (M2M) connections.
In response to this growth, mobile operators resort to flexible and efficient solutions to cope with the continuous demand on traffic. They have recently adopted HetNet solutions to offload traffic from a macro base station (BS) to a small cell BS, in the aim of improving the overall system performance. Yet, because of the load traffic disparity in DL and UL, it becomes essential to dynamically adjust UL/DL resources. In particular, the rapid growth in video streaming traffic results in asymmetric and dynamically changing UL and DL traffic loads. To support this new approach, dynamic time-division duplexing (TDD) ([2], [3]) has been proposed. Nevertheless, the importance of UL arises along with the evolution of social networking and cloud solutions. Therefore, it is of great interest to introduce novel techniques that mitigate UL interferences, improve UL and DL throughputs and allow as well, a better use of radio resources by providing adequate load balancing among UL and DL. Such an additional feature is the decoupled UL/DL access ([4], [5]).
Consequently and in order to address the aforementioned challenges, an important shift from classical HetNets to next-generation HetNets (5G) is emerging in the aim of improving overall system performance.

1.2 Heterogeneous Networks (HetNets)

The heterogeneous networks [6] approach consists in complementing the macro layer with low power nodes such as small cell base stations. This approach has been considered a way to improve the capacity and data rate in the areas covered by these low power nodes; they are mostly distributed depending on the areas that generate higher traffic. HetNets involve the use of different types of radio technology and employ low power nodes working together with the current macro cells; that is to say, they may coexist in the same geographical area sharing the same spectrum, so it is not necessary that they provide full area coverage. For this reason, while the location of the macro stations is generally carefully planned, the low power nodes are typically deployed in a relatively unplanned manner. Usually, the main aim of low power nodes is to eliminate coverage holes in the macro network, improve capacity in hotspots and improve cell edge throughput; that is why, the location chosen for their deployment is based on the knowledge of coverage issues and traffic density in the network.
Deploying low power nodes can be challenging, as performance depends on close proximity to where traffic is generated and, due to their reduced coverage range, a lot of them may be needed. Nevertheless, owing to their lower transmit power and smaller physical size, low power stations can offer flexible site acquisitions. Furthermore,

HetNets allow improving spectral efficiency per unit area and offer very high capacity and data rates in areas covered by the low power nodes. Therefore, it is an attractive solution in scenarios where users are highly clustered.

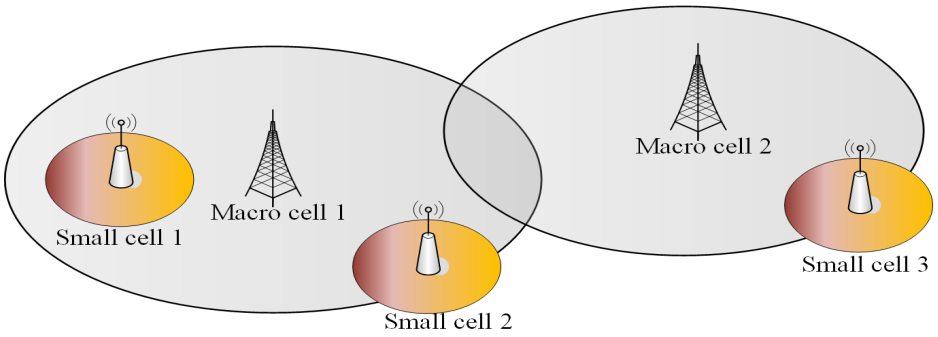

Figure 1.1: HetNet architecture.

1.2.1 HetNets Motivation

The concept of heterogeneous networks has attracted a lot of interest recently to optimize network performances. Spectral efficiency of current systems like WCDMA and LTE is approaching theoretical boundaries [7], LTE improves system performance by using more spectrum and since spectrum has been a scarce resource in the past few years a different approach must be considered to improve network performance. The main approach to enhance the performance is to improve the network topology. This is done in the scenario of heterogeneous networks by overlaying the planned network of high power macro base stations with smaller low power pico base stations that are distributed in an unplanned manner or simply in hotspots where a lot of traffic is generated (see Fig 1.2). By offloading macro base stations, these deployments can improve the overall capacity and the cell edge users' performance [8].

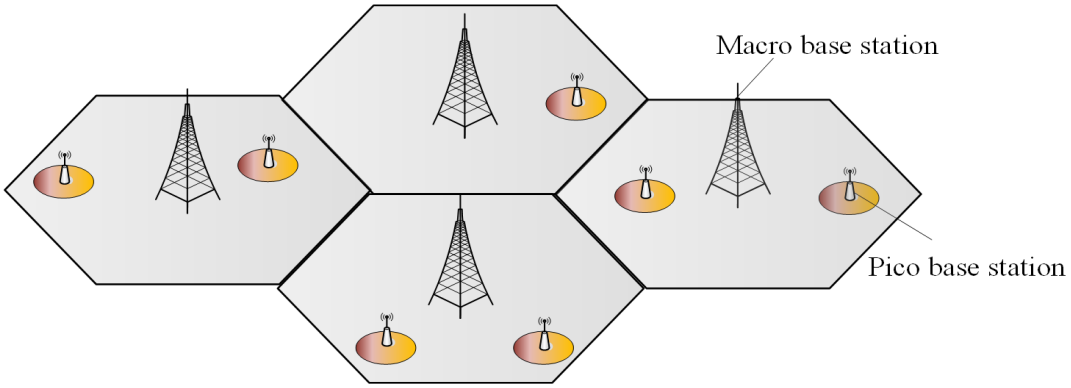

Figure 1.2: Heterogeneous network using pico base stations.

1.3 Key Techniques in HetNets

In reference to our research analysis, we have observed that the main driver of capacity growth is expected to come from network architecture advancements and novel techniques. In this section, we discuss the techniques that we expect to have the highest opportunity for increasing the system capacity in HetNets. These techniques are shown in Fig. 1.3. The main enhancement techniques tackled in this thesis are highlighted in yellow. In this work, we argue that analyzing the decoupling along with the dynamic TDD technique in a HetNet sharing the same RAT (radio access technologies) among cells, will report interesting results to the scientific community.

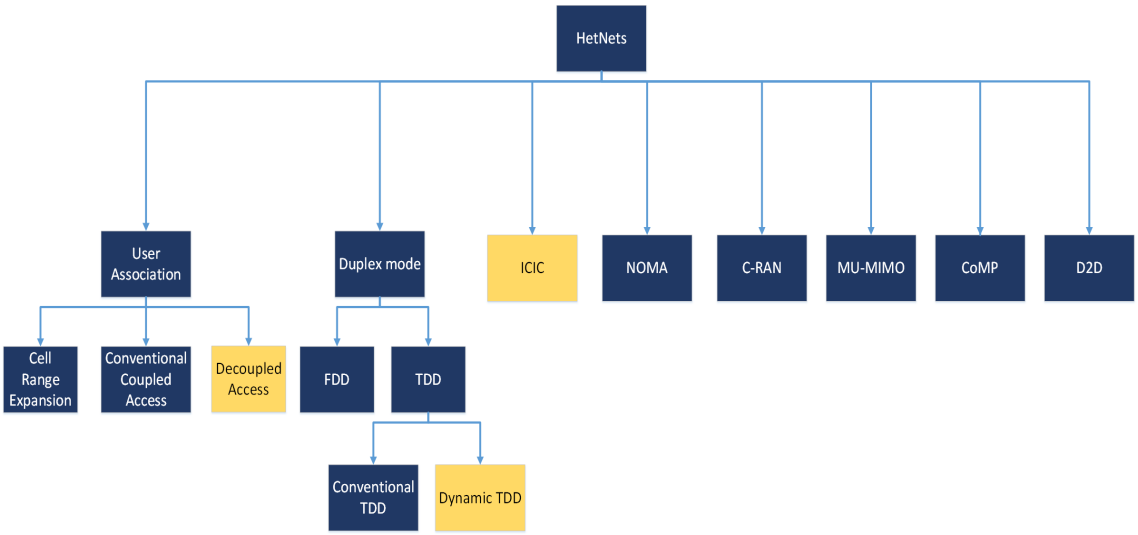

Figure 1.3: Key techniques in HetNets.

1.3.1 Non-Orthogonal Multiple Access (NOMA)

Multiple access techniques are used to allow sharing the available resources among a large number of UEs in the most effective way. As one of the most limited resources in a mobile network is the spectrum. In an multiple access system, different UEs have to simultaneously use the available bandwidth. Multiple access (MA) [9] schemes can be broadly classified into two categories: OMA (Orthogonal Multiple Access) and NOMA (Non-Orthogonal Multiple Access) [10]. OMA schemes have the advantage of avoiding intra-cell interference but they require careful cell planning to reduce inter-cell interference. The later can be achieved by having sufficient distance between the re-used channels, which results in a low spectral efficiency. On the contrary, NOMA schemes are prone to high intra-cell interference, but are robust against fading and inter-cell interference.
As a promising technique for future radio access (FRA) [11], NOMA was proposed by the mobile phone operator NTT DOCOMO [12] to enable multiple users to share the identical radio resource at the same time, which should be distinguished through different power levels [12]- [15]. To successfully retrieve the desired information from the overlapped signals, successive interference cancelation (SIC) technique is utilized at the receivers in NOMA networks [12].
In 4G long-term evolution (LTE), orthogonal frequency division multiple access (OFDMA) was chosen for the downlink. The selection of this MA scheme was a key step for increasing the capacity and improving the performance in 4G LTE. However, OFDMA might not be sufficient to cope with the expected traffic demands without considering new enhancement techniques, same as we did in our work. Hence, NOMA has gained a lot of attention as an MA technique that can boost the capacity of mobile networks, because of its ability to increase the spectral efficiency [16]- [18]. Other benefits of using NOMA include higher cell-edge throughput, relaxed channel feedback, and low transmission latency. As a result, NOMA technique dramatically attracts the attention of the academic community. The basic concepts of uplink and downlink NOMA networks were exploited in [12] and [20], and various challenges for NOMA networks involving power allocation and user scheduling were discussed in [20]. Power allocation therein plays a significant role in enhancing the system performance of NOMA networks since the signals of multiple users are superposed under certain power partitions, and thereby attracts a lot of research attention. For instance, the closed-form formula of outage probability and ergodic sum-rate were derived for two-user static power allocation NOMA system in [21]. Yang $et\ al.$ [22] analyzed the drawbacks of fixed power allocation in NOMA network and proposed a general two-user power allocation scheme. On the other hand, the influence of power allocation on fairness performance of NOMA network was investigated in [23], and the power allocation algorithms for two users NOMA networks were investigated under sum rate maximization and proportional fairness criteria in [24].

1.3.2 Cloud-Radio Access Networks (C-RAN)

The aforementioned mobile networks challenges are pushing mobile operators to adopt a new cost-effective RAN architecture. In that context, the C-RAN (cloud-radio access networks) architecture has been introduced, and has

been motivated in many projects, such as the “Interworking and Joint Design of an Open Access and Backhaul Network Architecture for Small Cells based on Cloud Networks” [25], launched in 2012 by the European Commission, and the “Mobile Cloud Networking (MCN)” [26], launched in 2013 also by the European Commission. Further, many Asian-Pacific MNOs have been tempted by the advantages of C-RAN architecture, and have already started to plan its deployment. For example, Korean SK Telecom and NTT-DoCoMO have announced early trials of C-RAN in 2019. The C-RAN consists of a new cloud architecture, aiming to face the need of TCOs reduction. This approach was conceived from the cloud computing concept. In C-RAN, BBUs (Baseband Units) are migrated from sites, to be gathered in a single location. The latter consists of a central office or a super macro site used to aggregate BBUs. RRHs (Remote Radio Heads) are connected to BBUs through high-bandwidth and low latency optical links. Precisely, baseband elements are employed efficiently and follow the instantaneous load conditions in the network, instead of adopting the maximum traffic of individual base stations. Consequently, processing power is reduced and adapts to network instantaneous load.

1.3.3 Multi-User MIMO (MU-MIMO)

Multiple antenna technology, known as MIMO, is playing an important role in 4G cellular networks, and is expected to be even more essential for meeting 5G target data rates [28]. One key such technique is multiuser MIMO (MU-MIMO), which allows a base station (BS) with many antennas to communicate simultaneously with numerous mobile units each with a very small number of antennas. Although multiuser MIMO also known as space division multiple access (SDMA) has been known for quite some time and previous implementation efforts have been relatively disappointing, enthusiasm has been recently renewed, as seen in the extensive recent literature on “massive MIMO” [29], as well as the very recent 3GPP standardization of full-dimension (FD) MIMO, which can support 64 antennas in a 2D array at the BS to communicate simultaneously with 32 mobile terminals [30].
Multi-antenna transmissions bring significant additional complexity to HetNet analysis, primarily due to the complexity of the random matrix channel. As shown in [31], the invariance property may be lost in multi-antenna HetNets, i.e., the outage probability will increase as the BS density increases. This is mainly because the distributions of both the signal and interference depend on the number of BS antennas and the adopted multi-antenna transmission strategy of each BS. The work [31] relied on stochastic ordering to compare different multi-antenna techniques, but such a method cannot be used for quantitative analysis, since the SINR and SIR distributions were not provided. That work was extended to incorporate load balancing and thus the achievable rate in [32]. Other notable efforts on MIMO HetNets include work limited to two tiers [33], [34], and the analysis in [35], which focused on the interference distribution.

1.3.4 User association

Conventional Coupled Access

In classical HetNets, conventional coupled UL/DL access mode is adopted, where each user is associated in downlink and uplink with a single cell. Cell association criteria in DL and UL is based on DL Reference Signal Received Power (RSRP) which is the conventional LTE user association policy. That is to say, each UE selects its serving cell ID according to the cell from which the largest RSRP is provided :

$$CellID_{serving} = argmax_i(RSRP_i).$$

Cell Range Expansion (CRE)

Cell selection in LTE is based on terminal measurements of the received power of the downlink signal or more specifically the cell specific reference (CRS) downlink signaling. However, in a heterogeneous network, there are different types of base stations with different transmission powers including different powers of CRS. This approach for cell selection would be unfair to the low power nodes (pico-eNBs), as most probably the terminal will choose the higher power base stations (macro-eNBs), even if the path loss to the pico-eNB is smaller and this will not be optimal in terms of:

1. Uplink coverage: As the terminal has a lower path loss to the pico-eNB but instead it will select the macro-eNB.

2. Downlink capacity: Pico-eNBs will be under-utilized as fewer users are connected to them while the macro-eNBs could be overloaded even if macro-eNBs and pico-eNBs are using the same resources in terms of spectrum, so the cell-splitting, also the offload gain is not large and the resources are not well utilized.

3. Interference: Due to the high transmission power of the macro-eNBs, then the Macro-eNB transmission is associated with a high interference to the pico-eNB users which denies them to use the same physical resources.

As a solution for the first two points, cell selection could be dependent on estimates of the uplink path loss, which in practice can be done by applying a cell-specific offset to the received power measurements used in typical cell selection. This offset would somehow compensate for the transmitting power differences between the macro-eNBs and pico-eNBs; it would also extend the coverage area of the Pico-eNB, or in other words extend the area where the pico-eNB is selected. This area is called "Range Expansion" [36].
In this technique, users are offloaded to smaller cells using an association bias or offset. Formally, if there are K candidate tiers available for a user to associate, then the index of the chosen tier is:

$$k^* = argmax_{i=1->k} B_i P_{rx,i}, \tag{1.1}$$

where B_i is the bias for tier i and $P_{rx,i}$ is the received power from tier i. By convention, tier 1 is the macro cell tier and has a bias of 1 (0 dB). For example a small cell bias of 10 dB means a UE would associate with the small cell up until its received power was more than 10 dB less than the macro cell base station.
However, the difference in transmission powers of the macro-eNBs and the pico-eNB in the range expansion area, makes the users in the range expansion area more prone to interference from the macro-eNB. So along with the benefits of range expansion, comes the disadvantage of the high inter-cell interference that the macro layer imposes on the users in the range expansion area of the pico layer.

UL/DL Decoupled Access

Cell association in cellular networks has been traditionally based on the downlink received signal power only [37], despite the fact that uplink and downlink transmission powers and interference levels differed significantly. This approach was adequate in homogeneous networks with macro base stations all having similar transmission power levels. However, with the growth of heterogeneous networks where a big disparity in the transmit power of the different base station types exists, this approach is highly inefficient. In this work, we study the notion of decoupled UL/DL access [38]. To understand this assertion, we consider a typical HetNet scenario with a macro cell and a small cell. The DL coverage of the macro cell is much larger than the small cell due to the large difference in the transmit powers. However, in the UL all the transmitters, which are battery powered mobile devices, have about the same transmit power and thus the same range. Therefore, a user equipment (UE) that is connected to a macro cell in the DL from which it receives the highest signal level might want to connect to a small cell in the UL where the pathloss is lower to that cell. As HetNets become denser and small cells smaller, the transmit power disparity between macro and small cells is increasing and, as a consequence, the gap between the optimal DL and UL cell boundaries increases. For the sake of optimal network operation, this necessitates a new design approach which is the Decoupled Uplink and Downlink access (DeUD) where the UL and DL are basically treated as separate network entities and a UE can connect to different serving nodes in the UL and DL (Fig. 1.4). The cell association criteria in DL is different than the cell association criteria in UL where the power imbalance between the macro cells and the small cells motivates the decoupling of both links.
As we have previously mentioned, CRE technique appears to improve the network performance in UL and degrade the performance in DL. On the other hand, the decoupling association policy appears to have potential benefits including network load balancing and performance improvement in UL without any performance degradation in DL. This will be investigated in the next chapters where we model and simulate a network with multiple association policies, including the CRE and the decoupling techniques.

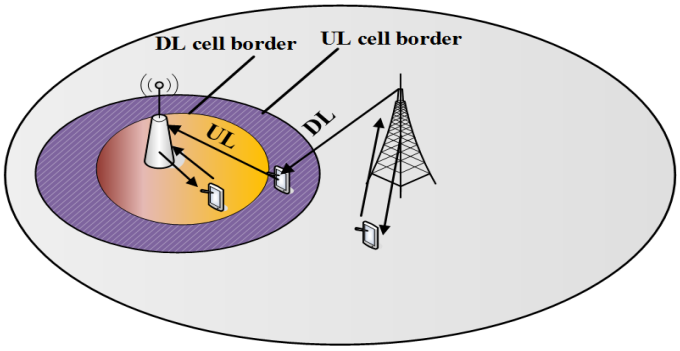

Figure 1.4: The concept of UL/DL decoupling [39].

1.3.5 Coordinated Multi-Point (CoMP)

In LTE-A (LTE-Advanced) Rel-11 coordinated multi-point (CoMP) transmission schemes were introduced as an alternative approach to cope with interference issues in HetNet systems [40] on a more dynamic basis than enhanced Inter-Cell Interference Coordination (eICIC). In contrast to eICIC, the interference between nodes in CoMP schemes is mitigated by the cooperation of a limited set of base stations having high capacity and low latency backhaul link connections with each other.
Owing to CoMPs significant effect on improving the spectral efficiency, it has also attracted attention from researchers who are focusing on energy efficiency study [41]. For example, authors in [42] gave an overview on the potential applications of CoMP transmission to increase energy efficiency for cell-edge users. Authors in [43] verified that combining CoMP and BS sleeping in conventional homogeneous networks can achieve improved energy efficiency. However, the system model in [43] is a one tier model and the deployment of BSs is based on a hexagonal grid which is not very realistic. Recently, in comparison to the conventional hexagonal grid based analysis, the stochastic geometry approach has gained increasing popularity for modelling wireless networks because it is accurate and tractable [44]. In stochastic geometry analysis, positions of BSs and users are modeled from certain stochastic point process. This approach is especially suitable to be used for HetNets where the deployment of small cells are far from symmetric distribution within the networks. Authors in [45] has formulated the coverage probability and the average data rate in homogeneous networks and [46] has extended the work in [45] to HetNets scenario.
In wireless cellular radio networks, the backhaul contribution to the total power consumption is generally overlooked because of its restrained effect compared with that of the radio BSs. However, satisfying the almost exponential increase in mobile data traffic demands a prominent number of (mainly small) BSs or macrocell along with remote antenna elements such as RRHs. Therefore, we can easily deduce that the deployment of the backhaul links in a CoMP-equipped HetNet will increase the expenditure (both CAPEX and OPEX) including more power consumption in the highly anticipated future green wireless system.

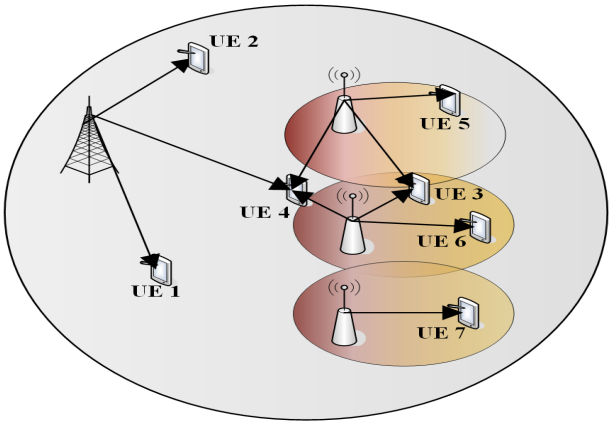

Figure 1.5: CoMP in HetNet [47].

1.3.6 UL/DL Decoupling and CoMP

Coordinated Multi-Point (CoMP) transmission or reception, has gained popularity in the context of HetNets as a means to increase the UE achievable throughput. eNBs within the same cluster communicate via backhaul links (i.e., via the X2 interface) with the objective of minimizing the inter-cell interference and capitalize on the benefits of distributed antenna systems. In fact, interference within a cooperation cluster can be effectively cancelled [48], [51]. This level of coordination and cooperation can be carried out in both UL and DL, and the realization of such coordination relies strongly on the availability of sufficient backhaul capacity, first to serve the UE in the cell cluster, and second to communicate with other cells in the cooperation cluster. This backhaul dependency can be very limiting in situations of high load, and in capacity limited links. The increased flexibility provided by decoupled UL and DL associations provides advantages when selecting UL and DL coordinated transmissions or receptions. In particular, there is no need to have both UL and DL simultaneous connection to the entire cooperating set of base stations and the UE could have unequal UL and DL active links (as in the case of CA). This flexible association inside the cluster, and the interoperability of DeUD with CoMP goes one step further in the device-centric network, since the UE can select independently the number and position of DL and UL serving cells, according to several input parameters, as backhaul capacity, power limitation, throughput maximization, among others

1.3.7 UL/DL Decoupling Enabler between CoMP and C-RAN

Implementing a decoupled cell association in a real network requires excellent connectivity and modest cooperation between different base stations. The main requirement DeUD imposes is a low latency connection between the downlink and the uplink base stations, to allow a fast exchange of control messages [52]. We emphasise that differently from the most sophisticated forms of CoMP (e.g. joint processing) where a high throughput backhaul connection between BSs is required to allow rapid data exchange, DeUD does not impose a tight requirement on the backhaul capacity. Put another way, DeUD allows gains similar to uplink joint processing (about 100% edge and average throughput gain), but with lower deployment costs. Compared to using MIMO or new spectrum to increase the throughput, the cost comparison is even more favorable to DeUD. The ongoing trend towards using partial or full Radio Access Network (RAN) centralization in deployments where a high-speed backhaul is available, will be an enabler for downlink and uplink decoupling, as signalling will be routed to a central processing unit with low-latency connections. In particular, partial centralization refers to those local deployments (e.g. indoor) where the transmission points serving the same local area are all connected to the same baseband processing central unit. Full centralization, often referred as Cloud-RAN, extends this approach to larger areas, where a large number of RF units are connected to the same baseband processing central unit. Given this already ongoing trend towards more centralized RAN architectures, which are underpinned by low-latency connectivity between BSs, the incremental cost of DeUD appears negligible in such scenarios.

1.3.8 Device to Device (D2D) Communications

With the spectral performance of the wireless link approaching the theoretical limits due to present cellular wireless networks, researchers have been working on various aspects in the framework of LTE-Advanced to further facilitate the mobile users in a ubiquitous and cost effective manner [53]. One of the ways of increasing the achievable rate in cellular communications is direct communication between closely located mobile users. This form of communication is referred to as device-to-device (D2D) communication [[55], [56]]. D2D communication, is a technique that is first introduced in 3GPP Release 12 and 13 [54]. Mobile devices involved in D2D communication form a direct link with each other, without the need of routing traffic via the cellular access network, resulting in lower transmit power and end-to-end delay, as well as freeing network resources. The lower transmit powers manifest through reduced interference levels in the system and battery power savings, while the improved rate is achieved as a result of low path-loss between any pair of devices involved in D2D communication [57]. The concept of D2D was presented in several studies as a promising solution to increase network capacity [58]. In this concept, the user can relay other user's traffic to light loaded small cell using its resource [59] [60].

1.3.9 Dynamic TDD

In classical HetNets, either FDD or conventional TDD technique is adopted. Sharing the same static TDD configuration between macro cell from one side and the small cell from the other side, is what we refer to as conventional TDD approach. However, the fifth-generation wireless communication systems (5G) are expected to support various

services, such as voice over IP (VoIP), online video, social networking, video sharing, etc. Due to the different uplink and downlink traffic demand of these services, the asymmetric traffic is one remarkable characteristics of future mobile communications. Besides, the instantaneous traffic condition of the network may vary significantly among adjacent cells. To satisfy this asymmetric and dynamic traffic demand, dynamic TDD is one promising solution since the UL/DL transmission direction can be changed dynamically to adapt the instantaneous traffic variation [61]. In the 3GPP standard, dynamic TDD is supported by seven configurations with respect to different uplink and downlink traffic ratios [62]. As shown in Fig. 1.6, each radio frame consists of 10 subframes, and the UL/DL ratio is different for each TDD frame configuration. This enables either the macro cell or the small cells base stations to select different configurations according to the traffic variation. As one special case of dynamic TDD, enhanced interference miti-

Uplink-downlink configuration	Downlink to uplink Switch-point periodicity (ms)	Subframe number									
		0	1	2	3	4	5	6	7	8	9
0	5	D	S	U	U	U	D	S	U	U	U
1	5	D	S	U	U	D	D	S	U	U	D
2	5	D	S	U	D	D	D	S	U	D	D
3	10	D	S	U	U	U	D	D	D	D	D
4	10	D	S	U	U	D	D	D	D	D	D
5	10	D	S	U	D	D	D	D	D	D	D
6	5	D	S	U	U	U	D	S	U	U	D

Figure 1.6: Supported TDD configurations in 3GPP [62].

gation and traffic adaptation (eIMTA) has been widely studied since LTE Rel.12 [63] where the UL/DL transmission direction is changed based on seven TDD configurations defined in LTE [62]. However, to enable more flexible traffic adaptation, fully dynamic TDD shall be supported in 5G where the UL/DL transmission direction can be changed per slot. Although dynamic TDD can provide flexible resource allocation, it also brings some new challenges due to the fact of misaligned UL/DL transmission direction among neighboring cells. The main challenge brought by dynamic TDD is the cross-link interference issue. As shown in Fig. 1.7, because of the different transmission directions among neighboring cells at a given time, two kinds of cross-link interference are introduced, i.e., BS-to-BS (DL to UL) interference and UE-to-UE (UL to DL) interference, which may degrade the system performance significantly. One step further in the optimization of HetNet, is the interdependency between UL and DL and how the association policies affect the system performance on both links in a way to mitigate the cross-link interference. Hence, the decoupled association policy has been introduced.

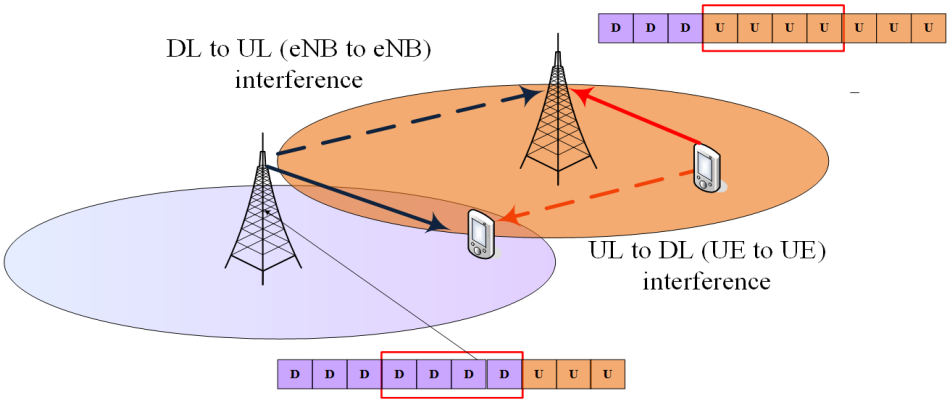

Figure 1.7: UL to DL and DL to UL interference in dynamic TDD system [61].

1.3.10 Inter-Cell Interference Coordination (ICIC)

The heterogeneity of all co-existing networks, that intend to enhance the radio coverage and considerably increase the offered capacity, will inevitably cause higher inter-cell interference if their operation is not coordinated. Orthogo-

nal Frequency Division Multiple Access (OFDMA) technology is widely accepted as the access scheme for the Third Generation Partnership (3GPP) LTE [64]. In the downlink, OFDMA allows assigning frequency sub-carriers to users within each cell in an orthogonal manner, each sub-carrier having a much lower bandwidth than the coherence bandwidth of the channel. With the use of cyclical prefix insertion, intra-cellular interference can be eradicated. Hence, OFDMA is very attractive as it enjoys high spectral efficiency and immunity to both frequency selective fading and inter-symbol interference (ISI) which encourages the use of a Reuse Factor equal to one. However, when the same Resource Block (RB) (the smallest time-frequency resource unit allotted to a mobile user) is used in neighboring cells, interference may occur which can degrade the Signal to Interference plus Noise Ratio (SINR) perceived by mobile users (especially those with bad channel quality usually situated on the edge cell as illustrated in Figure 1.8).

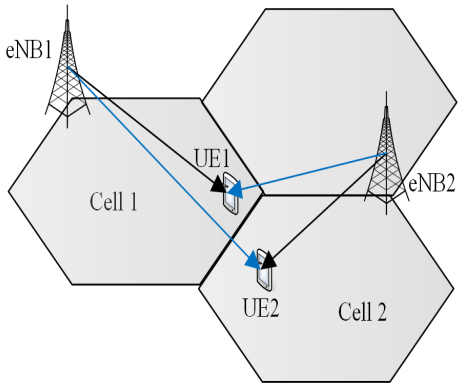

Figure 1.8: Cell-edge Inter-Cell Interference

Therefore, inter-cell interference is a central issue for the design of future cellular networks, especially at cell edges. Thus, investigation of Inter-cell Interference mitigation techniques is urgently required and facilitated by the flexibility in resource assignment in OFDMA. Inter-Cell Interference Coordination (ICIC) is considered as a key technique to combat interference. In our work, we study and statistically model several network performance metrics to analyze a TDD based HetNet. One important metric and key performance factor is the Inter-Cell Interference (ICI). Statistical modeling of ICI plays an imperative role in evaluating the system performance metrics and developing efficient interference mitigation techniques for 5G networks.

1.3.11 Motivation Behind Dynamic TDD and Decoupling Techniques in 5G

According to many studies, the decoupling technique which is developed in our manuscript, is expected to play an imperative role in the 5G architecture design. As stated in [65], the decoupling of the downlink and uplink is an emerging paradigm which will likely impact 5G design efforts.
As mentioned in [66] and in order to achieve extremely high spectral efficiency in 5G, three enabling technologies which are massive MIMO [67], mmWave [68] and densified heterogeneous networks (HetNets) with decoupling technique are mainly concerned.
According to [38], decoupling technique is a strong candidate for 5G architecture designs and it can be very useful in many applications like Machine Type Communications (MTC) where Uplink optimization is very critical. Most network technologies such as 3G or 4G were designed with macro cells in mind and heterogeneity was just an afterthought. This dramatic change in cellular networks requires a fresh look on how present networks are deployed and what fundamental changes and improvements need to be done for future networks to operate efficiently. Cellular networks have often been designed based on the downlink (DL); this is due to the fact that network traffic is mostly asymmetric in a way that the throughput required in the downlink is higher than the one required in the uplink. However, uplink is becoming more and more important with the increasing popularity of symmetric traffic applications, such as social networking, video calls, real-time video gaming, etc. As a consequence, the optimization of the uplink has become increasingly important.
Taking a real case scenario, Huawei has showcased in Nov. 2017 its ability to improve 5G coverage, capacity, and user experience by carrying uplink data via 4G LTE bands and downlink data on 5G bands [69] i.e. by using the decoupling technique. Huawei's "5G UL & DL Decoupling" receives 2019 GSMA award for best mobile technology breakthrough at the Mobile World Congress (MWC) in Feb 2019 [70]. This inter-band connectivity in 5G

networks [71] between two different radio technologies FR1 and FR2 has been clearly described in 3GPP Release 16. As an example, a mobile user hosting a video streaming session which generally requires a high downlink throughput, will be associated in DL to a mmwave BS that offers a large bandwidth and thus a high throughput. However in UL, the mobile user suffering from a transmitted signal power limitation will be associated to a low frequency LTE BS to compensate and increase its uplink coverage.

According to 3GPP Release 16 ([72], [73]) , TDD is widely used in 5G networks especially with high frequency bands (see Fig. 1.9). One of the main TDD features is the channel reciprocity, that will help in reducing the channel estimation overhead resulting from the MIMO technology and the multiple antennas implemented in 5G.

5G/NR - Operating in Frequency Range 2			
Band	Frequencies [GHz]	BW [MHz]	Duplex mode
n257	26.5 - 29.5	50 - 400	TDD
n258	24.25 - 27.5	50 - 400	TDD
n259	39.5 - 43.5	50 - 400	TDD
n260	37.0 - 40.0	50 - 400	TDD
n261	27.5 - 28.35	50 - 400	TDD

Figure 1.9: 5G operating in frequency range 2 with TDD [72].

Accordingly, 5G will adopt TDD [74] due to following reasons:

- The mmWave spectrum is mainly unpaired. It provides a single band used for both downlink and uplink.
- Guard period (GP) for link direction (UL/DL) switching can be kept small for small cells which are in focus for mmWave deployments.
- TDD operation makes the UL and DL channels reciprocal, which is important for massive MIMO operation (to estimate DL channel via uplink channel state information).
- DL/UL traffic can be very dynamic. Dynamic TDD matches the DL/UL traffic load of each small cell individually by adjusting the GP position.

1.4 Thesis Objectives

This thesis proposes studying next generation 5G HetNets using dynamic TDD configuration with uplink / downlink decoupling. Integrating TDD, uplink / downlink decoupling into the same model and the same simulator is the challenge that this thesis wishes to address in order to answer the following questions:

1. What are the HetNets' performances when implementing a dynamic TDD mechanism associated with uplink/downlink decoupling?

2. What are the benefits of an adaptive TDD and decoupling compared to conventional HetNets?

The answer to question 1 requires the development of a theoretical model (framework) to evaluate the performance of the system in terms of SINR (signal-to-noise ratio), spectral efficiency and throughput. This model will rely on probability and statistical tools to retrieve the probabilistic distributions of the above-mentioned performance indicators. Comparing this model with Monte Carlo simulations will validate its accuracy. In the next-generation HetNets,

deriving closed-form expressions for cross-tier/co-tier interference and user capacity in TDD HetNets helps in designing and optimizing advanced enhancement techniques, including but not limited to the decoupled access technique. Deriving these expressions reduces as well the need for time consuming Monte-Carlo simulations, especially in the case of multiple small cells deployment where the time required to run Monte-Carlo simulations significantly increases.

The answer to question 2 requires the implementation of these techniques in a system level simulator allowing an adaptive TDD and uplink / downlink decoupling in a HetNet based system. The optimization of a HetNet based system according to time-variant traffic loads with multiple small cells and multiple users, necessitates finding a system level simulator where we can present the motivation and accurately assess the role of both decoupling and dynamic TDD techniques in the optimization problem. Our aim is to create appropriate simulation environment that is relative to real scenarios i.e. simulations where multiple small cells are deployed in a heavy loaded HetNet system and under various traffic loads. These simulations consider random users distribution with scheduling decisions in both the uplink and the downlink directions. The gain provided by the proposed approaches will be evaluated based on the simulation results.

Chapter 2

Related Work & Contributions

In this chapter, we review works that relate to our thesis and discuss in detail how our solution advances the state of the art. In the comparison tables that follow, we indicate how the related articles contribute to each of the topics listed in the table columns. This will clearly show how our works (highlighted in yellow) lift a number of scientific locks addressed in the related articles.

2.1 Related Work

Modeling a TDD-based HetNet

Analyzing a TDD based HetNet requires modeling and studying several performance metrics. Interference modeling is considered a main metric in wireless communications as it plays a role in the design and analysis of wireless systems and the establishment of advanced interference mitigation techniques. Interference models can also be helpful in assessing the performance of a given network as a substitute to simulation-based approaches. The problem of interference modeling in small cell networks has been tackled recently using various tools and methods. Several recent studies considered the modeling of the Inter-Cell Interference (ICI), where closed-form formulas are derived to compute the network performance. Some of these studies tackled individually the downlink case, other works considered the uplink case.

For the downlink case, a semi-analytical distribution for the signal-to-interference-noise ratio (SINR) has been derived in [75] under path loss and log normal shadowing for femtocell networks.Numerical experiments were performed assuming various environments and deployment scenarios to examine the performance of femtocell networks. In [76], the applicability of the Gaussian and binomial distributions for modeling the downlink ICI is investigated. The influence of the closest interfering cells and time synchronization offsets were in the focus. In [77], an analytical approach based on geometric probability was developed for downlink performance analysis of a HetNet network model where the coverage probability and the spectral efficiency have been derived and verified by simulation. A novel circular interference model was introduced in [78] to facilitate statistical analysis in networks with regular grid layout. The key idea was to spread the power of the interferers uniformly along the circumcircle of the grid-shaping polygon. In [79], an interference model is obtained for the downlink of an OFDMA system with log-normal shadowing and Rayleigh fading. This work was extended in [80] for Ricean fading channels.

Several research works for the uplink appear in [81], [82] and [83]. An analytical model for the collisions for an arbitrary number of users in the different cells, was developed in [81]. In [82], an exact analytical expression for the collision probability was derived for an arbitrary number of base stations with non-coordinated schedulers. The expression was used to determine conditions under which ICI mitigation techniques may be required as well as to establish a baseline for performance comparison with ICI coordination schemes. In [83], the intercell interference was described as a random variable which is composed of many other random variables. The distributions, and in particular the mutual dependencies of those were carefully studied. In [84], a new approach based on Gaussian approximation was introduced to analyze the uplink signal to interference ratio (SIR) performance. In [85], the scheduling-based interference models for LTE networks was considered where the distance distribution and thus the interference distribution was derived for different resource allocation schemes such as proportional fair, greedy

and round robin scheduling schemes. In [86], uplink capacity (in bps/Hz) was derived with closed-form expressions in both dedicated and shared spectrum access scenarios. The proposed framework exploited the distance distributions based on geometric probability theory to characterize the co-tier and cross-tier uplink interferences.

As for the modeling of interference in TDD systems, the work in [87] introduced a statistical framework to analyze uplink/downlink interactions where analytical expressions for the four interference types in TDD systems were derived. For interference-aware scenarios, the distribution of the distance between the source and victim of interference was based on the scheduling algorithms defined in [85]. The distance distribution probability in [87] was scheduling based instead of geometric probability based. Moreover, it did not evaluate important network performance metrics such as average cell capacity. Instead, interference maps were generated to analyze the impact of TDD operation in a given network.

Analytical Evaluation of Decoupling in TDD HetNets

Several recent studies introduced the concept of downlink/uplink decoupling. The work in [88] focused on the architectural design and realization, identified and explained some key arguments in favor of DeUD.

A group of articles studied various link association policies and showed their performances based on simulations results. In [89], the notion of DeUD is studied, where the downlink cell association is based on the downlink received power, while the uplink is based on path loss. The follow-up work in [90] considered the cell-load as well as the available back-haul capacity within the association process. The work in [91] added a cell selection offset to the reference signals in small cells.

Other works focused on the analytical evaluation of a predefined association policy. The research work in [92] and [93] focused on the analytical characterization of the decoupled access, relying on the stochastic geometry framework and applying a specific association criteria (power received or transmitted). The main advantage of using stochastic geometry is the ability to develop a statistical model with randomly distributed small cells. The locations of BSs and the locations of devices in [92] are modeled by independent homogeneous Poisson Point Processes (PPPs). The work in [93] focused on the analytical characterization of the decoupled access by using the framework of stochastic geometry [94]. A joint analysis of the DL and UL association was performed using the same realization of the random process that describes spatial deployment of the BSs and devices. This analysis was applied for a two-tier cellular network, consisting of Macro BSs (MBSs) and Femto BSs (FBSs). Uplink performance improvement brought by a DeUD mode over a conventional CoUD mode, was investigated in [95]. A fractional power control was employed to determine location-dependent user transmit power. Two kinds of user equipment distributions, namely uniform and clustered distributions were considered and modeled as Poisson point and Neyman–Scott cluster processes, respectively. Also, the work in a [95] considered a HetNet which consists of k-tier BSs arranged according to an independent homogeneous PPP. A general analytical framework in a hybrid system (sub-6GHz and millimeter wave) was developed in [96] where the biased uplink and downlink cell association, as well as the rate coverage probability, were derived. A two-tier heterogeneous network was considered where Mcells and Scells (Small cells) are distributed uniformly according to independent homogeneous Poisson point processes (PPP). Specifically, a deployment of sub-6GHz Mcells overlaid by mmWave Scells is considered. The UEs are also assumed to be uniformly distributed according to a homogeneous PPP.

As for the modeling of TDD systems, the work in [97] introduced a statistical framework to model the UL/DL inter-cell interference in TDD networks. The distance distribution probability was scheduling-based and the users were associated according to the conventional downlink received power policy. As for the joint modeling of both decoupling and dynamic TDD techniques, it has not been covered in the recent literature. Instead, there is one study where these two techniques were simulated in a homogeneous small cells network. The main objective of this study is described next in the simulation section.

Adaptive TDD and Decoupling in 5G HetNets: Simulation-Based Evaluation

Several recent studies considered analyzing the UL/DL decoupling technique with simulations based on specific network simulators. A set of articles studied various link association policies (including the decoupled policy) and showed their performances based on simulations results. In [99], the concept of DeUD is studied, where the

downlink cell association is based on the downlink received power, while the uplink is based on path loss. The gains of this design approach were presented with simulations based on Vodafone's LTE field trial network in a dense urban area, employing a high resolution ray-tracing path loss prediction and realistic traffic maps based on live network measurements. The follow-up work in [100] considered the cell-load as well as the available back-haul capacity within the association process. The work in [101] added a cell selection offset to the reference signals in small cells.

Other works considered the analysis of both decoupling and TDD techniques under the same system level simulator or trial network. In [102], the problem of decoupled uplink and downlink in time division duplexing (TDD)-based small cell networks is studied. This work focused on the user association technique to solve the problem of dynamic user association in UL/DL decoupled small cell networks with dynamic TDD.

2.2 Thesis Contributions

The main contributions of this work can be summarized as follows:

1) TDD Statistical Model: We consider analyzing, in this work, both uplink/downlink interactions, whereas other works introduced either a downlink ICI model as in [76] and [77] or an uplink ICI model as in [85] and [86]. Few studies considered modeling a TDD system, however they either did not consider a HetNet system or did not evaluate any network performance indicator as in [87]. In this work, operating a TDD-based HetNet network necessitates four interference scenarios depending mainly on the geographical distance between the reference cell and the neighboring cell. In a multiple small cells scenario, the neighboring cell can be either the small cell or the macro cell. Thus, analyzing four interference scenarios is still applicable because of the TDD subframes distribution that is considered perfectly synchronized between the small cells (See Table 2.1 for illustration).

		TDD				
		UL Interactions Model	DL Interactions Model	TDD Model	HetNets	Total Throughputs (UL and DL)
TDD Model	[75] K. W. Sung, H. Haas, and S. McLaughlin, "A semi-analytical PDF of downlink SINR for femtocell networks," EURASIP J. Wireless Commun. and Networking, Jan. 2010.		✓			
	[76] S. Plass, X. G. Doukopoulos, and R. Legouable, "Investigations on link-level inter-cell interference in OFDMA systems," in Proc. 2006 IEEE Symposium on Communications and Vehicular Technology, pp. 49-52.		✓			
	[77] X. Yang and A. O. Fapojuwo, "Analysis of heterogeneous cellular network with hexagonal tessellated macrocells and randomly positioned small cells," IEEE WCNC, 2016.		✓		✓	
	[78] M. Taranetz and M. Rupp, "A circular interference model for wireless cellular networks," International Wireless Communications and Mobile Computing Conference, 2014.		✓			
	[81] S. Elayoubi, B. Haddada, and B. Fourestie, "Performance evaluation of fre- quency planning schemes in OFDMA based networks," IEEE Trans.Wireless Commun., vol. 7, no. 5, pp. 1623-1633, May 2008.	✓				
	[82] R. Kwan and C. Leung, "On collision probabilities in frequency-domain scheduling for LTE cellular networks," IEEE Commun. Lett., vol. 15, no. 9, pp. 965- 967, Sep. 2011.	✓				
	[83] I. Viering, A. Klein, M. Ivrlac, M. Castaneda, and J. A. Nossek, "On uplink intercell interference in a cellular system," in Proc. 2006 IEEE International Conference on Communications, pp. 2095-2100.	✓				
	[84] M. Ding, D. Lopez-Perez, G. Mao, and Z. Lin, "DNA-GA: A new approach of network performance analysis," Proc. IEEE ICC 2016,arXiv:1512.05429 [cs.IT], to be published.	✓				
	[85] H. Tabassum, Z. Dawy, E. Hossain, and M. S Alouini, "A framework for uplink intercell interference modeling with channel-based scheduling,"IEEE Trans. Wireless Commun., vol. 12, no. 1, pp. 206-217, Jan. 2013.	✓				
	[86] H. Tabassum, Z. Dawy, E. Hossain, and M. S Alouini, "Interference statistics and capacity analysis for uplink transmission in two-tier small cell networks: A geometric probability approach," IEEE Trans. Wireless Commun., vol. 13, no. 7, pp. 3837-3852, Jul. 2014.	✓			✓	
	[87] Ahmad El-Hajj, Naeem Akl, Bilal Hammoud, and Zaher Dawy, "On interference modeling for the analysis of uplink/downlink interactions in TDD-OFDMA networks," 2015 International Wireless Communications and Mobile Computing Conference (IWCMC), pp. 497-502, 2015.	✓	✓	✓		
	[103] B. Lahad, M. Ibrahim, S. Lahoud, K. Khawam and S. Martin, "A Statistical Model for Uplink/Downlink Intercell Interference and Cell Capacity in TDD HetNets", ICC 2018: 1-6.	✓	✓	✓	✓	✓

Table 2.1: Modeling a TDD-based HetNet [Related Work and Contribution].

2) Analytical Model Covering Various User Association Policies: Focusing on the decoupled access strategy, other similar works either developed an analytical model studying one specific association criteria ([92]- [96]) or investigated multiple association strategies based on simulation results ([89]- [91]). In this work, an analytical model covering four association policies is developed with the aim of studying the improvement that the decoupling access can bring to TDD HetNets among all other association policies (See Table 2.2 for illustration).

		Decoupling	
		Decoupling with Various Association Policies	Analytical Evaluation of Decoupling
UL/DL Decoupled Access	[89] H. Elshaer, F. Boccardi, M. Dohler, and R. Irmer, "Downlink and uplink decoupling: a disruptive architectural design for 5G networks," in GLOBECOM14. IEEE, 2014, pp. 1798-1803.	✓	
	[90] "Load & backhaul aware decoupled downlink/uplink access in 5G systems," arXiv preprint arXiv:1410.6680, 2014.	✓	
	[91] Qualcomm, "Range expansion for efficient support of heterogeneous networks," 3GPP TSG-RAN WG1 R1-083813, 2008	✓	
	[92] K. Smiljkovikj, H. Elshaer, P. Popovski, F. Boccardi, M. Dohler, L. Gavrilovska, and R. Irmer, "Capacity analysis of decoupled downlink and uplink access in 5G heterogeneous systems," arXiv preprint arXiv:1410.7270, 2014.		✓
	[93] K. Smiljkovikj, P. Popovski, and L. Gavrilovska, "Analysis of the decoupled access for downlink and uplink in wireless heterogeneous networks," Wireless Communications Letters, IEEE, vol. 4, no. 2, pp. 173-176, 2015.		✓
	[95] W. Nie, L. Zhang, and G. Fang, "Uplink Performance Improvement by Decoupling Uplink/Downlink Access in HetNets," IEEE Transactions on Vehicular Technology, IEEE, vol. 66, no. 8, pp. 6862-6876, 2017.		✓
	[96] H. E. Shaer, M. N. Kulkarni, F. Boccardi, J. G. Andrews, and M. Dohler, "Downlink and Uplink Cell Association in Sub-6GHz and Millimeter Wave 5G Heterogeneous Networks," Globecom Workshops (GC Wkshps), 2016 IEEE.		✓
	[117] B. Lahad, M. Ibrahim, S. Lahoud, K. Khawam and S. Martin, "Analytical Evaluation of Decoupled Uplink and Downlink Access in TDD 5G HetNets", PIMRC 2018: 1-7.	✓	✓

Table 2.2: Analytical model covering various user association policies [Related Work and Contribution].

3) Joint Modeling of TDD and Decoupled UL/DL access in Multiple Small Cells HetNets: Studying the next-generation wireless 5G HetNets with respect to TDD and UL/DL decoupled access. Other works investigated either a TDD system as in [87] and [103] or the decoupled access technique as in [89]- [96]. In fact, considering a TDD model jointly with a decoupled association policy appears to be a viable solution to address UL and DL throughput degradation challenges (See Table 2.3 for illustration). The work in [117] studied both decoupling and TDD techniques, however it was limited to one small cell case study.
In our model, we consider a network consisting of one macro cell along with a reference small cell located at a certain distance from the macro cell. Multiple instances of interfering small cells are deployed at specific distances from the reference small cell in order to be aligned as much as possible with real case scenarios. We consider this specific network model, as simple as it shows in regards to BS distribution, to focus on the main thesis objective which is the modeling of TDD and decoupling in a scenario that is close to real cases, and at the same time to avoid adding further complexity to the model itself. Instead, including any other BS distribution (stochastic for example), will bring significant additional complexity to our HetNet analysis, especially that our aim is to combine both decoupling and dynamic TDD techniques under one statistical model. Our model is based on geometric approach contrary to most of the recent articles, where the model is based on stochastic probability and the user association is based on UL/DL received power. However, we will rely on the recent literature on decoupling ([104], [105]) to retrieve the small cell bias/offset (power based) and apply it in our system level simulations that analyze different association policies among them, a power based policy. The latter will be discussed in details in Chapter5.

		TDD					Decoupling		Multiple small cells
		UL Interactions Model	DL Interactions Model	TDD Model	HetNets	Total Throughput	Decoupling with Various Association Policies	Analytical Evaluation of Decoupling	Multiple small cells
UL/DL Decoupled Access	[89] H. Elshaer, F. Boccardi, M. Dohler, and R. Irmer, "Downlink and uplink decoupling: a disruptive architectural design for 5G networks," in GLOBECOM14. IEEE, 2014, pp. 1798-1803.				✓		✓		✓
	[90] "Load & backhaul aware decoupled downlink/uplink access in 5G systems," arXiv preprint arXiv:1410.6680, 2014.				✓		✓		✓
	[91] Qualcomm, "Range expansion for efficient support of heterogeneous networks," 3GPP TSG-RAN WG1 R1-083813, 2008				✓		✓		✓
	[92] K. Smiljkovikj, H. Elshaer, P. Popovski, F. Boccardi, M. Dohler, L. Gavrilovska, and R. Irmer, "Capacity analysis of decoupled downlink and uplink access in 5G heterogeneous systems," arXiv preprint arXiv:1410.7270, 2014.	✓	✓		✓	✓		✓	✓
	[93] K. Smiljkovikj, P. Popovski, and L. Gavrilovska, "Analysis of the decoupled access for downlink and uplink in wireless heterogeneous networks," Wireless Communications Letters, IEEE, vol. 4, no. 2, pp. 173-176, 2015.	✓			✓			✓	✓
	[95] W. Nie, L. Zhang, and G. Fang, "Uplink Performance Improvement by Decoupling Uplink/Downlink Access in HetNets," IEEE Transactions on Vehicular Technology, IEEE, vol. 66, no. 8, pp. 6862-6876, 2017.	✓			✓			✓	✓
	[96] H. E. Shaer, M. N. Kulkarni, F. Boccardi, J. G. Andrews, and M. Dohler, "Downlink and Uplink Cell Association in Sub-6GHz and Millimeter Wave 5G Heterogeneous Networks," Globecom Workshops (GC Wkshps), 2016 IEEE.	✓	✓		✓	✓		✓	✓
	[117] B. Lahad, M. Ibrahim, S. Lahoud, K. Khawam and S. Martin, "Analytical Evaluation of Decoupled Uplink and Downlink Access in TDD 5G HetNets", PIMRC 2018: 1-7.	✓	✓	✓	✓	✓	✓	✓	
Joint TDD and Decoupled Access with multiple small cells	[130] B. Lahad, M. Ibrahim, S. Lahoud, K. Khawam and S. Martin, "Joint Modeling of TDD and Decoupled Uplink/Downlink Access in 5G HetNets with Multiple Small Cells Deployment", *in IEEE Transactions on Mobile Computing*,2020.	✓	✓	✓	✓	✓	✓	✓	✓

Table 2.3: Joint modeling of TDD and Decoupling in multiple small cells HetNets [Related Work and Contribution].

4) Adaptive TDD and Decoupling in 5G HetNets: Simulation-Based Evaluation: We conduct simulations using a system level simulator where we consider analyzing a system supporting a dynamic TDD resource allocation along with UL/DL decoupled access in a dense HetNet deployment. Other works proposed various link association policies (coupled and decoupled policies) and showed their performance gain with simulations based on LTE field trial network, without considering any dynamic TDD configuration [99]- [101].
Few studies considered simulating both decoupling and dynamic TDD techniques as in [102], however these techniques were not implemented under a system simulator with scheduling decisions to dynamically allocate UL/DL resources. Note that the implementation of scheduling algorithms plays an important role in ensuring a fair and efficient distribution of resources, whether in the uplink or downlink. Moreover, the work in [102] did not consider the case of a HetNet deployment in the presence of macro cells, it considered small cell networks instead (See Table 2.4 for illustration).

		Simulations				
		TDD	Decoupling	Various Association Policies	HetNets	System Level Simulator
Uplink/Downlink Decoupled Access with Dynamic TDD - Simulations	[99] H. Elshaer, F. Boccardi, M. Dohler, and R. Irmer, "Downlink and uplink decoupling: a disruptive architectural design for 5G networks," in GLOBECOM14. IEEE, 2014, pp. 1798-1803.		✓	✓	✓	
	[100] "Load & backhaul aware decoupled downlink/uplink access in 5G systems," arXiv preprint arXiv:1410.6680, 2014.		✓	✓	✓	
	[101] Qualcomm, "Range expansion for efficient support of heterogeneous networks," 3GPP TSG-RAN WG1 R1-083813, 2008		✓	✓	✓	
	[102] M. S. ElBamby, M. Bennis, and M. Latva-aho, "UL/DL decoupled userassociation in dynamic TDD small cell networks," in 2015 International Symposium on Wireless Communication Systems (ISWCS), Aug 2015,pp. 456460.	✓	✓	✓		
	[131] B. Lahad, M. Ibrahim, S. Lahoud, K. Khawam and S. Martin, "Uplink/Downlink Decoupled Access with Dynamic TDD in 5G HetNets", IWCMC 2020: 1-6.	✓	✓	✓	✓	✓

Table 2.4: Adaptive TDD and Decoupling in 5G HetNets: Simulation-Based evaluation [Related Work and Contribution].

2.3 Thesis Organization

The remaining of this thesis is organized as follows: In Chapter 3, we develop a joint TDD/decoupling model in 5G HetNets with multiple small cells deployment. We conduct both downlink and uplink performance comparison study for four various cell association rules in TDD HetNet. Two cases are considered with UL/DL coupled access and two others with decoupled access. This chapter considers the modeling of both cross-tier and co-tier interferences in a multiple small cells environment. More insight into the benefits of decoupling mode, is provided in this chapter in terms of UL and DL decoupling gains. Moreover, we consider the uplink power control and the case of an unsynchronized TDD configuration between small cells.
In Chapter 4, we evaluate the analytical and simulation results based on the closed-form expressions derived in Chapter 3. We show the benefits that the decoupling access mode can bring to a HetNet TDD based system, in terms of UL and DL spectral efficiencies. Monte-Carlo simulation results are provided to validate the accuracy of the analytical model including 95% confidence intervals of disparity measures.
In Chapter 5, we create appropriate simulation environment that is relative to real scenarios, i.e. simulations where multiple small cells are deployed in a heavy loaded HetNet system and under various traffic loads. These simulations consider random users distribution with scheduling decisions in both the uplink and the downlink directions. In this chapter, we propose a new procedure to jointly implement a dynamic TDD based system with coupled/decoupled user association policies and to analyze the outcome resulting from this joint optimization. To proceed with these simulations, we consider an existing system level simulator to which we have added customized features/modules to motivate our system model. The added modules include, in addition to the decoupling and dynamic TDD techniques, many other customization that are described in details in this chapter. Finally, Chapter 6 draws the conclusion and gives recommendations for future works.

Chapter 3

Joint Modeling of TDD and Decoupling in 5G HetNets

3.1 Introduction

3.1.1 Motivation

In this chapter, we develop a statistical and analytical model for a HetNet based system where decoupling and dynamic TDD are jointly deployed. On the one hand, this model should capture the complexity of the system by taking into account its main radio and topological design parameters. On the other hand, we aim for closed-form analytical expressions of the system performance metrics such as the average capacity and the decoupling gain.
By meeting these contradictory requirements and constraints, the proposed model offers a simple analysis tool to assess a given TDD/Decoupling-based HetNet deployment. The analytical formulas provide relevant insights about network performance without the need for time consuming Monte-Carlo Simulations. This tool is also useful for network designers who can use it to determine the range of deployment parameters given a target QoS.
In the remaining of this section, we provided some insights on our modeling approach and identify the main challenges to overcome, especially those related to complex interference scenarios. We then describe our proposed solution that uses geometric probability approach to compute the probability distributions of the radio signals involved in a user communication.

3.1.2 TDD Modeling Insights and Challenges

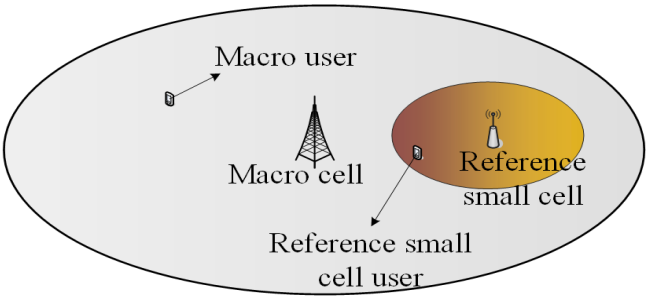

Figure 3.1: HetNet system - single small cell.

Let us consider a HetNet system which consists of one macro cell along with one small cell (see Fig. 3.1). Our main focus will be evaluating users' performance inside the small cell. This small cell is referred to as a reference small cell. Assuming randomly distributed macro and small cell users, the model will compute the statistical distribution of SINR at the reference small cell. From the SINR, an important performance metric can be calculated, which is the average user capacity at the reference small cell.
However, obtaining the SINR requires both the statistical distribution for the signal of interest (S) of one user inside

the reference cell and the statistical distribution for the interference (I). Note that the interference suffered by the reference small cell is caused by the macro cell that uses the same frequency.
Incorporating the dynamic TDD technique into our HetNet based system imposes a new type of interference and thus, brings a new challenge in deriving closed-form expressions for the interference I in general. This new type of interference is called the cross-link interference. Because of the different transmission directions among neighboring cells at a given time, two kinds of cross-link interference are introduced, i.e., BS-to-BS (DL to UL) interference and UE-to-UE (UL to DL) interference. The most challenging part is to derive a closed-form expression for the UE to UE interference which involves two randomly distributed variables: the macro user position and the small cell user position. The interference incurred at one tier (reference small cell) arising from the other tier (macro cell) is referred to as cross-tier interference. As shown in Fig. 3.2, four kinds of cross-tier interference are introduced in order to cover all UL/DL TDD possible combinations between the macro cell from a side and the small cell from the other side. Hence, we consider analyzing four scenarios in our model as follows:

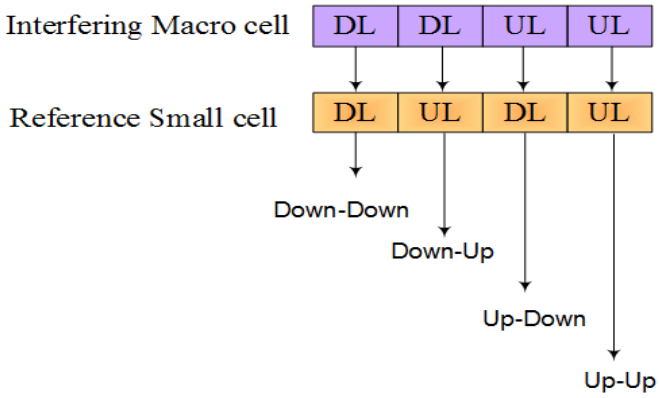

Figure 3.2: Four possible TDD combinations.

1. **Down - Down** scenario defines a situation where both macro and small cells are operating in downlink.
2. **Up - Down** scenario defines a situation where the macro cell is operating in uplink and the small cell in downlink.
3. **Up - Up** scenario defines a situation where both macro and small cells are operating in uplink.
4. **Down - Up** scenario defines a situation where the macro cell is operating in downlink and the small cell in uplink.

Figure 3.3 illustrates the cross-tier interference (I) and the signal of interest (S) corresponding to each of the aforementioned scenarios. As mentioned earlier, the challenge is to derive closed-form expressions for these interferences and specifically for the UE to UE interference in the Up - Down scenario.

3.1.3 Joint TDD - Decoupling Modeling Insights and Challenges

Deploying the decoupling policy on top of our TDD HetNet system necessitates the modeling of various association policies in order to highlight the benefits that the decoupling policy can bring to that system in comparison with the other policies. We consider a geographical area between the reference small cell and the macro cell where the users inside this area can be either coupled or decoupled. Users are coupled when they are associated in UL and DL with the same base station. However, users are decoupled when they are associated in UL with a base station and in DL with another base station. Decoupling technique is the case when the users are associated in UL with the small cell and in DL with the macro cell (see Fig. 3.4). Each adopted association policy will have direct impact on the users in the expanded area and on the users inside the reference small cell as well. Hence, average capacity for both small cell users and expanded area users must be evaluated in this case. This will require the derivation of closed form expressions for the interferences that occur at both the expanded area and the reference small cell area. Deriving expressions for these interferences will depend on the TDD subframe and the association policy selected at a specific time. Let's consider a decoupling technique adopted in a Down - Up scenario; users in the expanded area

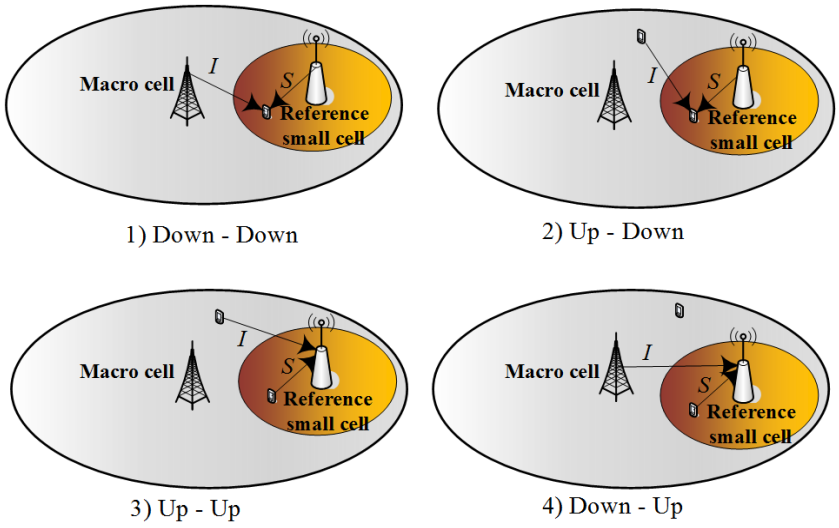

Figure 3.3: Illustration of the four possible scenarios.

are at the same time operating in DL with the macro cell that is enabling the DL transmission and in UL with the small cell that is enabling the UL transmission. The challenge here is to derive expressions for all possible interferences and specifically the uplink interference experienced from the small cell user at the expanded area user operating in DL. Deriving a closed form expression for this interference must take into account the random distribution of both the expanded area users and the small cell users. On the other hand, while adopting the decoupling technique in a Up - Down scenario, users in the expanded area are associated in DL with the macro cell whilst the latter is enabling only UL transmissions. Also, users in the expanded area are associated in UL with the small cell whilst the latter is enabling only DL transmissions. In this case, users in the expanded area will enter an idle state.
As a summary and despite the fact that we have incorporated both the decoupling and the dynamic TDD techniques into our system, we continue to work towards deriving closed-form expressions for S and I. From these expressions, we can evaluate the average user capacity in different scenarios. Accordingly, we will be able to analyze and assess the impact of both techniques on the system performance.

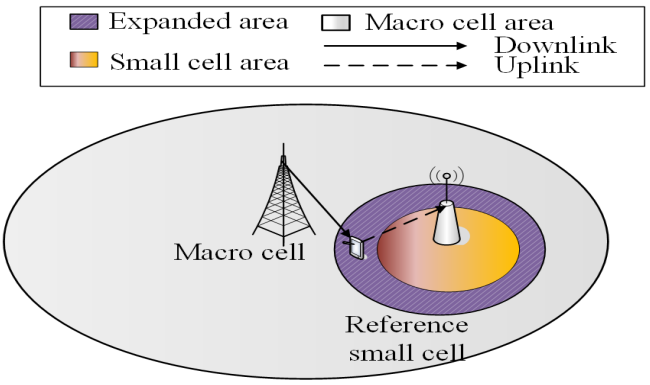

Figure 3.4: HetNet system with decoupling - single small cell.

3.1.4 Solution Approach

Our main objective is to develop a statistical and analytical model by deriving closed-form expressions for S and I in a HetNet based system, where decoupling and dynamic TDD techniques are jointly deployed. The model should take into account the main radio and network parameters in order to compute the system performance metrics such as spectral efficiency, decoupling gain, and power consumption. These metrics are detailed under Section 3.2.4. Such model will help in optimizing the system design parameters under various radio and network conditions (see

Fig. 3.5).

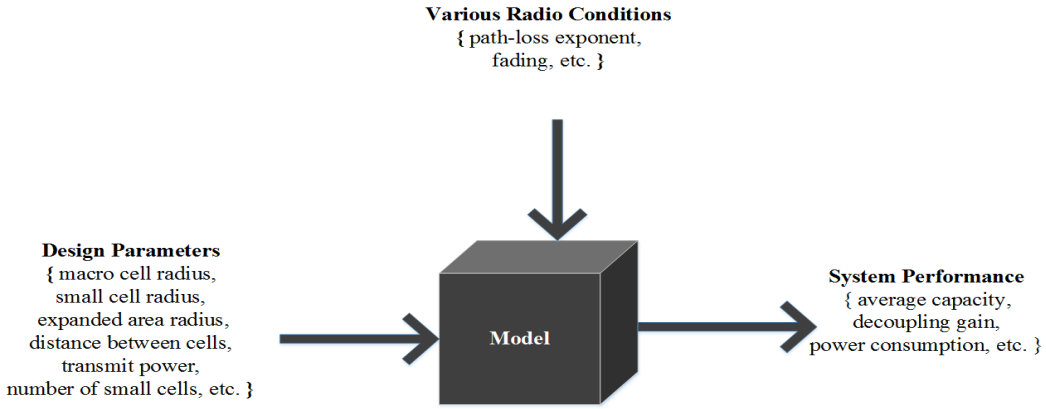

Figure 3.5: Model overview.

To start building our model, we will go through three important phases (see Fig. 3.6):

- **Geometric method**: In our model, we consider that macro and small cell users are both uniformly distributed in defined geometric places and they can be anywhere in their respective places. Hence, we can rely on a geometric probability approach to derive statistical expressions for the reference small cell user location and the interferers locations. This geometric method captures the main model design parameters e.g. macro cell radius, small cell radius, distance between cells, etc.

- **Probabilistic distribution**: Based on the statistical closed-form expressions derived in the previous phase, CDF of S and CDF of I can then be retrieved taking into account various radio conditions (path-loss, fading, etc.). From the CDF of S and I, we can obtain their corresponding PDFs.

- **Average capacity**: In order to calculate the average of the SINR and thus, the average user capacity of the reference small cell user, we need to apply a specific lemma that requires having the MGF of S and the MGF of I. Both MGFs can then be obtained from their corresponding and previously derived PDFs.

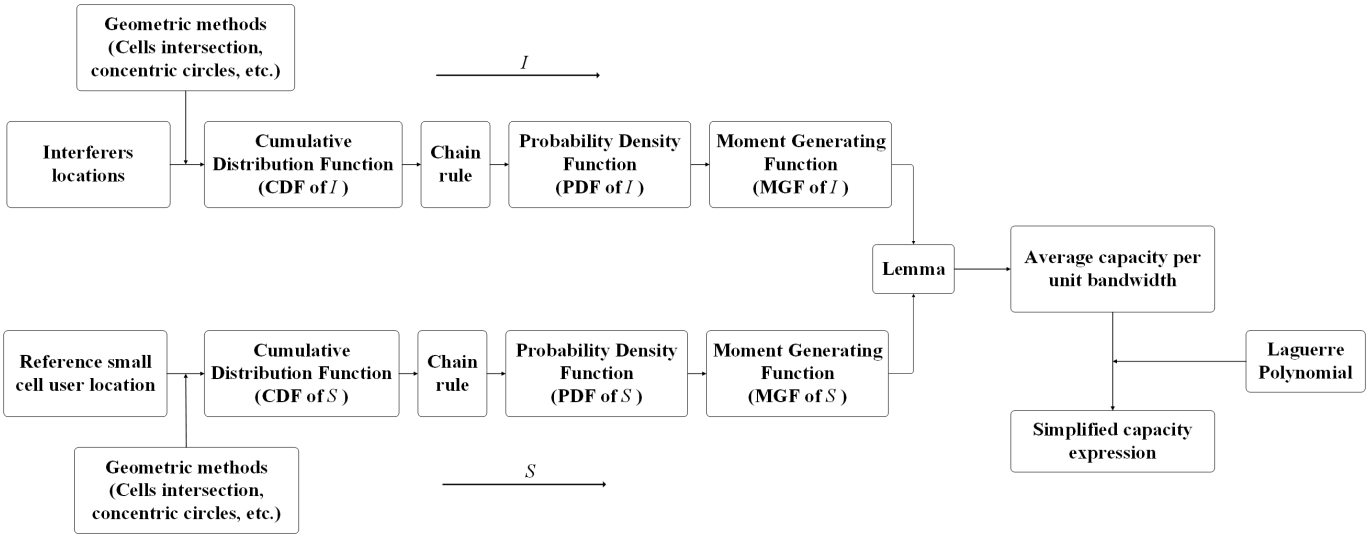

Figure 3.6: Model block diagram.

3.1.5 Chapter Organization

This chapter can be divided into four main sections as shown below:

- **System Model for Single Small cell Scenario**: We describe the system model of a network consisting of one macro cell and one small cell.
- **Ergodic Capacity in TDD 5G HetNets - Single Small Cell Scenario**: We model the uplink/downlink intercell interference and the cell capacity in TDD HetNets, for the single small cell scenario.
- **Modeling TDD 5G HetNets with Decoupling - Single Small Cell Scenario**: We analytically investigate a joint TDD and DeUD statistical model based on a geometric probability approach, for the single small cell scenario.
- **Analytical Evaluation in TDD 5G HetNets with Decoupling - Multiple Small Cells Scenario**: We derive analytical expressions for the capacity and the cross-tier/co-tier interference, considering a network of one macro cell and multiple small cells. We build on the derived capacity expressions to measure the decoupling gain and thus, identify the location of the interfering small cell where the decoupled mode maintains a higher gain in both DL and UL. Moreover, we add the uplink power control to the developed model and we consider an unsynchronized TDD configuration across small cells.

3.2 System Model for Single Small Cell Scenario

3.2.1 Network Topology

We consider a two-tier heterogeneous cellular network consisting of one macro cell and one reference small cell. The performance metrics will be evaluated inside this small cell.
The macro cell and small cell coverage areas are discs of radius R and R_s respectively. We assume that the small cell is totally covered by the macro cell. (see Fig. 3.7). There will be no coverage holes thanks to the presence of macro cell covering the overall area. We are making sure to avoid any coverage hole by selecting the appropriate system parameters. The reference small cell center (or BS) is located at distance d from the macro cell center.
In order to assess the impact of decoupling and other association policies on our HetNet system, we need to isolate

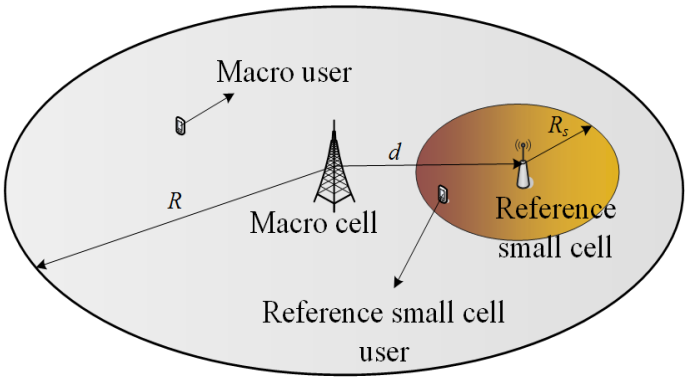

Figure 3.7: Geometrical illustration of the network model - without decoupling.

a specific area between the macro and the small cell that is called the expanded area. Users inside this expanded area can be either coupled or decoupled at a specific time t. They are located at a distance r_e from the center of the reference small cell where $R_s < r_e < R_e$ (see Fig. 3.8). Let the radius of the expanded area R_e, be a tunable variable and a new design parameter in our model. This new parameter is referred to, in our study, as the small cell offset factor.

Figure 3.8 depicts all distances involved in our model. We define in Table 3.1 the notations of these distances for which statistical expressions are derived in the next sections.

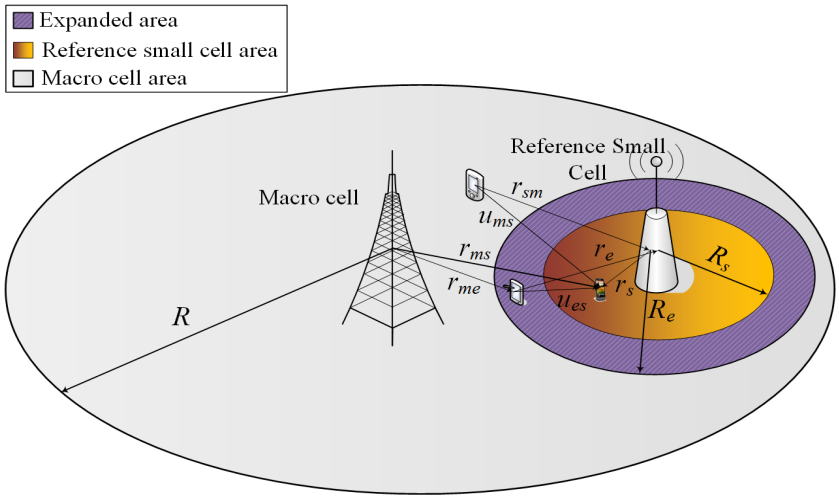

Figure 3.8: Geometrical illustration of the network model - with decoupling.

d	Distance between the reference small cell and the macro cell
R	Macro cell radius
R_e	Small cell offset factor
r_e	Distance of the user in the expanded area from the small cell BS
r_{me}	Distance of the user in the expanded area from the macro cell BS
r_{ms}	Distance of the small cell user from the macro cell BS
R_s	Small cell radius
r_s	Distance of the small cell user from the small cell BS
r_{sm}	Distance of the small cell BS from the macro user
u_{es}	Distance between the user in the expanded area and the small cell user
u_{ms}	Distance between the small cell user and the macro user

Table 3.1: Distances notations

3.2.2 Radio Model

In our HetNet system, the transmission power of the macro BS and the small cell BS is denoted by P_m and P_s respectively. The transmission power of the macro user and the small cell user is denoted by P_{um} and P_{us} respectively. We will use the variable P_t to generically designate the transmit power of either a base station or a mobile user.
We consider using the same RAT and the same frequency among the macro cell and the small cell. This will lead to an interference that occurs between these two tiers. This interference is called a cross-tier interference. In our model, we denote by I the interference experienced from the interfering source at the target receiver. In our case, the target receiver is either the reference small cell BS or the reference small cell user. Also, we denote by S the signal of interest or the desired signal received by the user or the BS inside the reference small cell. In uplink direction, S and I are measured at the BS level whereas in downlink direction, they are measured at the user level. Knowing the transmit power P_t, we are still in need of a propagation model in order to calculate both signals S and I at the receiver. For this purpose, we will use the same generic path-loss propagation model across macro and small cells. Hence, S and I or more generically the received signal power P_r at the receiver can be written as follows:

$$P_r = KL_0P_tl^{-\gamma}, \tag{3.1}$$

where K is the composite fading, L_0 the path-loss constant, γ the path-loss exponent and l is the length of the radio link between the transmitter and the receiver in meters. L_0 depends on the carrier frequency and the propagation environment.
Considering a suburban environment, the path-loss expression in dB can be written as follows [106] [107]:

$$PL(dB) = 122.08 + 20log_{10}f_c + 10\gamma log_{10}l, \tag{3.2}$$

where f_c is the carrier frequency in GHz and l is the length of the radio link between the transmitter and the receiver in kilometers. L_0 in (3.1) can be then retrieved by mapping (3.1) to (3.2) as follows:

$$PL(dB) = 10log_{10}L_0 - 10\gamma log_{10}l = -122.08 - 20log_{10}f_c - 10\gamma log_{10}\frac{l}{1000}, \tag{3.3}$$

where l is the length of the radio link between the transmitter and the receiver in meters.
Since the users are randomly distributed inside macro and small cells, we can conclude that l is a random variable. Accordingly and based on (3.1), S and I will be two random variables as well.

Moreover, considering the dynamic TDD technique in our HetNet system imposes the analysis of the four scenarios described previously in Section 3.1.1, and which are Down - Down, Up - Down, Down - Up and Up - Up scenarios. In our model, closed-form expressions for S and I will be derived in each of these scenarios.

Assumption 1. *In this model, the composite fading denoted by K is considered as a constant. It combines both the shadowing and the fast fading.*
Nonetheless, we have simulated exactly the same scenarios under random variable fading. A log-normal shadowing and an exponential distribution with parameter $\lambda = 1$ as an approximation of the Rayleigh fading, were considered. As a result, we obtained nearly the same throughput values in UL and DL and the same behavior as in the case of a constant composite fading; the impact of the decoupling in comparison with other association policies remained the same. Consequently, a constant fading was adopted in this model. In the next chapter, we will assess and show the impact of the variable fading under section 4.2.2.

Assumption 2. *In this model, we consider the interference (I) and the signal of interest (S) as two statistically independent random variables. To justify our assumption, we have statistically derived the correlation coefficient to measure the dependency between the two variables S and I. Referring to the path-loss formula in (3.1) and to the Assumption 1, we can conclude that S is a function of the reference small cell user position. In some rare cases, I might be indirectly a function of the same reference small cell user position. Accordingly, some cases show exactly a zero correlation, others show nearly zero values.*
In the next chapter, we will show under section 4.3.1 the correlation between S and I in order to validate our assumption.

3.2.3 Traffic Model

We consider uniformly distributed users in both macro and small cells. Hence, both the interference experienced from one single user inside each interfering cell and the signal of interest of one single user inside the reference small cell, must be statistically derived. In this case, the total system bandwidth will be allocated to that single user in each cell, whether a macro or a small cell. This full load assumption characterizes our system traffic model.

3.2.4 Performance Metrics

In this model, we study several network performance metrics based on the expressions derived for the interference and the signal of interest. We present hereafter the definition and the motivation of each of these metrics:

Spectrum Efficiency or Ergodic Capacity per Unit Bandwidth

Spectrum efficiency (in bps/Hz) refers to the maximum information rate that can be transmitted over a given bandwidth in a specific communication system. With the surge of data traffic and limited spectrum resources, a high spectrum efficiency is a mandatory requirement of next generation networks. In our model, we consider analyzing

the average spectral efficiency per user inside a specific reference cell. The spectral efficiency is evaluated in the case of one small cell (cf. Section 3.3 and Section 3.4) and multiple small cells (cf. Section 3.5). It is considered as well in the case of synchronized and unsynchronized TDD configuration between small cells. We denote by C_s the average user capacity in the small cell area and by C_e the average user capacity in the expanded area. C_{es} denotes the average user capacity in both the small cell area and the expanded area.

Power Consumption

Uplink power control is used in 3rd Generation Partner Project (3GPP) Long Term Evolution (LTE) and LTE-A systems [108] to mitigate uplink ICI and save the energy consumption of UE batteries. Hence, we add the uplink power control to the developed model under Section 3.5.7. This power control mechanism is based on the open-loop power control strategy standardized in 3GPP LTE [109]. Moreover, we define and evaluate the average reduction in UEs power consumption under the same section.

Decoupling Gain

The main purpose of introducing the decoupling gain metric is to highlight the benefits that the decoupling access mode can bring to a HetNet TDD based system, in terms of UL and DL throughput gains, mainly in a multiple small cells environment. Since the decoupling gain will be a function of both the distance between small cells and the small cell offset factor (R_e), this will help to identify the position of interfering small cells and choose the optimal offset factor for a higher decoupling gain. In this model, we evaluate the decoupling gain in the case of both synchronized and unsynchronized TDD configuration between small cells. The exact definition of the decoupling gain is given under [Section 3.5.9, Definition 1].

3.2.5 Terms, Notations & Summary of Model Variables

Terms Definitions

Specific terms used in this manuscript are defined and described in Table 3.2.

Term	Definition
Interfering source	User or BS that causes the interference
Target receiver	User or BS that receives the interference
Interfering link	Radio link between the interfering source and the target receiver
Interfering distance	Length of the interfering link

Table 3.2: Terms definitions

Mathematical Notations

Let Z be a random variable, the probability density function (PDF) of Z can be written as $f_Z(z)$. The cumulative distribution function (CDF) of Z is defined as a function mapped to the probability that Z is less than z: $F_Z(z) = P(Z \leq z) = \int_{-\infty}^{z} f_Z(t)dt$.
The moment generating function (MGF) of Z is defined as the integral of $f_Z(z)$: $M_Z(t) = \int_0^{\infty} e^{-tz} f_Z(z)dz$.
$A(a, b, R_c)$ is a circle with radius R_c and centered at a point having a as abscissa and b as ordinate.

Summary of Model Variables

The below Table 3.3 summarizes all the model variables defined so far:

Variable	Description	Random Variable
γ	Path-loss exponent	
C_e	Average user capacity in the expanded area	
C_{es}	Average user capacity in both the expanded area and the small cell area	
C_s	Average user capacity in the small cell area	
d	Distance between the reference small cell and the macro cell	
f_c	Carrier frequency	
I	Interference signal at the target receiver	✓
K	Composite fading	
K_c	Defined constant	
L_0	Path-loss constant	
P_m	Macro BS transmission power	
P_r	Received signal power	
P_s	Small cell BS transmission power	
P_t	Transmit power	
P_{um}	Macro user transmission power	
P_{us}	Small cell user transmission power	
R	Macro cell radius	
R_e	Small cell offset factor	
r_e	Distance of the user in the expanded area from the small cell BS	✓
r_{me}	Distance of the user in the expanded area from the macro cell BS	✓
r_{ms}	Distance of the small cell user from the macro cell BS	✓
R_s	Small cell radius	
r_s	Distance of the small cell user from the small cell BS	✓
r_{sm}	Distance of the small cell BS from the macro user	✓
S	Signal of interest or desired signal at the target receiver	✓
u_{es}	Distance between the user in the expanded area and the small cell user	✓
u_{ms}	Distance between the small cell user and the macro user	✓

Table 3.3: Model variables summary

3.3 Ergodic Capacity in TDD 5G HetNets - Single Small Cell Scenario

In this section, an analytical framework is developed to evaluate the performance of a TDD system in heterogeneous networks which considers a concurrent uplink and downlink transmission in two different types of cells, macro and small cells.
Referring to our model diagram (Fig. 3.6) and in order to compute the average user capacity, we need to apply a specific lemma that requires having the MGF of S and the MGF of I. However and in order to retrieve the MGFs, we require first deriving probabilistic/statistical expressions for S and I. Both S and I expressions can be derived using the path-loss formula in (3.1). Since the composite fading K is considered as constant according to Assumption 1, the only random variable parameter that will be impacting S and I is the distance l between the transmitter and the receiver. In order to find the probability distribution of S, we need to derive the probability distribution of the distance between the reference small cell user and the small cell BS. It depends on the position of the reference small cell user, whether uplink or downlink direction is considered. In order to find the probability distribution of I, we have to derive the probability distribution of the length of the interfering link, i.e. the distance between the interfering source and the target receiver.

In this section, we will show how statistical expressions for both the reference user position and the interfering link length can be derived using the proposed geometric approach.

3.3.1 Signal of Interest Modeling

A. Downlink Direction

The signal power received by a randomly selected user at the reference small cell on a downlink channel is defined using equation (3.1) with $P_t = P_s$ the transmit power and $l = r_s$ the reference user position. Consequently, S can be written as follows:

$$S = KL_0P_sr_s^{-\gamma}, \tag{3.4}$$

Since we consider uniformly distributed users, the distribution of the distance r_s of a small cell user will be following the distribution of a random point inside a disk of radius R_s:

$$f_{r_s}(r) = \frac{2r}{R_s^2}, \quad 0 \leq r \leq R_s, \tag{3.5}$$

According to Assumption 1, K is considered as constant. Consequently, the CDF of S can be formulated as:

$$F_S(s) = P(S \leq s) = P(KL_0P_sr_s^{-\gamma} \leq s) = P(r_s^{-\gamma} \leq \frac{s}{KL_0P_s}) = P\Big(r_s \leq (\frac{s}{KL_0P_s})^{-\frac{1}{\gamma}}\Big) = 1 - F_{r_s}\Big((\frac{s}{K_c})^{-\frac{1}{\gamma}}\Big), \tag{3.6}$$

where $K_c = KL_0P_s$ and $F_{r_s}(r)$ is the CDF of r_s.

Applying the chain rule [111], the PDF of the received signal S can be formulated as:

$$f_S(s) = \frac{1}{s\gamma} f_{r_s}\Big((\frac{s}{K_c})^{-\frac{1}{\gamma}}\Big)(\frac{s}{K_c})^{\frac{-1}{\gamma}}. \tag{3.7}$$

By replacing (3.5) in (3.7), the PDF of S can be written as:

$$f_S(s) = \beta s^{-(\frac{2+\gamma}{\gamma})}, \tag{3.8}$$

where $\beta = \frac{2K_c^{\frac{2}{\gamma}}}{\gamma R_s^2}$.

Consequently, the MGF of S can be given as:

$$M_S(t) = \mathbb{E}[e^{(-tS)}] = \int_0^\infty e^{-ts} f_S(s) ds. \tag{3.9}$$

$$M_S(t) = \int_a^\infty \beta s^{-(\frac{2+\gamma}{\gamma})} e^{-ts} ds, \tag{3.10}$$

where $a = K_cR_s^{-\gamma}$.

B. Uplink Direction

When the small cell is operating in uplink mode, the signal power received at the reference small cell on an uplink channel from a randomly selected user is defined using equation (3.1) with $P_t = P_{us}$ and $l = r_s$. Same formulas are applied to the PDF and MGF of the signal of interest while changing the constant K_c to $K_c = KL_0P_{us}$.

3.3.2 Interference Modeling

In order to characterize the statistics of each interference scenario that could occur in TDD-based HetNets, the proposed framework analyzes in details both the downlink and uplink interferences (see Fig. 3.9). This will require considering the four interference scenarios described previously: Down - Down, Up - Down, Down - Up and Up -

Up.
In each scenario, the distance between the interfering source and the target receiver has a different probability distribution. Accordingly, a new probability distribution of I will be derived in each scenario. For example, in Down - Down scenario, the interfering source (macro BS) position is fixed whereas the target receiver (small cell user) position is changing. However, in Up - Down scenario, both interfering source (macro user) and target receiver (small cell user) positions are changing.

Figure 3.9: Four interference scenarios.

Based on the path-loss formula in (3.1), I can be written as $I = KL_0P_tl^{-\gamma}$ where l is the interfering distance. The value of P_t and the distance variable representing l depend on the interference scenario.
According to Assumption 1, K is considered as constant. Consequently, the CDF of interference I can be formulated similarly to (3.6):

$$F_I(i) = 1 - F_l\Big((\frac{i}{K_c})^{-\frac{1}{\gamma}}\Big), \tag{3.11}$$

where $K_c = KL_0P_t$ and $F_l(r)$ is the CDF of l.
Applying the chain rule, the PDF of I can be written as:

$$f_I(i) = \frac{1}{i\gamma} f_l\Big((\frac{i}{K_c})^{-\frac{1}{\gamma}}\Big)(\frac{i}{K_c})^{\frac{-1}{\gamma}}. \tag{3.12}$$

Consequently, a closed-form expression for the MGF of I can be derived based on (3.12) as follows:

$$M_I(t) = \int_0^\infty e^{-ti} f_I(i)di. \tag{3.13}$$

From (3.12), we see that the statistical distribution of I can be obtained based on the distribution of the interfering distance. Accordingly and in order to obtain closed-form expressions for I, we will derive in this section the probability distribution of the interfering distance ($f_l(r)$) in each interference scenario, based on the proposed geometric approach.

A. Down - Down mode

In this mode, since both macro and small cells are operating in downlink, the macro BS is the source of the interference suffered by the small cell user. Therefore, on the interfering link between these two entities, $P_t = P_m$ and $l = r_{ms}$ and the received interference signal can be written as $I = KL_0P_mr_{ms}^{-\gamma}$.
In order to find the probability distribution of r_{ms}, we will start by deriving its CDF.
By definition, the CDF of r_{ms} can be written as follows:

$$F_{r_{ms}}(r) = P(r_{ms} \leq r). \tag{3.14}$$

Geometric approach:

$P(r_{ms} \leq r)$ can be seen as the percentage of small cell users located at distance $r_{ms} \leq r$ from the macro BS, out of all the small cell users distributed inside the small cell area (see Fig. 3.10). Since the users are uniformly distributed inside this cell, the probability of locating a small user at distance $r_{ms} \leq r$ is equal to the probability that this same user is inside the intersection area of two circles: a circle centered at the macro BS with radius r and a

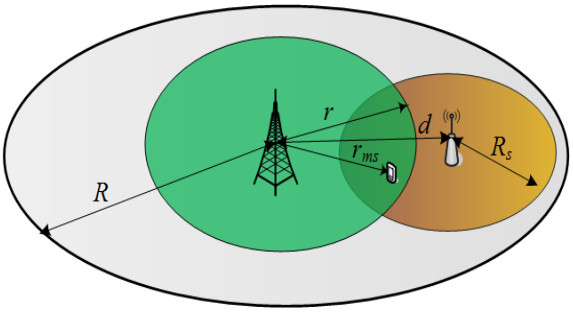

Figure 3.10: Down - Down mode.

circle centered at the small cell BS with radius R_s. Note that in this case, the distance between the circles' centers is d with $d > R_s$.
In order to calculate this cell intersection based on a geometric approach, we will adopt a Cartesian coordinate system having the macro BS as origin (see Fig. 3.11). As shown in Fig. 3.11, we define $A_{r_{ms}}$ as the intersection

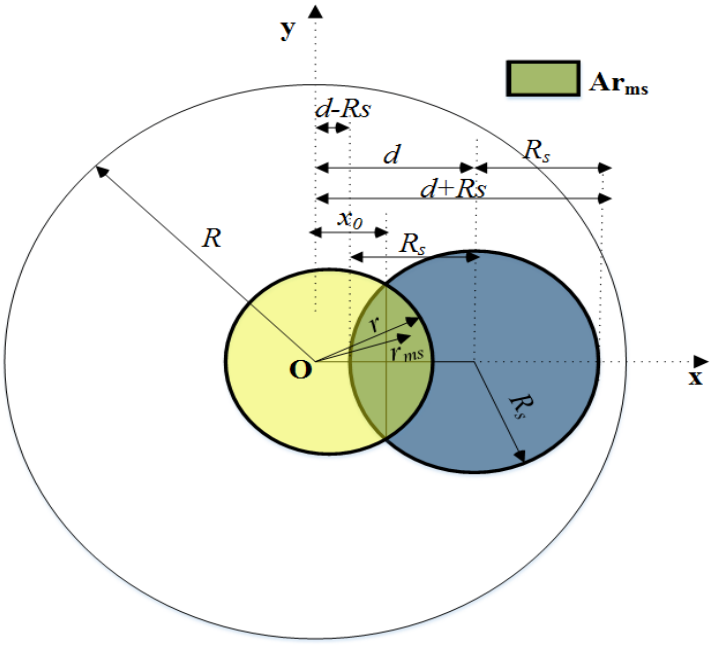

Figure 3.11: Down - Down geometric presentation.

area of the two circles $A(0,0,r)$ with radius r and $A(d,0,R_s)$ with radius R_s.
Consequently, $P(r_{ms} \leq r)$ can be written as follows:

$$F_{r_{ms}}(r) = P(r_{ms} \leq r) = \frac{A_{r_{ms}}}{\text{Small cell area}} = \frac{A_{r_{ms}}}{\pi R_s^2}, \tag{3.15}$$

$$F_{r_{ms}}(r) = \begin{cases} \frac{A_{r_{ms}}}{\pi R_s^2} = \frac{0}{\pi R_s^2} = 0, & r < d - R_s \\ \frac{A_{r_{ms}}}{\pi R_s^2}, & d - R_s \leq r \leq d + R_s \\ \frac{A_{r_{ms}}}{\pi R_s^2} = \frac{\pi R_s^2}{\pi R_s^2} = 1, & r > d + R_s. \end{cases} \tag{3.16}$$

We denote by x_0 the distance between the origin and the segment formed by the intersection point of the two circles i.e., it is the abscissa of the intersection points. The equations of the two intersected circles can be written as:

$$x^2 + y^2 = r^2 \tag{3.17}$$

$$(x - d)^2 + y^2 = R_s^2 \tag{3.18}$$

At the intersection points of abscissa x_0, (3.17) and (3.18) are equal, which gives:

$$(x_0 - d)^2 + (r^2 - x_0^2) = R_s^2. \tag{3.19}$$

Multiplying through and rearranging gives:

$$x_0^2 - 2dx_0 + d^2 - x_0^2 = R_s^2 - r^2. \tag{3.20}$$

Solving for x_0 results in:

$$x_0 = \frac{d^2 - R_s^2 + r^2}{2d}. \tag{3.21}$$

From another side, since $A_{r_{ms}}$ is the sum of areas under the two circles, integrals can be used to calculate it as follows (see Fig. 3.11):

$$A_{r_{ms}} = 2\int_{d-R_s}^{x_0} \sqrt{(R_s^2 - (d-x)^2)}dx + 2\int_{x_0}^{r} \sqrt{(r^2 - x^2)}dx. \tag{3.22}$$

After replacing x_0 by its value from (3.21), solving the integrals of (3.22) yields to:

$$A_{r_{ms}} = \frac{\pi}{2}(r^2 + R_s^2) - r^2 \arcsin(\frac{d^2 + r^2 - R_s^2}{2dr}) + R_s^2 \arcsin(\frac{r^2 - d^2 - R_s^2}{2dR_s}) - 1/2\sqrt{(r^2 - (d-R_s)^2)((d+R_s)^2 - r^2)} \tag{3.23}$$

$$A_{r_{ms}} = R_s^2 \arccos(\frac{d^2 + R_s^2 - r^2}{2dR_s}) + r^2 \arccos(\frac{d^2 + r^2 - R_s^2}{2dr}) - 1/2\sqrt{4d^2r^2 - (d^2 - R_s^2 + r^2)^2}. \tag{3.24}$$

The CDF of r_{ms} can now be obtained by substituting (3.24) in (3.16):

$$F_{r_{ms}}(r) = \begin{cases} 0, & r < d - R_s \\ \frac{R_s^2 \arccos(\frac{d^2+R_s^2-r^2}{2dR_s}) + r^2 \arccos(\frac{d^2+r^2-R_s^2}{2dr})}{\pi R_s^2} - \frac{1/2\sqrt{4d^2r^2-(d^2-R_s^2+r^2)^2}}{\pi R_s^2}, & d - R_s \leq r \leq d + R_s \\ 1, & r > d + R_s. \end{cases} \tag{3.25}$$

The PDF is obtained by deriving (3.25) as a function of distance r:

$$f_{r_{ms}}(r) = \begin{cases} 0, & r < d - R_s \\ \frac{1}{\pi R_s^2}(\pi r - 2r \arcsin(\frac{d^2+r^2-R_s^2}{2dr})), & d - R_s \leq r \leq d + R_s \\ 0, & r > d + R_s. \end{cases} \tag{3.26}$$

$$\boxed{f_{r_{ms}}(r) = \begin{cases} \frac{1}{\pi R_s^2}(\pi r - 2r \arcsin(\frac{d^2+r^2-R_s^2}{2dr})), & d - R_s \leq r \leq d + R_s \\ 0, & elsewhere. \end{cases}} \tag{3.27}$$

N.B. The obtained result in (3.27) will be frequently used in our model to derive PDF expressions for distances other than r_{ms}. It can be generalized to any circular cell of radius R_s intersecting with a circle of radius r, with a distance d between the centers of the two circles.

B. Up - Up mode

In this mode, since both macro and small cells are operating in uplink, the macro user is the source of the interference suffered by the small cell BS. Therefore, on the interfering link between these two entities, $P_t = P_{um}$ and $l = r_{sm}$, and the received interference signal can be written as $I = KL_0P_{um}r_{sm}^{-\gamma}$. As in the down-down, we will use a geometric approach to derive the CDF and the PDF of r_{sm}.

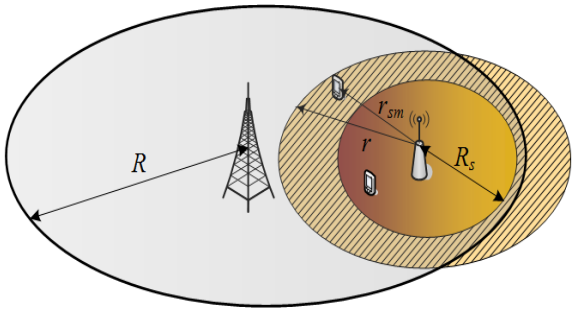

Figure 3.12: Up - Up mode.

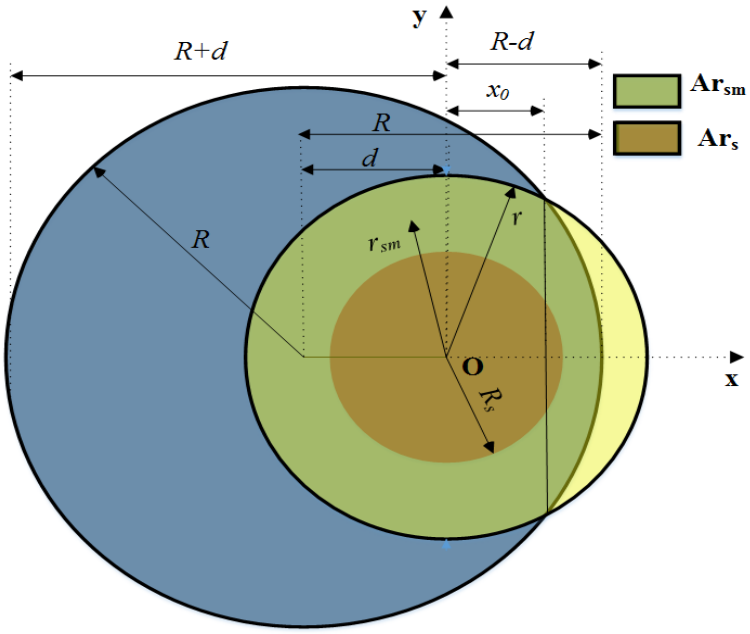

Figure 3.13: Up - Up geometric presentation with $r > R - d$.

Geometric approach:

$P(r_{sm} \leq r)$ is the probability of finding the interfering macro user at a distance less then r from the small cell BS. We denote by $A_{r_{sm}}$ the area around the small cell where the macro user location verifies $r_{sm} < r$. Knowing that the macro user can be anywhere in the macro cell area, excluding the small cell area, we can write:

$$F_{r_{sm}}(r) = P(r_{sm} \leq r) = \frac{A_{r_{sm}}}{\text{Macro cell area} - \text{Small cell area}}. \tag{3.28}$$

In order to calculate the $A_{r_{sm}}$ area, we will use a Cartesian coordinate system having the small cell BS as origin. We consider the circle $A(0, 0, r)$ which is a circle of radius r whose center is the small cell BS and the circle $A(-d, 0, R)$ which is the macro cell circle. If we denote by A_{int} the intersection area of these two circles, we notice that $A_{int} = A_{r_{sm}} + \text{Small cell area}$ with $A_{r_s} = \text{Small cell area}$ (see Fig. 3.13). Hence, $A_{r_{sm}} = A_{int} - \pi R_s^2$ and the CDF of r_{sm} becomes:

$$F_{r_{sm}}(r) = P(r_{sm} \leq r) = \frac{A_{int} - \pi R_s^2}{\pi R^2 - \pi R_s^2}, \tag{3.29}$$

which can be calculated, thanks to A_{int}, using a circle intersection approach.
Note that the distance between the circles' centers is d with $d < R$. This means that the centers of the two intersected circles are both inside the same circle $A(-d, 0, R)$ with radius R.

Two cases are considered for the calculation of A_{int}:

1. $r > R - d$

   In this case, a part of the circle $A(0, 0, r)$ is outside the macro cell area (see Fig. 3.13). Let x_0 denote the distance between the origin and the intersection points of the two circles $A(0, 0, r)$ and $A(-d, 0, R)$. The equations of these two circles can be written as:

$$x^2 + y^2 = r^2 \tag{3.30}$$

$$(x + d)^2 + y^2 = R^2 \tag{3.31}$$

   At the intersection points of abscissa x_0, (3.30) and (3.31) are equal, which gives:

$$(x_0 + d)^2 + (r^2 - x_0^2) = R^2. \tag{3.32}$$

   Multiplying through and rearranging gives:

$$x_0^2 + 2dx_0 + d^2 - x_0^2 = R^2 - r^2. \tag{3.33}$$

   Solving for x_0 results in:

$$-x_0 = \frac{d^2 - R^2 + r^2}{2d}. \tag{3.34}$$

   From another side, since A_{int} is the sum of areas under the two circles, integrals can be used to calculate it as follows:

$$A_{int} = 2\int_{x_0}^{R-d} \sqrt{(R^2 - (d + x)^2)}dx + 2\int_{-r}^{x_0} \sqrt{(r^2 - x^2)}dx. \tag{3.35}$$

   After replacing x_0 by its value from (3.34), solving the integrals of (3.35) yields to:

$$A_{int} = R^2 \arccos(\frac{d^2 + R^2 - r^2}{2dR}) + r^2 \arccos(\frac{d^2 + r^2 - R^2}{2dr}) - 1/2\sqrt{4d^2r^2 - (d^2 - R^2 + r^2)^2}. \tag{3.36}$$

   Therefore, substituting (3.36) in (3.28) yields to:

$$F_{r_{sm}}(r) = \frac{R^2 \arccos(\frac{d^2+R^2-r^2}{2dR}) + r^2 \arccos(\frac{d^2+r^2-R^2}{2dr})}{\pi R^2 - \pi R_s^2} - \frac{1/2\sqrt{4d^2r^2 - (d^2 - R^2 + r^2)^2}}{\pi R^2 - \pi R_s^2} - \frac{\pi R_s^2}{\pi R^2 - \pi R_s^2} \tag{3.37}$$

   The PDF is obtained by deriving (3.37) as a function of distance r:

$$f_{r_{sm}}(r) = \frac{1}{\pi R^2 - \pi R_s^2}(\pi r - 2r \arcsin(\frac{d^2 + r^2 - R^2}{2dr})). \tag{3.38}$$

2. $r < R - d$

   In this case, the circle $A(0, 0, r)$ is entirely inside the macro cell area (see Fig. 3.14) and A_{int} is simply :

$$A_{int} = \pi r^2. \tag{3.39}$$

   Therefore, substituting (3.39) in (3.28) yields to:

$$F_{r_{sm}}(r) = \frac{\pi r^2 - \pi R_s^2}{\pi R^2 - \pi R_s^2}. \tag{3.40}$$

   The PDF is obtained by deriving (3.40) as a function of distance r:

$$f_{r_{sm}}(r) = \frac{2\pi r}{\pi R^2 - \pi R_s^2}. \tag{3.41}$$

Adding both cases, the PDF of r_{sm} can be written as follows:

$$f_{r_{sm}}(r) = \begin{cases} \frac{1}{\pi R^2 - \pi R_s^2}(2\pi r), & R_s \leq r < R - d \\ \frac{1}{\pi R^2 - \pi R_s^2}(\pi r - 2r \arcsin(\frac{d^2+r^2-R^2}{2dr})), & R - d \leq r \leq R + d \\ 0, & elsewhere. \end{cases} \tag{3.42}$$

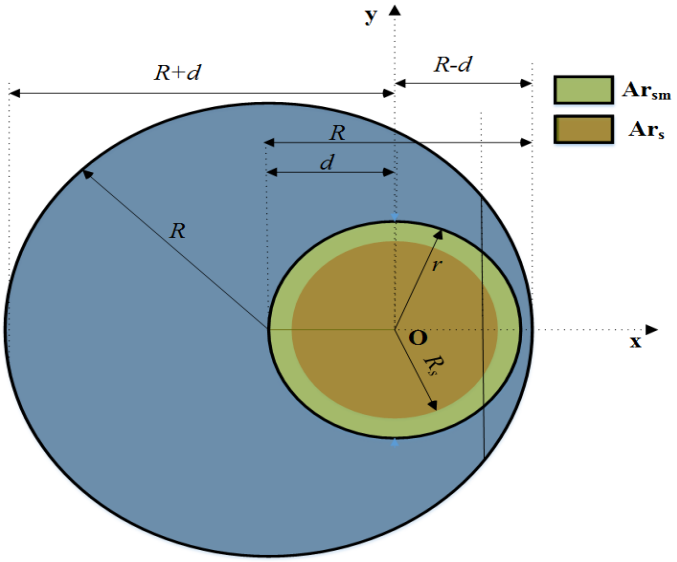

Figure 3.14: Up - Up geometric presentation with $r < R - d$.

C. Up - Down mode

In this mode, the macro cell is operating in uplink while the small cell is in downlink mode. The macro user is generating interference at the small cell user. Therefore, on the interfering link between these two users, $P_t = P_{um}$ and $l = u_{ms}$ and the received interference signal can be written as $I = KL_0P_{um}u_{ms}^{-\gamma}$. Note that in this case, transmitter and receiver of the interfering link have variable positions.

In order to compute the CDF of the interfering distance u_{ms} we will need to jointly consider the random vari-

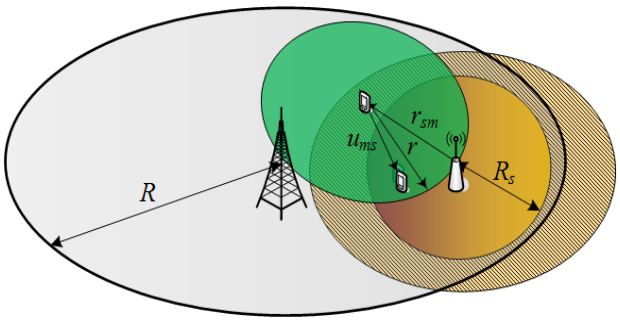

Figure 3.15: Up - Down mode.

able r_{sm} (distance between the macro user and the small cell BS). Let us denote by $f_{u_{ms},r_{sm}}$ the joint pdf of u_{ms} and r_{sm}, and by $f_{u_{ms}|r_{sm}}$ the conditional pdf of u_{ms} given r_{sm}.

Using marginal and conditional distributions mathematical definitions, the CDF of u_{ms} is derived as follows:

$$F_{u_{ms}}(r) = P(u_{ms} \leq r) = \int_{-\infty}^{r} f_{u_{ms}}(x)dx = \int_{-\infty}^{r} \Big[\int_{-\infty}^{+\infty} f_{u_{ms},r_{sm}}(x,y)dy\Big]dx = \int_{-\infty}^{r} \Big[\int_{-\infty}^{+\infty} f_{u_{ms}|r_{sm}=y}(x)f_{r_{sm}}(y)dy\Big]dx$$

Since the densities are non-negative measurable functions, Fubini–Tonelli theorem can be applied in order to switch the order of integration yielding to:

$$F_{u_{ms}}(r) = \int_{-\infty}^{+\infty} \Big[\int_{-\infty}^{r} f_{u_{ms}|r_{sm}=y}(x)dx\Big]f_{r_{sm}}(y)dy$$

The term $\int_{-\infty}^{r} f_{u_{ms}|r_{sm}=y}(x)dx$ is the conditional CDF of u_{ms} , denoted by $F_{u_{ms}|r_{sm}}$, obtained by fixing the distance r_{sm} between the macro user and small cell BS. The CDF of u_{ms} can then be rewritten as:

$$F_{u_{ms}}(r) = \int_{-\infty}^{+\infty} F_{u_{ms}|r_{sm}}(r) f_{r_{sm}}(y)dy, \qquad 0 \leq r \leq R + d + R_s. \tag{3.43}$$

The pdf of r_{sm} ($f_{r_{sm}}$) has already been calculated in the Up-Up scenario. Hence, from (3.42) we have:

$$f_{r_{sm}}(r_{sm}) = \begin{cases} \frac{1}{\pi R^2 - \pi R_s^2}(2\pi r_{sm}), & R_s \leq r_{sm} < R - d \\ \frac{1}{\pi R^2 - \pi R_s^2}(\pi r_{sm} - 2r_{sm} \arcsin(\frac{d^2 + r_{sm}^2 - R^2}{2dr_{sm}})), & R - d \leq r_{sm} \leq R + d. \end{cases} \tag{3.44}$$

N.B. The reader would have noticed the abuse of notation in (3.44) regarding the use of the symbol r_{sm}. In fact, in $f_{r_{sm}}(r_{sm})$, the subscript r_{sm} designates, as it should be, the random variable, while in the argument, it designate a value of r_{sm}. We think that this makes the formulas easier to read.

Given a fixed value of r_{sm}, calculating $F_{u_{ms}|r_{sm}}$ is geometrically similar to the Down-Down scenario where the macro cell is replaced with the macro user. Therefore, (3.25) can be used after replacing d with r_{sm}.

$$F_{u_{ms}|r_{sm}}(r) = \begin{cases} 0, & r < r_{sm} - R_s \\ \frac{R_s^2 \arccos(\frac{r_{sm}^2 + R_s^2 - r^2}{2r_{sm}R_s}) + r^2 \arccos(\frac{r_{sm}^2 + r^2 - R_s^2}{2r_{sm}r})}{\pi R_s^2} - \frac{1/2\sqrt{4r_{sm}^2 r^2 - (r_{sm}^2 - R_s^2 + r^2)^2}}{\pi R_s^2}., & r - R_s \leq r_{sm} \leq r + R_s \\ 1, & r > r_{sm} + R_s. \end{cases} \tag{3.45}$$

In this context, $F_{u_{ms}}(r)$ can be derived from (3.43), (3.44) and (3.45) as follows:

$$F_{u_{ms}}(r) = 0P(r_{sm} > r + R_s) + 1P(r_{sm} < r - R_s) + \int_{r-R_s}^{r+R_s} F_{u_{ms}|r_{sm}}(r) f_{r_{sm}}(r_{sm})dr_{sm},$$

$$F_{u_{ms}}(r) = F_{r_{sm}}(r - R_s) + \int_{r-R_s}^{r+R_s} F_{u_{ms}|r_{sm}}(r) f_{r_{sm}}(r_{sm})dr_{sm}, \tag{3.46}$$

given that the lowest and the highest values of r_{sm} are respectively R_s and $R + d$.

The same logic applies for the PDF:

$$f_{u_{ms}}(r) = \int_{r-R_s}^{r+R_s} f_{u_{ms}|r_{sm}}(r) f_{r_{sm}}(r_{sm})dr_{sm}, \qquad 0 \leq r \leq R + d + R_s, \tag{3.47}$$

where $f_{u_{ms}|r_{sm}}(r) = \frac{1}{\pi R_s^2}(\pi r - 2r \arcsin(\frac{r_{sm}^2 + r^2 - R_s^2}{2r_{sm}r}))$ and $f_{r_{sm}}(r_{sm})$ as follows:

$$f_{r_{sm}}(r_{sm}) = \begin{cases} \frac{1}{\pi R^2 - \pi R_s^2}(2\pi r_{sm}), & R_s \leq r_{sm} < R - d \\ \frac{1}{\pi R^2 - \pi R_s^2}(\pi r_{sm} - 2r_{sm} \arcsin(\frac{d^2 + r_{sm}^2 - R^2}{2dr_{sm}})), & R - d \leq r_{sm} \leq R + d. \end{cases} \tag{3.48}$$

D. Down - Up mode

In this mode, the macro cell is operating in downlink while the small cell is in uplink mode. The macro BS is generating interference at the small cell BS. Therefore, on the interfering link between these two entities, $P_t = P_m$ and $l = d$ and the received interference signal can be written as $I = KL_0P_m d^{-\gamma}$. Note that in this case, transmitter and receiver of the interfering link have fixed positions.
In this case, I is a constant. Accordingly, the MGF of I will be defined as:

$$\boxed{M_I(t) = \mathbb{E}[e^{(-tI)}] = e^{-tI_c}} \tag{3.49}$$

where $I_c = KL_0P_m d^{-\gamma}$ (see Fig. 3.16 for illustration).

Table 3.4 summarizes different interfering distance distribution of each interference scenario.

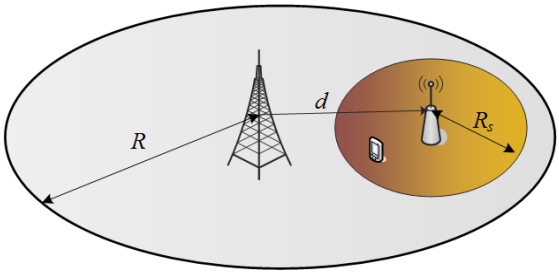

Figure 3.16: Down - Up mode.

Macro	Small cell	Scenario	Interfering Distance Distribution
Down	Down	BS-MS	$f_{r_{ms}}(r) = \frac{1}{\pi R_s^2}(\pi r - 2r\arcsin(\frac{d^2+r^2-R_s^2}{2dr})), \qquad d - R_s \leq r \leq d + R_s$
Up	Up	MS-BS	$f_{r_{sm}}(r) = \begin{cases} \frac{1}{\pi R^2 - \pi R_s^2}(2\pi r), & R_s \leq r < R - d \\ \frac{1}{\pi R^2 - \pi R_s^2}(\pi r - 2r\arcsin(\frac{d^2+r^2-R^2}{2dr})), & R - d \leq r \leq R + d \end{cases}$
Up	Down	MS-MS	$f_{u_{ms}}(r) = \int_{r-R_s}^{r+R_s} f_{u_{ms}\|r_{sm}}(r) f_{r_{sm}}(r_{sm}) dr_{sm}, \qquad 0 \leq r \leq R + d + R_s,$ $f_{u_{ms}\|r_{sm}}(r) = \frac{1}{\pi R_s^2}(\pi r - 2r\arcsin(\frac{r_{sm}^2 + r^2 - R_s^2}{2r_{sm}r}))$ $f_{r_{sm}}(r_{sm}) = \begin{cases} \frac{1}{\pi R^2 - \pi R_s^2}(2\pi r_{sm}), & R_s \leq r_{sm} < R - d \\ \frac{1}{\pi R^2 - \pi R_s^2}(\pi r_{sm} - 2r_{sm}\arcsin(\frac{d^2+r_{sm}^2-R^2}{2dr_{sm}})), & R - d \leq r_{sm} \leq R + d \end{cases}$
Down	Up	BS-BS	$d = constant$

Table 3.4: Summary of interfering distances distributions.

3.3.3 Capacity Analysis in Single Small Cell Scenario

The average user capacity per unit bandwidth i.e. the spectral efficiency at the reference small cell, is defined as the achievable average rate of the link to the allocated bandwidth (B), expressed mathematically by the modified Shannon's formula as:

$$C_s = \mathbb{E}\Big[\frac{B\ln(1+\frac{S}{I+\sigma^2})}{B}\Big] = \mathbb{E}\Big[\ln(1+\frac{S}{I+\sigma^2})\Big], \tag{3.50}$$

with σ^2 the thermal noise power variance.

The latter can be calculated using the lemma proposed in [112] as follows:

$$C_s = \mathbb{E}[\ln(1+\frac{S}{I+\sigma^2})] = \int_0^\infty \frac{M_I(t) - M_S(t)M_I(t)}{t} e^{-(\sigma^2)t} dt = \int_0^\infty \frac{M_I(t) - M_S(t)M_I(t)}{te^{-at}} e^{-(\sigma^2+a)t} dt, \tag{3.51}$$

where S and I are considered independent for all cases. In this work, the a parameter was introduced to resolve the scaling problem in Laguerre polynomial, more specifically in the $M(t)$ expression.
This expression can be solved efficiently by expressing it in terms of the weights w_e and abscissas x_e of the Laguerre orthogonal polynomial [113]. The Laguerre orthogonal polynomial formula can be expressed as follows:

$$\int_0^{\infty} f(x)e^{-x}dx \simeq \sum_{e=1}^{n} w_e f(x_e), \tag{3.52}$$

where the weights w_e and abscissas x_e can be obtained from the tables provided in [114].

Therefore, mapping (3.51) to(3.52) with a change in variables, yields to:

$$\boxed{C_s = \sum_{e=1}^{n} w_e \Big(\frac{M_I(x_e/(\sigma^2+a))}{x_e e^{-(ax_e)/(\sigma^2+a)}} - \frac{M_S(x_e/(\sigma^2+a))M_I(x_e/(\sigma^2+a))}{x_e e^{-(ax_e)/(\sigma^2+a)}} \Big).} \tag{3.53}$$

Note that this formula has been generalized under Section3.5.6 to include the multiple small cells scenario.

3.4 Modeling TDD 5G HetNets with Decoupling - Single Small Cell Scenario

In this section, we analytically investigate a joint TDD and DeUD statistical model based on a geometric probability approach, considering a network consisting of one macro cell and one small cell. This section complements the previous work by modeling the decoupling technique on top of the TDD HetNet model developed in Section 3.3. Taking all possible TDD subframes combinations between the macro and small cells, four coupled and decoupled cell associations strategies for users in the expanded area are investigated in details.
A good assessment of DeUD requires a thorough comparison study with the conventional coupled UL/DL access (CoUD) mode. For further analysis and to ensure the generality of our study, we investigate the CoUD scenario by taking into account two cases:

1) Users in the expanded area are coupled in UL and DL with macro cell.

2) Users in the expanded area are coupled in UL and DL with small cell, i.e. it represents the CRE scenario.

Two cases, as well, can be part of the DeUD mode:

1) Forward decoupling where users in the expanded area are associated in UL to the small cell and in DL to the macro cell. In the remaining, this case will be called simply "decoupling" instead of "forward decoupling".

2) Reverse Decoupling, where users in the expanded area are associated in UL to the macro cell and in DL to the small cell.

As mentioned previously, each adopted association policy will have direct impact on the users in the expanded area and on the users inside the reference small cell as well. Hence, average capacity for both small cell users and expanded area users must be evaluated in this case. This will require the derivation of closed form expressions for the signal of interest and interference that occur at both the expanded area and the reference small cell area.
The above mentioned variables of interest are summarized in the Table 3.5 that complements the Table 3.3.

In order to cover all possible UL/DL TDD combinations, we will analyze in this section the four TDD scenarios for each association policy (see Fig. 3.17). In each scenario, closed form expressions for the pdf of I_e, S_e, I_s and S_s will be derived. The full ergodic capacity analysis will be completed in the next section. Note that the same ergodic capacity formula will be used to calculate both C_s and C_e.

Variable	Description
C_e	Average user capacity in the expanded area
C_{es}	Average user capacity in both the expanded area and the reference small cell area
C_s	Average user capacity in the reference small cell area
I_e	Interference signal at the expanded area
I_s	Interference signal at the reference small cell area
S_e	Signal of interest at the expanded area
S_s	Signal of interest at the reference small cell area

Table 3.5: Complementary model variables for the joint TDD/Decoupling single small cell model

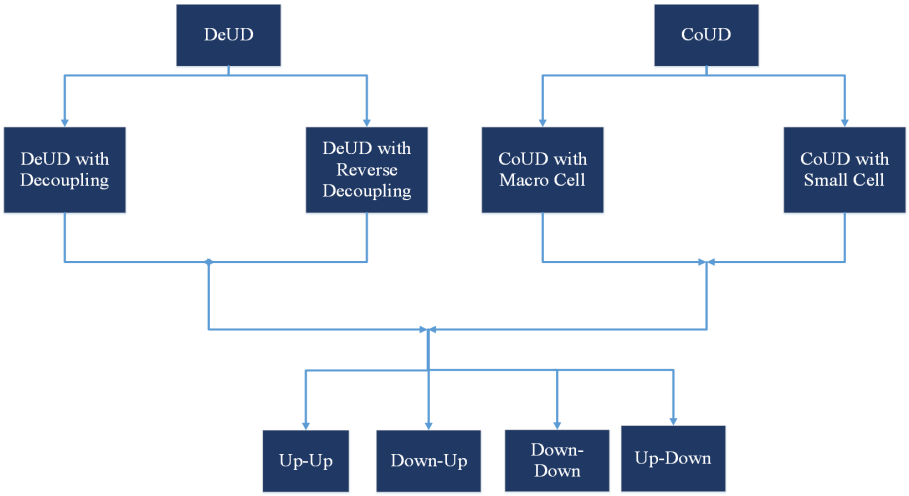

Figure 3.17: All possible TDD/CoUD/DeUD scenarios

3.4.1 Capacity Analysis with CoUD

In this section, we will consider the users in the extended area associated in UL and DL with a single cell. Two cases are considered, users in this area are either coupled to the macro cell or to the small cell.

CoUD with Macro Cell

This is the default case where users in the expanded area are associated to the macro cell without any special coupling or decoupling strategy (see Fig. 3.18). All the subsequent coupling and decoupling strategies will be compared to this reference scenario.

In each of the below possible UL/DL combinations, we derive the statistics of users in both expanded area and small cell.

A. Down - Down Scenario

The downlink interference I_e is experienced from the small cell BS at the mobile user in the expanded area. On this link, $P_t = P_s$ and $l = r_e$.

Since we consider uniformly distributed users, the CDF of the distance r_e of users in the expanded area bounded between R_s and R_e is given by:

$$F_{r_e}(r) = \frac{\pi r^2 - \pi R_s^2}{\pi R_e^2 - \pi R_s^2}, \quad R_s \leq r \leq R_e. \tag{3.54}$$

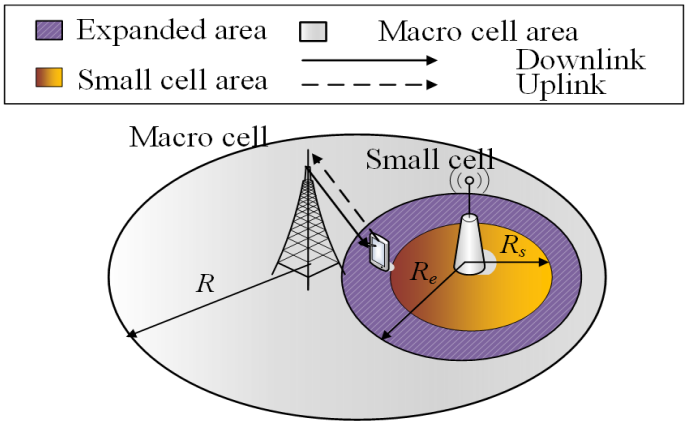

Figure 3.18: CoUD with macro cell illustration

Consequently, the PDF of r_e is given by:

$$f_{r_e}(r) = \frac{2r}{R_e^2 - R_s^2}, \quad R_s \leq r \leq R_e. \tag{3.55}$$

The signal of interest S_e of the mobile user in the expanded area is defined on a link having $P_t = P_m$ and $l = r_{me}$.

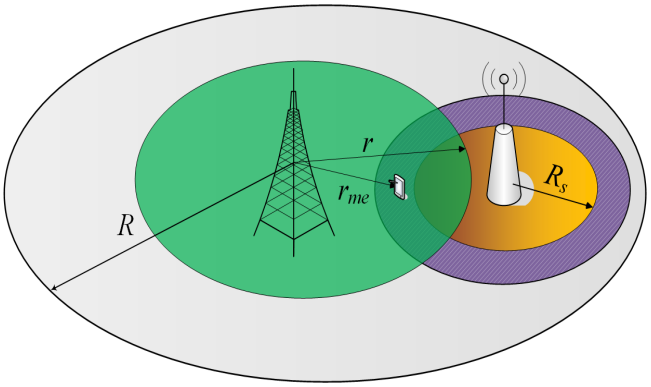

Figure 3.19: Illustration of r_{me} distance.

Three cases are considered to derive the PDF of r_{me} (see Fig. 3.19 for illustration):

1. $d - R_e \leq r \leq d - R_s$

   The CDF of r_{me} in this case can be a result of cell intersection with circle of radius R_e, dividing it by the entire expanded area i.e. $\pi R_e^2 - \pi R_s^2$. Consequently, the PDF of r_{me} as follows:

$$f_{r_{me}}(r) = \frac{1}{(\pi R_e^2 - \pi R_s^2)}(\pi r - 2r \arcsin(\frac{d^2 + r^2 - R_e^2}{2dr})). \tag{3.56}$$

2. $d - R_s \leq r \leq d + R_s$

   The CDF of r_{me} in this case can be a result of cell intersection with circle of radius R_e minus the result of cell intersection with circle of radius R_s , dividing it by the entire expanded area i.e. $\pi R_e^2 - \pi R_s^2$. Consequently, the PDF of r_{me} as follows:

$$f_{r_{me}}(r) = \frac{1}{(\pi R_e^2 - \pi R_s^2)}\Big((\pi r - 2r \arcsin(\frac{d^2 + r^2 - R_e^2}{2dr})) - (\pi r - 2r \arcsin(\frac{d^2 + r^2 - R_s^2}{2dr}))\Big). \tag{3.57}$$

3. $d + R_s \leq r \leq d + R_e$

The CDF of r_{me} in this case is defined as:

$$F_{r_{me}}(r) = F_3(r) - \frac{\pi R_s^2}{(\pi R_e^2 - \pi R_s^2)}, \tag{3.58}$$

with $F_3(r)$ a CDF that results from a cell intersection with a circle of radius R_e .
By applying the derivative of $F_{r_{me}}(r)$ and since the second term is a constant, the PDF $f_{r_{me}}(r)$ will be:

$$f_{r_{me}}(r) = f_3(r) = \frac{1}{(\pi R_e^2 - \pi R_s^2)}(\pi r - 2r \arcsin(\frac{d^2 + r^2 - R_e^2}{2dr})), \tag{3.59}$$

with $f_3(r)$ defined as the derivative of $F_3(r)$.

Adding the three cases, the probability density function (PDF) of r_{me} can be written as:

$$f_{r_{me}}(r) = \begin{cases} \frac{1}{(\pi R_e^2 - \pi R_s^2)}(\pi r - 2r \arcsin(\frac{d^2+r^2-R_e^2}{2dr})), & d - R_e \leq r \leq d - R_s \\ \frac{1}{(\pi R_e^2 - \pi R_s^2)}\Big((\pi r - 2r \arcsin(\frac{d^2+r^2-R_e^2}{2dr})) - (\pi r - 2r \arcsin(\frac{d^2+r^2-R_s^2}{2dr}))\Big), & d - R_s \leq r \leq d + R_s \\ \frac{1}{(\pi R_e^2 - \pi R_s^2)}(\pi r - 2r \arcsin(\frac{d^2+r^2-R_e^2}{2dr})), & d + R_s \leq r \leq d + R_e. \end{cases} \tag{3.60}$$

As for the statistics related to the small cell users, the downlink interference I_s is experienced from the macro BS at the small cell users. On this link, $P_t = P_m$ and $l = r_s$. Based on the expression (3.27) derived in the previous section, the PDF of r_{ms} can be obtained as a result of cell intersection with circle of radius R_s:

$$f_{r_{ms}}(r) = \frac{1}{\pi R_s^2}(\pi r - 2r \arcsin(\frac{d^2 + r^2 - R_s^2}{2dr})). \tag{3.61}$$

The signal of interest S_s of the small cell user is defined on a link having $P_t = P_s$ and $l = r_s$.
Since we consider uniformly distributed users, the distribution of the distance r_s of a small cell user is given by:

$$f_{r_s}(r) = \frac{2r}{R_s^2}, \quad 0 \leq r \leq R_s. \tag{3.62}$$

Note that the same distribution of r_s will be applicable for all coming scenarios.

B. Up - Down Scenario

The uplink interference I_e is experienced from the small cell BS at the macro BS. On this link, $P_t = P_s$ and $l = d$.
The uplink desired signal S_e of the mobile user in the expanded area is defined on a link having $P_t = P_{um}$ and $l = r_{me}$.
Repeating the same analysis as in (3.60), the PDF of r_{me} can be written as:

$$f_{r_{me}}(r) = \begin{cases} \frac{1}{(\pi R_e^2 - \pi R_s^2)}(\pi r - 2r \arcsin(\frac{d^2+r^2-R_e^2}{2dr})), & d - R_e \leq r \leq d - R_s \\ \frac{1}{(\pi R_e^2 - \pi R_s^2)}\Big((\pi r - 2r \arcsin(\frac{d^2+r^2-R_e^2}{2dr})) - (\pi r - 2r \arcsin(\frac{d^2+r^2-R_s^2}{2dr}))\Big), & d - R_s \leq r \leq d + R_s \\ \frac{1}{(\pi R_e^2 - \pi R_s^2)}(\pi r - 2r \arcsin(\frac{d^2+r^2-R_e^2}{2dr})), & d + R_s \leq r \leq d + R_e. \end{cases} \tag{3.63}$$

As for the statistics related to the small cell users, the downlink interference I_s is experienced from the macro cell user at the small cell user. On this link, $P_t = P_{um}$ and $l = u_{ms}$.
Based on the expression (3.47) derived in the Up - Down scenario, the PDF of u_{ms} can be written as follows:

$$f_{u_{ms}}(r) = \int_{r-R_s}^{r+R_s} f_{u_{ms}|r_{sm}}(r) f_{r_{sm}}(r_{sm}) dr_{sm}, \qquad 0 \leq r \leq R + d + R_s, \tag{3.64}$$

where $f_{u_{ms}|r_{sm}}(r) = \frac{1}{\pi R_s^2}(\pi r - 2r \arcsin(\frac{r_{sm}^2 + r^2 - R_s^2}{2r_{sm}r}))$ and $f_{r_{sm}}(r_{sm})$ defined as follows:

$$f_{r_{sm}}(r_{sm}) = \begin{cases} \frac{1}{\pi R^2 - \pi R_s^2}(2\pi r_{sm}), & R_s \leq r_{sm} < R - d \\ \frac{1}{\pi R^2 - \pi R_s^2}(\pi r_{sm} - 2r_{sm} \arcsin(\frac{d^2 + r_{sm}^2 - R^2}{2dr_{sm}})), & R - d \leq r_{sm} \leq R + d. \end{cases} \tag{3.65}$$

The signal of interest S_s of the small cell user is defined on a link having $P_t = P_s$ and $l = r_s$.

C. Up - Up Scenario

The uplink interference I_e is experienced from the small cell user at the macro BS. On this link, $P_t = P_{us}$ and $l = r_{ms}$.
The PDF of r_{ms} can be defined as:

$$f_{r_{ms}}(r) = \frac{1}{\pi R_s^2}(\pi r - 2r\arcsin(\frac{d^2+r^2-R_s^2}{2dr})), \qquad d - R_s \leq r \leq d + R_s$$

The uplink desired signal S_e of the mobile user in the expanded area is defined on a link having $P_t = P_{um}$ and $l = r_{me}$.
The PDF of r_{me} can be defined similarly as in (3.60):

$$f_{r_{me}}(r) = \begin{cases} \frac{1}{(\pi R_e^2 - \pi R_s^2)}(\pi r - 2r\arcsin(\frac{d^2+r^2-R_e^2}{2dr})), & d - R_e \leq r \leq d - R_s \\ \frac{1}{(\pi R_e^2 - \pi R_s^2)}\Big((\pi r - 2r\arcsin(\frac{d^2+r^2-R_e^2}{2dr})) - (\pi r - 2r\arcsin(\frac{d^2+r^2-R_s^2}{2dr}))\Big), & d - R_s \leq r \leq d + R_s \\ \frac{1}{(\pi R_e^2 - \pi R_s^2)}(\pi r - 2r\arcsin(\frac{d^2+r^2-R_e^2}{2dr})), & d + R_s \leq r \leq d + R_e. \end{cases} \tag{3.66}$$

As for the statistics related to the small cell users, the uplink interference I_s is experienced from the macro cell user at the small cell BS. On this link, $P_t = P_{um}$ and $l = r_{sm}$.
The PDF of r_{sm} can be deducted from the expression (3.42) in the Up - Up scenario as follows:

$$f_{r_{sm}}(r) = \begin{cases} \frac{1}{\pi R^2 - \pi R_s^2}(2\pi r), & R_s \leq r < R - d \\ \frac{1}{\pi R^2 - \pi R_s^2}(\pi r - 2r\arcsin(\frac{d^2+r^2-R^2}{2dr})), & R - d \leq r \leq R + d. \end{cases} \tag{3.67}$$

The signal of interest S_s of the small cell user is defined on a link having $P_t = P_{us}$ and $l = r_s$.

D. Down - Up Scenario

The downlink interference I_e is experienced from the small cell user BS at the mobile user in the expanded area. On this link, $P_t = P_{us}$ and $l = u_{es}$.
Since u_{es} refers to the distance between two randomly selected nodes in concentric circles and in this case the two nodes are uniformly distributed, then the PDF of u_{es} can be derived using the closed form expression obtained in [115]. The inner concentric circle is the one in which the small cell users are located and its radius is equal to R_s. In the outer concentric circle, the users in the expanded area are located and its radius is equal to R_e.
In this context, the PDF of u_{es} can be written as:

$$f_{u_{es}}(r) = \begin{cases} \frac{2r}{R_e^2}, & 0 \leq r \leq R_e - R_s \\ \frac{r}{\pi}\Big(\frac{2v(r)-\sin(2v(r))}{R_e^2} + \frac{2w(r)-\sin(2w(r))}{R_s^2}\Big), & R_e - R_s \leq r \leq R_e + R_s, \end{cases} \tag{3.68}$$

where $v(r) = \arccos(\frac{r^2-R_e^2+R_s^2}{2rR_s})$ and $w(r) = \arccos(\frac{r^2+R_e^2-R_s^2}{2rR_e})$.

The signal of interest S_e of the mobile user in the expanded area is defined on a link having $P_t = P_m$ and $l = r_{me}$. Repeating the same analysis as in (3.60), the PDF of r_{me} can be written as:

$$f_{r_{me}}(r) = \begin{cases} \frac{1}{(\pi R_e^2 - \pi R_s^2)}(\pi r - 2r\arcsin(\frac{d^2+r^2-R_e^2}{2dr})), & d - R_e \leq r \leq d - R_s \\ \frac{1}{(\pi R_e^2 - \pi R_s^2)}\Big((\pi r - 2r\arcsin(\frac{d^2+r^2-R_e^2}{2dr})) - (\pi r - 2r\arcsin(\frac{d^2+r^2-R_s^2}{2dr}))\Big), & d - R_s \leq r \leq d + R_s \\ \frac{1}{(\pi R_e^2 - \pi R_s^2)}(\pi r - 2r\arcsin(\frac{d^2+r^2-R_e^2}{2dr})), & d + R_s \leq r \leq d + R_e. \end{cases} \tag{3.69}$$

As for the statistics related to the small cell users, the uplink interference I_s is experienced from the macro BS at the small cell BS. On this link, $P_t = P_m$ and $l = d$.
The signal of interest S_s of the small cell user is defined on a link having $P_t = P_{us}$ and $l = r_s$.

CoUD with Small Cell or CRE Scenario

A major issue in HetNet planning is to ensure that the small cells actually serve enough users. One way to do that is to increase the area served by the small cell, which can be done through the use of a positive cell selection offset to the received power of the small cell. Extending the coverage of a cell by means of connecting a UE to a cell whose signal is weaker than the strongest detected cell signal, is referred to as cell range extension (CRE) [116]. Figure 3.20 illustrates the CRE concept, where users in the expanded area are associated in both UL and DL directions with the small cell.

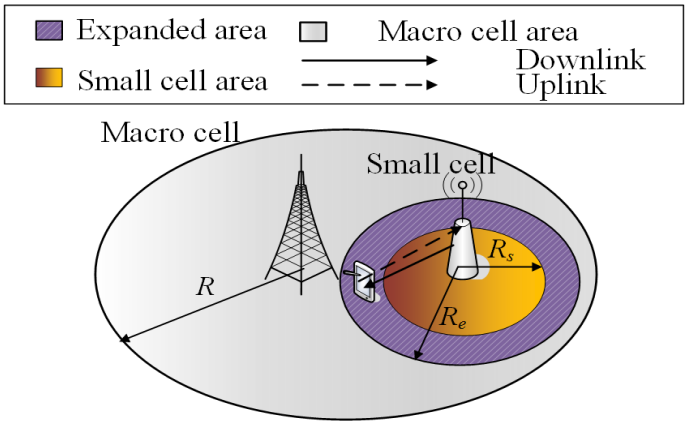

Figure 3.20: CRE illustration

In each of the following scenario under CRE, we will derive the statistics of users in the expanded area apart, in addition to the the small users' figures.

A. Down - Down Scenario

The downlink interference I_e is experienced from the macro BS at the mobile user in the expanded area. On this link, $P_t = P_m$ and $l = r_{me}$.
Repeating the same analysis as in (3.60), the PDF of r_{me} can be written as:

$$f_{r_{me}}(r) = \begin{cases} \frac{1}{(\pi R_e^2 - \pi R_s^2)}(\pi r - 2r\arcsin(\frac{d^2+r^2-R_e^2}{2dr})), & d - R_e \leq r \leq d - R_s \\ \frac{1}{(\pi R_e^2 - \pi R_s^2)}\Big((\pi r - 2r\arcsin(\frac{d^2+r^2-R_e^2}{2dr})) - (\pi r - 2r\arcsin(\frac{d^2+r^2-R_s^2}{2dr}))\Big), & d - R_s \leq r \leq d + R_s \\ \frac{1}{(\pi R_e^2 - \pi R_s^2)}(\pi r - 2r\arcsin(\frac{d^2+r^2-R_e^2}{2dr})), & d + R_s \leq r \leq d + R_e. \end{cases} \quad (3.70)$$

The signal of interest S_e of the mobile user in the expanded area is defined on a link having $P_t = P_s$ and $l = r_e$.
The distribution of r_e is given by (3.55).

As for the statistics related to the small cell users, the downlink interference I_s is experienced from the macro BS at the small cell users. On this link, $P_t = P_m$ and $l = r_{ms}$.
The PDF of r_{ms} can be obtained as a result of cell intersection with circle of radius R_s:

$$f_{r_{ms}}(r) = \frac{1}{\pi R_s^2}(\pi r - 2r\arcsin(\frac{d^2+r^2-R_s^2}{2dr})), \qquad d - R_s \leq r \leq d + R_s. \quad (3.71)$$

The signal of interest S_s of the small cell user is defined on a link having $P_t = P_s$ and $l = r_s$.

B. Up - Down Scenario

The downlink interference I_e is experienced from the macro cell user at the small cell user that is located inside the area bounded by R_e. On this link, $P_t = P_{um}$ and $l = u_{ms}$.
The PDF of u_{ms} is given by replacing R_s with R_e in (3.64):

$$f_{u_{ms}}(r) = \int_{r-R_e}^{r+R_e} f_{u_{ms}|r_{sm}}(r) f_{r_{sm}}(r_{sm}) dr_{sm}, \qquad 0 \leq r \leq R + d + R_e, \quad (3.72)$$

where $f_{u_{ms}|r_{sm}}(r) = \frac{1}{\pi R_e^2}(\pi r - 2r\arcsin(\frac{r_{sm}^2+r^2-R_e^2}{2r_{sm}r}))$ and $f_{r_{sm}}(r_{sm})$ formulated as:

$$f_{r_{sm}}(r_{sm}) = \begin{cases} \frac{1}{\pi R^2 - \pi R_e^2}(2\pi r_{sm}), & R_e \leq r_{sm} < R - d \\ \frac{1}{\pi R^2 - \pi R_e^2}(\pi r_{sm} - 2r_{sm}\arcsin(\frac{d^2+r_{sm}^2-R^2}{2dr_{sm}})), & R - d \leq r_{sm} \leq R + d \end{cases} \tag{3.73}$$

The signal of interest S_e of the mobile user in the expanded area is defined on a link having $P_t = P_s$ and $l = r_e$.
The distribution of r_e is given by (3.55).

As for the statistics related to the small cell users, the downlink interference I_s is experienced from the macro cell user at the small cell user that is located inside the area bounded by R_e. On this link, $P_t = P_{um}$ and $l = u_{ms}$.
The distribution of u_{ms} is given by (3.72). For simplicity, we considered the same distance u_{ms} to measure the distance from the macro user to either the small cell user or the user in the expanded area. This approximation is valid due to the notably smaller size of small cells comparing to the macro cell. The signal of interest S_s of the small cell user is defined on a link having $P_t = P_s$ and $l = r_s$.

C. Up - Up Scenario

The uplink interference I_e is experienced from the macro cell user that is located outside the area bounded by R_e at the small cell BS. On this link, $P_t = P_{um}$ and $l = r_{sm}$.
The PDF of r_{sm} is derived as in (3.73) where R_e is replacing R_s:

$$f_{r_{sm}}(r) = \begin{cases} \frac{1}{\pi R^2 - \pi R_e^2}(2\pi r), & R_e \leq r < R - d \\ \frac{1}{\pi R^2 - \pi R_e^2}(\pi r - 2r\arcsin(\frac{d^2+r^2-R^2}{2dr})), & R - d \leq r \leq R + d. \end{cases} \tag{3.74}$$

The uplink desired signal S_e of the mobile user in the expanded area is defined on a link having $P_t = P_{us}$ and $l = r_e$.
The distribution of r_e is given by (3.55).

As for the statistics related to the small cell users, the uplink interference I_s is defined on a link having $P_t = P_{um}$ and $l = r_{sm}$.
Same distance r_{sm} as in (3.74) will be studied for simplicity. The accuracy of this approximation will be validated in the next chapter using Monte-Carlo simulations.
The signal of interest S_s of the small cell user is defined on a link having $P_t = P_{us}$ and $l = r_s$.

D. Down - Up Scenario

The uplink interference I_e is experienced from the macro cell BS at the small cell BS. On this link, $P_t = P_m$ and $l = d$.
The signal of interest S_e of the mobile user in the expanded area is defined on a link having $P_t = P_{us}$ and $l = r_e$.
The distribution of r_e is given by (3.55).

As for the statistics related to the small cell users, they can be modeled by replacing r_e with r_s in the expressions derived for the mobile users in the expanded area under this same scenario.

3.4.2 Capacity Analysis with DeUD

In this section, we will consider the users in the extended area simultaneously connected to two cells, one for the downlink and one for the uplink. Two cases are considered, decoupling access or reverse decoupling access.

DeUD with Decoupling

Figure 3.21 illustrates the DeUD with decoupling case, where users in the expanded area are associated in UL to the small cell and in DL to the macro cell.

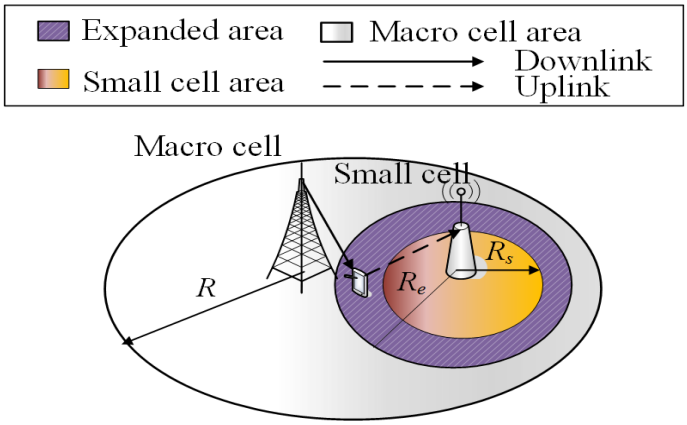

Figure 3.21: DeUD with decoupling illustration

A. Down - Down Scenario

The downlink interference I_e is experienced from the small cell BS at the mobile user in the expanded area. On this link, $P_t = P_s$ and $l = r_e$.
The distribution of r_e is given by (3.55). The signal of interest S_e of the mobile user in the expanded area is defined on a link having $P_t = P_m$ and $l = r_{me}$.
The distribution of r_{me} is defined as in (3.70).

As for the statistics related to the small cell users, the downlink interference I_s is experienced from the macro BS at the small cell users. On this link, $P_t = P_m$ and $l = r_{ms}$.
The PDF of r_{ms} can be obtained as a result of cell intersection with circle of radius R_s:

$$f_{r_{ms}}(r) = \frac{1}{\pi R_s^2}(\pi r - 2r \arcsin(\frac{d^2 + r^2 - R_s^2}{2dr})), \qquad d - R_s \leq r \leq d + R_s. \tag{3.75}$$

The signal of interest S_s of the small cell user is defined on a link having $P_t = P_s$ and $l = r_s$.

B. Up - Down Scenario

In this scenario, users with a decoupled access will be in a silent mode. Consequently, the average throughput for the users in the expanded area won't be considered.

As for the statistics related to the small cell users, the downlink interference I_s is experienced from the macro cell user at the small cell user that is located inside the area bounded by R_e. On this link, $P_t = P_{um}$ and $l = u_{ms}$.
The distribution of u_{ms} is given by (3.72) where R_e is replacing R_s.
The signal of interest S_s of the small cell user is defined on a link having $P_t = P_s$ and $l = r_s$.

C. Up - Up Scenario

In this scenario, same expressions will be derived as in the Up-Up scenario defined for the CoUD with small cell case.

D. Down - Up Scenario

In this scenario, users in the expanded area can operate at the same time in uplink and downlink. The downlink interference I_e is experienced from the small cell user BS at the mobile user in the expanded area. On this link, $P_t = P_{us}$ and $l = u_{es}$.

Referring to (3.68), the PDF of u_{es} can be written as:

$$f_{u_{es}}(r) = \begin{cases} \frac{2r}{R_e^2}, & 0 \leq r \leq R_e - R_s \\ \frac{r}{\pi}\left(\frac{2v(r)-\sin(2v(r))}{R_e^2} + \frac{2w(r)-\sin(2w(r))}{R_s^2}\right), & R_e - R_s \leq r \leq R_e + R_s, \end{cases} \tag{3.76}$$

where $v(r) = \arccos(\frac{r^2-R_e^2+R_s^2}{2rR_s})$ and $w(r) = \arccos(\frac{r^2+R_e^2-R_s^2}{2rR_e})$.

The downlink desired signal S_e of the user in the expanded area is defined on a link having $P_t = P_m$ and $l = r_{me}$.
The PDF of r_{me} is given by (3.70).

As for the uplink transmission, the interference I_e is experienced from the macro BS at the small cell BS. On this link, $P_t = P_m$ and $l = d$.
The uplink desired signal S_e in this case, is defined on a link having $P_t = P_{us}$ and $l = r_s$.

As for the statistics related to the small cell users, the uplink interference I_s is experienced from the macro BS at the small cell BS. On this link, $P_t = P_m$ and $l = d$.
The signal of interest S_s of the small cell user is defined on a link having $P_t = P_{us}$ and $l = r_s$.

DeUD with Reverse Decoupling

Figure 3.22 illustrates the DeUD with reverse decoupling case, where users in the expanded area are associated in UL to the macro cell and in DL to the small cell.

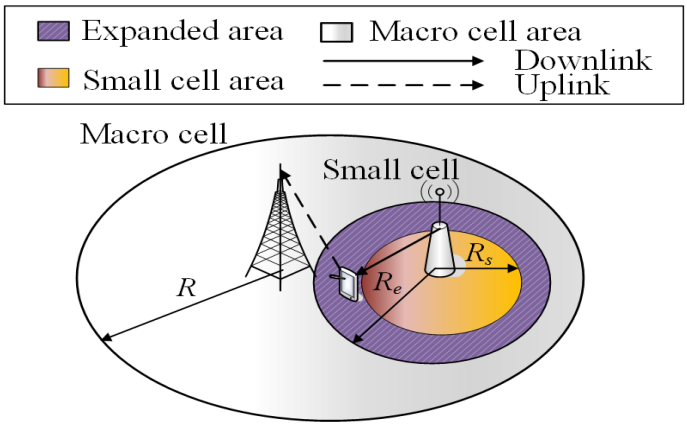

Figure 3.22: DeUD with reverse decoupling illustration

A. Down - Down Scenario

The downlink interference I_e is experienced from the macro BS at the mobile user in the expanded area. On this link, $P_t = P_m$ and $l = r_{me}$.
The PDF of r_{me} is formulated as in (3.70).
The signal of interest S_e of the mobile user in the expanded area is defined on a link having $P_t = P_s$ and $l = r_e$.
The distribution of r_e is given by (3.55).
As for the statistics related to the small cell users, the downlink interference I_s is experienced from the macro BS at the small cell users. On this link, $P_t = P_m$ and $l = r_{ms}$.
The PDF of r_{ms} can be obtained as a result of cell intersection with circle of radius R_s:

$$f_{r_{ms}}(r) = \frac{1}{\pi R_s^2}(\pi r - 2r\arcsin(\frac{d^2+r^2-R_s^2}{2dr})), \qquad d - R_s \leq r \leq d + R_s$$

The signal of interest S_s of the small cell user is defined on a link having $P_t = P_s$ and $l = r_s$.

B. Up - Down Scenario

In this scenario, users in the expanded area can operate at the same time in uplink and downlink . The downlink interference I_e is experienced from the macro cell user at the small cell user that is located inside the area bounded by R_e. On this link, $P_t = P_{um}$ and $l = u_{ms}$.
The PDF of u_{ms} is given by (3.72).
The downlink desired signal S_e of the user in the expanded area is defined on a link having $P_t = P_s$ and $l = r_e$.
The distribution of r_e is given by (3.55).

The uplink interference I_e is experienced from the small cell BS at the macro BS. On this link, $P_t = P_s$ and $l = d$.
The uplink desired signal S_e of the mobile user in the expanded area is defined on a link having $P_t = P_{um}$ and $l = r_{me}$.
The PDF of r_{me} is given by (3.70).

As for the statistics related to the small cell users, the downlink interference I_s is experienced from the macro cell user at the small cell user that is located inside the area bounded by R_e. On this link, $P_t = P_{um}$ and $l = u_{ms}$.
For simplicity, we considered the same distance u_{ms} to measure the distance from the macro user to either the small cell user or the user in the expanded area. This approximation is valid due to the notably smaller size of small cells comparing to the macro cell.
The signal of interest S_s of the small cell user is defined on a link having $P_t = P_s$ and $l = r_s$.

C. Up - Up Scenario

In this scenario, same expressions will be derived as in the Up-Up scenario defined for the CoUD with macro cell case.

D. Down - Up Scenario

In this scenario, users with a reversed decoupled access will be in a silent mode. Consequently, the average throughput for the users in the expanded area won't be considered.

As for the statistics related to the small cell users, the uplink interference I_s is experienced from the macro BS at the small cell BS. On this link, $P_t = P_m$ and $l = d$.
The signal of interest S_s of the small cell user is defined on a link having $P_t = P_{us}$ and $l = r_s$.

3.5 Analytical Evaluation in TDD 5G HetNets with Decoupling - Multiple Small Cells Scenario

In the previous sections (3.3 and 3.4), the developed models were built with the assumption of one macro cell and one small cell. However and in order to provide more insight into the benefits of decoupling mode in multiple small cells environment, we derive in this section, analytical expressions for the capacity and the interference, considering a network of one macro cell and multiple small cells. In this environment, we will consider at least one interfering small cell as a second source of interference affecting the reference small cell, in addition to the first source which is the macro cell. In the previous sections, the interference incurred at one tier (reference small cell) arising from the other tier (macro cell) is referred to as cross-tier interference. It may also be worth mentioning that, since multiple small cells are being deployed in this section as an overlay to the macro cell, the modeling of the interference incurred at the reference small cell arising from other small cells is becoming essential to evaluate the overall system performance. This type of interference is referred to as co-tier interference. Under this context, closed-form expressions for this new type of interference must be derived as well in order to calculate the average capacity at the reference small.
Moreover, we build on the derived capacity expressions to measure the decoupling gain and thus, identify the location of the interfering small cell where the decoupled mode maintains a higher gain in both DL and UL.

3.5.1 System Model for Multiple Small Cells Scenario

We consider a two-tier heterogeneous cellular network consisting of one macro cell and multiple small cells. The system model (topology, radio and traffic) for the macro and the reference small cell is the same as in section (3.2). However, this model should be extended in order to account for multiple small cells.
We denote by N_s the number of small cells. In this work and for simplicity, we consider $N_s = 2$ with one interfering small cell. However, the model scope can be expanded to include multiple interfering small cells which will definitely incur huge computational complexity (see Model Scalability Section 3.5.4).
We denote by d_{12} the distance from the reference small cell to the interfering small cell to be a new design parameter in this section. All small cells are considered synchronized with the same TDD configuration. Macro users are uniformly distributed in the macro cell. Similarly, small cell users are uniformly distributed inside their respective small cell. The reference small cell is located at a distance d from the center of the macro cell. The interfering small cell is located at a distance d_{12} and d_2 from the reference small cell and the macro cell respectively. Figure 3.23 depicts all distances involved in this model. In the following, we will define the major notations of these distances:

- $\psi = \{s, m, i\}$ denotes a set of base stations. The small cell reference BS is designated by s, the interfering macro cell BS by m and the interfering small cell BS by i. Note that e designates the expanded area at the reference small cell s.
- The interference experienced from the macro cell m and the interfering small cell i at the reference small cell s, is denoted by I_m and I_i respectively.
- $u_{k,j}$ denotes the distance between the user in the cell k and the user in the cell j, where j and $k \in \psi$.
- $r_{k,j}$ denotes the distance from the cell k to the user in the cell j, where j and $k \in \psi$. If k=j, $r_{k,j} = r_k$.
- $d_{k,j}$ denotes the distance from the cell k to the cell j, where j and $k \in \psi$.

For simplicity, we redefine $d_{k,j}$ notations in Table 3.6.

$d_{k,j}$ = d; k=m & j=s	Distance between the macro cell and the reference small cell
$d_{k,j} = d_{12}$; k=s & j=i	Distance between the reference small cell and the interfering small cell
$d_{k,j} = d_2$; k=m & j=i	Distance between the macro cell and the interfering small cell

Table 3.6: $d_{k,j}$ Notations

3.5.2 Cross-tier Interference Modeling

Cross-tier interference is the interference experienced from the macro cell m at the reference small cell s. In a multiple small cells environment, we have observed that nearly the same analytical expressions for the four interference types can be derived as in the case of one small cell (cf. Section 3.3).
However, some exceptions occurred, where introducing additional small cells leads to a change in the cross-tier interference expressions ((3.42) and (3.48)) derived under the Up - Up and Up - Down scenarios respectively. We can notice that the main interferer in these scenarios is the macro cell user. In this context, the area occupied by the small cells should be excluded when deriving the cumulative distribution function (CDF) of the interference experienced from the macro user at the reference small cell.
We define hereby the function $g(r)$ as a result of cell intersection with circle of radius R, with a distance d between the centers of the two circles:

$$g(r) = \pi r - 2r \arcsin(\frac{d^2 + r^2 - R^2}{2dr}), \tag{3.77}$$

and $h(r)$ as a result of cell intersection with the interfering small cell of radius R_s, with a distance d_{12} between the centers of the two circles:

$$h(r) = \pi r - 2r \arcsin(\frac{d_{12}^2 + r^2 - R_s^2}{2d_{12}r}). \tag{3.78}$$

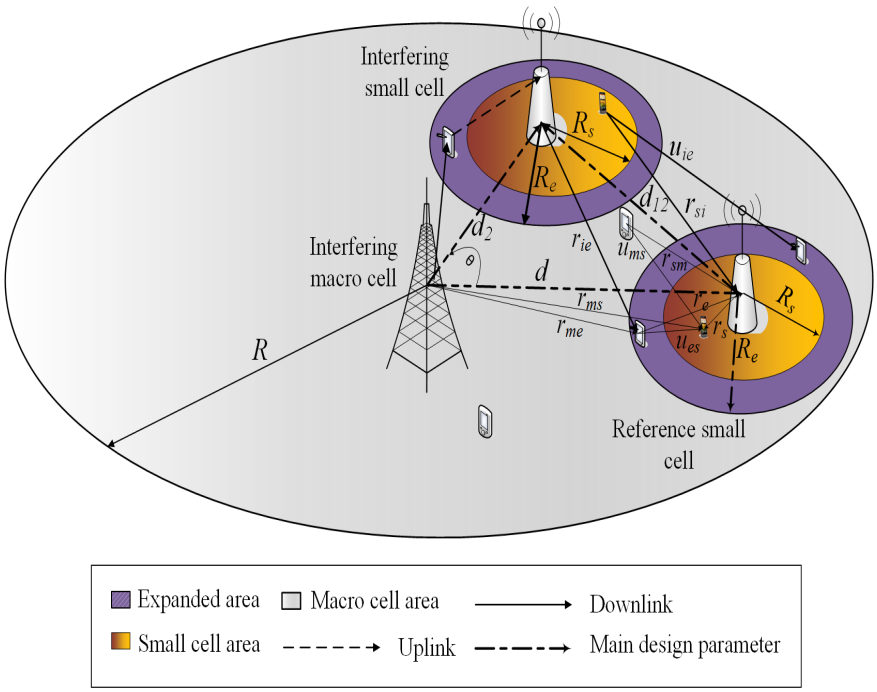

Figure 3.23: Geometrical illustration of all possible distances in the case of multiple small cells environment

Consequently, the PDF of r_{sm} in (3.42) and (3.48) is updated to include the distance between small cells (d_{12}) as follows:

$$f_{r_{sm}}(r) = \begin{cases} \frac{2\pi r}{\pi R^2 - 2\pi R_s^2}, & R_s \leq r < R - d \\ \frac{g(r)}{(\pi R^2 - 2\pi R_s^2)}, & R - d \leq r \leq d_{12} - R_s \\ \frac{g(r) - h(r)}{(\pi R^2 - 2\pi R_s^2)}, & d_{12} - R_s \leq r \leq d_{12} + R_s \\ \frac{g(r)}{(\pi R^2 - 2\pi R_s^2)}, & d_{12} + R_s \leq r \leq R + d. \end{cases} \tag{3.79}$$

3.5.3 Co-tier Interference Modeling

In order to model the cumulative interference at the reference small cell in a multiple small cells HetNet, we derive hereafter closed-form expressions for the co-tier interference to complement the cross-tier interference expressions derived in the previous section. We consider as co-tier interference the interference experienced at the reference small cell s from the interfering small cell i (see Fig. 3.23). Since the small cells are considered synchronized in uplink and downlink, the following two scenarios must be taken into account to derive expressions for the co-tier interference:

Small cell in Downlink Mode

The downlink co-tier interference is experienced from the interfering small cell BS at the mobile user associated with the reference small cell BS. On this link, $P_t = P_s$ and $l = r_{is}$.

Similar to the BS-MS scenario in (3.27), the PDF of r_{is} can be written as:

$$f_{r_{is}}(r) = \frac{1}{\pi R_s^2}\left(\pi r - 2r \arcsin\left(\frac{d_{12}^2 + r^2 - R_s^2}{2 d_{12} r}\right)\right), \qquad d_{12} - R_s \leq r \leq d_{12} + R_s, \tag{3.80}$$

where d_{12} represents in this case the distance between the centers of two intersecting circles.

Small cell in Uplink Mode

The uplink co-tier interference is experienced from the interfering small cell user at the reference small cell BS. On this link, $P_t = P_s$ and $l = r_{si}$.
The PDF of r_{si} can be obtained as a result of cell intersection with the interfering small cell of radius R_s:

$$f_{r_{si}}(r) = \frac{1}{\pi R_s^2}\Big(\pi r - 2r\arcsin(\frac{d_{12}^2 + r^2 - R_s^2}{2d_{12}r})\Big), \qquad d_{12} - R_s \leq r \leq d_{12} + R_s. \tag{3.81}$$

3.5.4 Model Scalability

Although in this section the model is built with two small cells, however its scope can be expanded to include multiple interfering small cells f located at distance d_{1f} from the reference small cell respectively. Accordingly, in order to derive expressions for the interference experienced from different interfering small cells, the PDF of r_{is} (to be denoted by r_{fs}) in (3.80) is revised by replacing d_{12} with d_{1f}, same for the PDF of r_{si} (to be denoted by r_{sf}) in (3.81). On the other hand, the PDF of the interference experienced from the macro users and thus, the PDF of r_{sm} in (3.79) is carefully revised and can be written as follows:

$$f_{r_{sm}}(r) = \begin{cases} \frac{2\pi r}{\pi R^2 - N_s \pi R_s^2}, & R_s \leq r < R - d \\ \frac{g(r)}{(\pi R^2 - N_s \pi R_s^2)}, & R - d \leq r \leq d_f - R_s \\ \frac{g(r) - \sum_{f=2}^{N_s} h_f(r)}{(\pi R^2 - N_s \pi R_s^2)}, & d_f - R_s \leq r \leq D_f + R_s \\ \frac{g(r)}{(\pi R^2 - N_s \pi R_s^2)}, & D_f + R_s \leq r \leq R + d, \end{cases} \tag{3.82}$$

where $g(r) = \pi r - 2r\arcsin(\frac{d^2 + r^2 - R^2}{2dr})$, $D_f = \max\limits_{2 \leq f \leq N_s} d_{1f}$, $d_f = \min\limits_{2 \leq f \leq N_s} d_{1f}$ and

$$h_f(r) = \begin{cases} \pi r - 2r\arcsin(\frac{d_{1f}^2 + r^2 - R_s^2}{2d_{1f}r}), & d_{1f} - R_s \leq r \leq d_{1f} + R_s \\ 0, & elsewhere. \end{cases} \tag{3.83}$$

3.5.5 Signal of Interest Modeling

The signal power received by a randomly selected user at the reference small cell on a downlink channel is defined as: $S = KL_0P_s r_s^{-\gamma}$ where r_s is the distance of the user from the small cell BS s. The distribution of S remains the same as in the case of a single small cell:

$$f_S(s) = \beta s^{-(\frac{2+\gamma}{\gamma})}, \tag{3.84}$$

where $\beta = \frac{2K_c^{\frac{2}{\gamma}}}{\gamma R_s^2}$ and $K_c = KL_0P_s$. Note that same logic applies to derive similar expressions on the uplink channel.

3.5.6 Capacity Analysis in Multiple Small Cells Scenario

The average user capacity per unit bandwidth i.e. the spectral efficiency at the reference small cell, in a multiple small cells environment is defined as follows:

$$C_s = \mathbb{E}\Big[\frac{B\ln(1 + \frac{S}{I_{tot} + \sigma^2})}{B}\Big] = \mathbb{E}\Big[\ln(1 + \frac{S}{I_{tot} + \sigma^2})\Big], \tag{3.85}$$

where σ^2 is the thermal noise power variance and I_{tot} the cumulative interference defined as: $I_{tot} = I_m + I_i$. I_m is the interference experienced from the macro cell and I_i is the interference experienced from the interfering small cells, at the reference small cell. S and I_{tot} are considered as two independent variables. In the following, we will provide an approximation to the generic function of the capacity C_s:

The interference, in general, can be written as: $I = KL_0P_t l^{-\gamma} = K_c l^{-\gamma}$ where $K_c = KL_0P_t$, l denotes the interfering distance, P_t the transmitted power and K the composite fading. Applying the chain rule to the CDF of I,

the corresponding PDF can be written as $f_I(i) = \frac{1}{i\gamma} f_l\Big((\frac{i}{K_c})^{-\frac{1}{\gamma}}\Big)(\frac{i}{K_c})^{\frac{-1}{\gamma}}$. Accordingly, a closed-form expression for the MGF of the interference I can be formulated as $M_I(t) = \int_0^\infty e^{-ti} f_I(i)di$. Note that the same steps apply for the derivation of the MGF of the signal of interest ($M_S(t)$).
Denote by I_{tot} the cumulative interference from the macro cell (I_m) and the interfering small cells (I_i), at the reference small cell. Consequently, I_{tot} can be written as: $I_{tot} = I_m + I_i$. Considering I_m and I_i as independent variables, the MGF of the cumulative interference I_{tot} can be calculated as follows: $M_{I_{tot}}(t) = M_{I_m}(t)M_{I_i}(t)$.
Based on the MGF expressions derived for S and I_{tot}, the average capacity per unit bandwidth can be calculated using the lemma proposed in [112] as follows:

$$C_s = \mathbb{E}[\ln(1 + \tfrac{S}{I_{tot}+\sigma^2})] = \int_0^\infty \tfrac{M_{I_{tot}}(t) - M_S(t)M_{I_{tot}}(t)}{t} e^{-(\sigma^2)t} dt$$

$$C_s = \int_0^\infty \tfrac{M_{I_m}(t)M_{I_i}(t) - M_S(t)M_{I_m}(t)M_{I_i}(t)}{te^{-at}} e^{-(\sigma^2+a)t} dt.$$

This expression can be solved efficiently by expressing it in terms of the weights w_e and abscissas x_e of a Laguerre orthogonal polynomial [113] [114], as follows:

$$C_s = \sum_{e=1}^{n} w_e \Big(\frac{M_{I_m}(x_e/(\sigma^2+a))M_{I_i}(x_e/(\sigma^2+a))}{x_e e^{-(ax_e)/(\sigma^2+a)}} - \frac{M_S(x_e/(\sigma^2+a))M_{I_m}(x_e/(\sigma^2+a))M_{I_i}(x_e/(\sigma^2+a))}{x_e e^{-(ax_e)/(\sigma^2+a)}} \Big). \quad (3.86)$$

In this work, the a parameter was introduced to resolve the scaling problem in Laguerre polynomial, more specifically in the $M(t)$ expression. Adding the a parameter will ensure scalable values of the MGF expression with $M(x_e/(\sigma^2+a))$. a is set to 10^{-4} in the scenarios where the macro cell is in a DL mode and to 10^{-6} in the scenarios where the macro cell is in an UL mode.

Special Case: $\psi = \{s, m\}$, *i.e.* $N_s = 1$ *and* $I_i = 0$: In case of a network consisting of one macro cell and one reference small cell, the latter will be purely affected by the interfering macro cell and therefore $I_{tot} = I_m = I$. Accordingly, the capacity expression can be formulated as follows:

$$C_s = \sum_{e=1}^{n} w_e \Big(\frac{M_I(x_e/(\sigma^2+a))}{x_e e^{-(ax_e)/(\sigma^2+a)}} - \frac{M_S(x_e/(\sigma^2+a))M_I(x_e/(\sigma^2+a))}{x_e e^{-(ax_e)/(\sigma^2+a)}} \Big). \quad (3.87)$$

3.5.7 Uplink Power Control

Uplink power control can also be added to the developed model. Based on the open-loop power control strategy standardized in 3GPP LTE [109], the transmit power of a mobile user is given by:

$$P_t = min(P_{max}, P_0 r_s^\gamma), \quad (3.88)$$

where r_s is the distance of the reference small cell user from its serving BS, P_0 is the desired received signal level at the BS and P_{max} denotes the maximum transmit power capability per user. Consequently, the uplink signal power received at the reference BS with power control can be given as $S = KL_0P_t r_s^{-\gamma}$ with:

$$S = \begin{cases} KL_0P_0, & P_{max} > P_0 r_s^\gamma \\ KL_0P_{max} r_s^{-\gamma}, & P_{max} \leq P_0 r_s^\gamma, \end{cases} \quad (3.89)$$

and the interference caused at a reference BS (or user) from a given interfering small cell (or macro cell), can then be derived as $I = KL_0P_t l^{-\gamma}$ with:

$$I = \begin{cases} KL_0P_0 r_s^\gamma l^{-\gamma}, & P_{max} > P_0 r_s^\gamma \\ KL_0P_{max} l^{-\gamma}, & P_{max} \leq P_0 r_s^\gamma, \end{cases} \quad (3.90)$$

where l is the length of the interfering link. The PDF of I can be derived by averaging over r_s the PDF of $f_l(r)_{|r_s}$.
It is important to note that the power control mechanism leads in average to reduction in power consumption when a user in a specific position is able to compensate the overall path loss with $P_0 r_s^{\gamma} < P_{max}$. In this case, average reduction in power consumption (PR) can be defined as: $PR = \mathbb{E}[P_{max} - P_0 r_s^{\gamma}]$.
Simulation results showing the impact of power control on the system throughput and the network power consumption, will be discussed in the next chapter under Section 4.5.2.

3.5.8 Unsynchronized TDD Configuration

Although in this chapter the model is developed based on a synchronized TDD configuration assumption across small cells, it can be well adapted to consider an unsynchronized TDD configuration by deriving two additional expressions for the co-tier interference experienced from the interfering small cell at the reference small cell:

1) In the case where the interfering small cell operates in uplink and the reference small cell operates in downlink, the PDF of the distance from the interfering small cell user to the reference small cell user (u_{is}) can be derived similarly to the PDF of u_{ms} in (3.47):

$$f_{u_{is}}(r) = \int_{r-R_s}^{r+R_s} f_{u_{is}|r_{si}}(r) f_{r_{si}}(r_{si}) dr_{si}, \qquad 2(R_e - R_s) \leq r \leq d + 2R_s, \quad (3.91)$$

where $f_{u_{is}|r_{si}}(r) = \frac{1}{\pi R_s^2}(\pi r - 2r \arcsin(\frac{r_{si}^2 + r^2 - R_s^2}{2 r_{si} r}))$ and $f_{r_{si}}(r_{si})$ defined as follows:

$$f_{r_{si}}(r_{si}) = \frac{1}{\pi R_s^2}\Big(\pi r_{si} - 2 r_{si} \arcsin(\frac{d_{12}^2 + r_{si}^2 - R_s^2}{2 d_{12} r_{si}})\Big), \quad (3.92)$$

2) In the case where the interfering small cell operates in downlink and the reference small cell operates in uplink, the distance from the interfering small cell to the reference small cell is constant and equal to d_{12}.

Simulation results showing the impact of considering an unsynchronized TDD configuration, will be discussed in the next chapter under Section 4.5.3.

3.5.9 Decoupling Gain Analysis in Multiple Small Cells Scenario

In the previous sections, we have calculated the average user capacity per association policy mainly, in order to compare the performance of the decoupling strategy with other association strategies. However and in order to provide more insights about the gain that the decoupling strategy can bring in comparison with the coupled with macro case, we focus in this section on the analytical evaluation of this gain that is referred to as the decoupling gain. Under this context, we investigate the decoupling gain mainly in multiple small cells scenario where it appears to be dependent on the distance between the reference small cell and the interfering small cells.

Definition 1. The decoupling gain, denoted as η_d, is defined as the ratio between the throughput achieved when decoupling is adopted and the throughput achieved without decoupling (in the coupled with macro (CM) case):

$$\eta_d = \frac{Throughput_d(\text{Decoupling}) \text{ - } Throughput_d(\text{CM})}{Throughput_d(\text{CM})}, \quad (3.93)$$

where $d \in \{UL, DL\}$.

To analyze the decoupling gain in a multiple small cells TDD HetNet, it is important to develop a complete model for both the CM and the decoupling cases. Moreover, calculating the decoupling gain in one direction (UL or DL) necessitates measuring C_{es} in that direction for both CM and decoupling cases. C_{es} is computed by adding the average users capacity in the small cell area (C_s) to the average users capacity in the expanded area (C_e). For simplicity, we consider in the below calculations $N_s = 2$ with one interfering small cell.

Uplink Decoupling Gain

In the Down - Up and Up - Up scenarios, small cell users along with the users in the expanded area are operating in uplink. Hence, the latter two scenarios present a considerable part of the overall uplink capacity (C_{es}), whereas the Up - Down case considers a negligible part ($C_{es} = C_e \simeq 0$).

A. Down - Up Scenario

a) CM Case: For the C_s calculation, closed-form expressions are derived for:

- $I_m = KL_0P_md$.
- $I_i = KL_0P_{us}r_{si}$, where $d_{12} - R_s \leq r_{si} \leq d_{12} + R_s$.
- $S_s = KL_0P_{us}r_s$, where $0 \leq r_s \leq R_s$.

The PDF $f_{r_{si}}(r)$ is given by (3.81), an expression derived in the case of two small cells:

$$f_{r_{si}}(r) = \frac{1}{\pi R_s^2}\Big(\pi r - 2r\arcsin(\frac{d_{12}^2 + r^2 - R_s^2}{2d_{12}r})\Big), \qquad d_{12} - R_s \leq r \leq d_{12} + R_s. \tag{3.94}$$

In this case, $C_e = 0$.

b) Decoupling Case: For the C_s calculation, closed-form expressions are derived for:

- $I_m = KL_0P_md$.
- $I_i = KL_0P_{us}r_{si}$, where $d_{12} - R_e \leq r_{si} \leq d_{12} + R_e$.
- $S_s = KL_0P_{us}r_s$, where $0 \leq r_s \leq R_s$.

The PDF $f_{r_{si}}(r)$ is given by replacing R_s with R_e in (3.94):

$$f_{r_{si}}(r) = \frac{1}{\pi R_e^2}\Big(\pi r - 2r\arcsin(\frac{d_{12}^2 + r^2 - R_e^2}{2d_{12}r})\Big), \qquad d_{12} - R_e \leq r \leq d_{12} + R_e. \tag{3.95}$$

The same interference expressions will be derived for the calculation of C_e. However, S_e is defined as: $S_e = KL_0P_{us}r_e$, where $R_s \leq r_e \leq R_e$.

B. Up - Up Scenario

a) CM Case: For the C_s calculation, closed-form expressions are derived for:

- $I_m = KL_0P_{um}r_{sm}$, where $R_s \leq r_{sm} \leq R + d$.
- $I_i = KL_0P_{us}r_{si}$, where $d_{12} - R_s \leq r_{si} \leq d_{12} + R_s$.
- $S_s = KL_0P_{us}r_s$, where $0 \leq r_s \leq R_s$.

The PDF of r_{sm} is derived as follows:

$$f_{r_{sm}}(r) = \begin{cases} \frac{2\pi r}{(\pi R^2 - 2\pi R_s^2)}, & R_s \leq r < R - d \\ \frac{g(r)}{(\pi R^2 - 2\pi R_s^2)}, & R - d \leq r \leq d_{12} - R_s \\ \frac{g(r) - h(r)}{(\pi R^2 - 2\pi R_s^2)}, & d_{12} - R_s \leq r \leq d_{12} + R_s \\ \frac{g(r)}{(\pi R^2 - 2\pi R_s^2)}, & d_{12} + R_s \leq r \leq R + d, \end{cases} \tag{3.96}$$

where $g(r) = \pi r - 2r\arcsin(\frac{d^2 + r^2 - R^2}{2dr})$ and $h(r) = \pi r - 2r\arcsin(\frac{d_{12}^2 + r^2 - R_s^2}{2d_{12}r})$.

The PDF of r_{si} is given by (3.94).
In this case, $C_e \simeq 0$.

b) Decoupling Case: For the C_s calculation, closed-form expressions are derived for:

- $I_m = KL_0P_{um}r_{sm}$, where $R_e \leq r_{sm} \leq R + d$.
- $I_i = KL_0P_{us}r_{si}$, where $d_{12} - R_e \leq r_{si} \leq d_{12} + R_e$.
- $S_s = KL_0P_{us}r_s$, where $0 \leq r_s \leq R_s$.

The PDF $f_{r_{sm}}(r)$ is given by replacing R_s with R_e in (3.96):

$$f_{r_{sm}}(r) = \begin{cases} \frac{2\pi r}{(\pi R^2 - 2\pi R_e^2)}, & R_e \leq r < R - d \\ \frac{g(r)}{(\pi R^2 - 2\pi R_e^2)}, & R - d \leq r \leq d_{12} - R_e \\ \frac{g(r) - i(r)}{(\pi R^2 - 2\pi R_e^2)}, & d_{12} - R_e \leq r \leq d_{12} + R_e \\ \frac{g(r)}{(\pi R^2 - 2\pi R_e^2)}, & d_{12} + R_e \leq r \leq R + d, \end{cases} \tag{3.97}$$

where $g(r) = \pi r - 2r \arcsin(\frac{d^2 + r^2 - R^2}{2dr})$ and $i(r)$ computed as a result of cell intersection with the interfering small cell of radius R_e, with a distance d_{12} between the centers of the two circles:

$$i(r) = \pi r - 2r \arcsin(\frac{d_{12}^2 + r^2 - R_e^2}{2d_{12}r}). \tag{3.98}$$

The PDF of r_{si} is given by (3.95).
The same interference expressions will be derived for the calculation of C_e. However, S_e is defined as: $S_e = KL_0P_{us}r_e$.

Downlink Decoupling Gain

In the Up - Down and Down - Down scenarios, small cell users along with the users in the expanded area are operating in downlink. Hence, the latter two scenarios present a considerable part of the overall downlink capacity (C_{es}), whereas the Down - Up case considers a negligible part ($C_{es} = C_e \simeq 0$).

A. Up - Down Scenario

a) CM Case: For the C_s calculation, closed-form expressions are derived for:

- $I_m = KL_0P_{um}u_{ms}$, where $0 \leq u_{ms} \leq R + d + R_s$.
- $I_i = KL_0P_sr_{is}$, where $d_{12} - R_s \leq r_{is} \leq d_{12} + R_s$.
- $S_s = KL_0P_sr_s$, where $0 \leq r_s \leq R_s$.

u_{ms} represents the distance from the macro cell user to the small cell user that is located inside the area bounded by R_s. The PDF of u_{ms} is derived by averaging over the PDF of r_{sm} ($f_{r_{sm}}(r_{sm})$):

$$f_{u_{ms}}(r) = \int_{r-R_s}^{r+R_s} f_{u_{ms}|r_{sm}}(r) f_{r_{sm}}(r_{sm}) dr_{sm}, \qquad 0 \leq r \leq R + d + R_s, \tag{3.99}$$

where r_{sm} is the distance of the reference small cell BS from the macro cell user and $f_{u_{ms}|r_{sm}}(r)$ denotes the PDF of u_{ms} conditioned on r_{sm}.
In this case, the expanded areas of both small cells are part of the macro user region and thus, $f_{r_{sm}}$ will be derived using R_s as the main parameter to determine the macro user area boundaries as in (3.96). Since C_s represents the average capacity of the reference small cell users located inside the area bounded by R_s, the integral of $f_{u_{ms}|r_{sm}}(r)$ will range from $r - R_s$ to $r + R_s$. The PDF $f_{r_{is}}(r)$ is given by (3.80), an expression derived in the case of two small cells:

$$f_{r_{is}}(r) = \frac{1}{\pi R_s^2}\Big(\pi r - 2r \arcsin(\frac{d_{12}^2 + r^2 - R_s^2}{2d_{12}r})\Big), \qquad d_{12} - R_s \leq r \leq d_{12} + R_s. \tag{3.100}$$

In the CM case under the Up - Down scenario, $C_e = 0$ and thus, $C_{es} = C_s$.
b) Decoupling Case: For the C_s calculation, closed-form expressions are derived for:

- $I_m = KL_0P_{um}u_{ms}$, where $R_e - R_s \leq u_{ms} \leq R + d + R_s$.

- $I_i = KL_0P_sr_{is}$, where $d_{12} - R_s \leq r_{is} \leq d_{12} + R_s$.
- $S_s = KL_0P_sr_s$, where $0 \leq r_s \leq R_s$.

u_{ms} represents the distance from the macro cell user to the small cell user that is located inside the area bounded by R_s. The PDF of u_{ms} is derived by averaging over the PDF of r_{sm} ($f_{r_{sm}}(r_{sm})$):

$$f_{u_{ms}}(r) = \int_{r-R_s}^{r+R_s} f_{u_{ms}|r_{sm}}(r) f_{r_{sm}}(r_{sm}) dr_{sm}, \qquad R_e - R_s \leq r \leq R + d + R_s. \tag{3.101}$$

Contrary to the CM case, the expanded areas of both small cells are out of the macro user region and thus, $f_{r_{sm}}$ will be derived using R_e as the main parameter to determine the macro user area boundaries:

$$f_{r_{sm}}(r) = \begin{cases} \frac{2\pi r}{(\pi R^2 - 2\pi R_e^2)}, & R_e \leq r < R - d \\ \frac{g(r)}{(\pi R^2 - 2\pi R_e^2)}, & R - d \leq r \leq d_{12} - R_e \\ \frac{g(r) - i(r)}{(\pi R^2 - 2\pi R_e^2)}, & d_{12} - R_e \leq r \leq d_{12} + R_e \\ \frac{g(r)}{(\pi R^2 - 2\pi R_e^2)}, & d_{12} + R_e \leq r \leq R + d, \end{cases} \tag{3.102}$$

where $g(r) = \pi r - 2r \arcsin(\frac{d^2 + r^2 - R^2}{2dr})$ and $i(r) = \pi r - 2r \arcsin(\frac{d_{12}^2 + r^2 - R_e^2}{2d_{12}r})$.

Consequently, u_{ms} will range from $R_e - R_s$ to $R + d + R_s$. Similar to the CM case and since C_s represents the average capacity of the reference small cell users located inside the area bounded by R_s, the integral of $f_{u_{ms}|r_{sm}}(r)$ will range from $r - R_s$ to $r + R_s$.
Note that $r_{is}(r)$ follows the same statistical distribution as in the CM case. Whether the user located in the expanded area, is in decoupling or CM state, $r_{is}(r)$ will be reflecting the interference experienced from the interfering small cell independently of the small cell user access policy.
In this case, $C_e = 0$ and thus, $C_{es} = C_s$.

B. Down - Down Scenario

Under this scenario, same expressions are derived for both CM and decoupling cases. Theoretically, it means there is no downlink decoupling gain ($\eta_{DL} = 0$).
For the C_s calculation, closed-form expressions are derived for:

- $I_m = KL_0P_mr_{ms}$, where $d - R_s \leq r_{ms} \leq d + R_s$.
- $I_i = KL_0P_sr_{is}$, where $d_{12} - R_s \leq r_{is} \leq d_{12} + R_s$.
- $S_s = KL_0P_sr_s$, where $0 \leq r_s \leq R_s$.

The PDF of r_{ms} can be obtained as a result of the cell intersection with the circle of radius R_s:

$$f_{r_{ms}}(r) = \frac{1}{\pi R_s^2}\Big(\pi r - 2r \arcsin(\frac{d^2 + r^2 - R_s^2}{2dr})\Big), \qquad d - R_s \leq r \leq d + R_s. \tag{3.103}$$

The PDF of r_{is} is given by (3.100).
As for the C_e calculation, closed-form expressions are derived for:

- $I_m = KL_0P_mr_{me}$, where $d - R_e \leq r_{me} \leq d + R_e$.
- $I_i = KL_0P_sr_{ie}$, where $d_{12} - R_e \leq r_{ie} \leq d_{12} + R_e$.
- $S_e = KL_0P_sr_e$, where $R_s \leq r_e \leq R_e$.

The PDF of r_{me} can be defined similarly as in (3.60). As for the distribution of r_{ie}, it is given by replacing d with d_{12} in (3.60):

$$f_{r_{ie}}(r) = \begin{cases} \frac{i(r)}{(\pi R_e^2 - \pi R_s^2)}, & d_{12} - R_e \leq r \leq d_{12} - R_s \\ \frac{i(r) - h(r)}{(\pi R_e^2 - \pi R_s^2)}, & d_{12} - R_s \leq r \leq d_{12} + R_s \\ \frac{i(r)}{(\pi R_e^2 - \pi R_s^2)}, & d_{12} + R_s \leq r \leq d_{12} + R_e, \end{cases} \tag{3.104}$$

where $i(r) = \pi r - 2r \arcsin(\frac{d_{12}^2 + r^2 - R_e^2}{2 d_{12} r})$ and $h(r) = \pi r - 2r \arcsin(\frac{d_{12}^2 + r^2 - R_s^2}{2 d_{12} r})$.

3.6 Conclusion

In this chapter, we have developed a statistical and analytical model for a HetNet based system where decoupling and dynamic TDD are jointly deployed. The proposed model offers a simple analysis tool to assess a given TDD/Decoupling-based HetNet deployment. The analytical formulas provide relevant insights about network performance without the need for time consuming Monte-Carlo Simulations. This tool is also useful for network designers who can use it to determine the range of deployment parameters given a target QoS.
In our analysis, we have considered a network consisting of one macro cell along with one small cell. Our main focus will be evaluating users' performance inside the small cell. This small cell is referred to as a reference small cell.
Firstly, the case of one small cell has been considered. Incorporating the dynamic TDD technique into the HetNet based system has imposed the modeling of four kinds of cross-tier interference in order to cover all UL/DL TDD possible combinations between the macro cell from a side and the small cell from the other side. Moreover, deploying the decoupling policy on top of the TDD HetNet system has necessitated the modeling of various association policies in order to highlight the benefits that the decoupling policy can bring to that system in comparison with the other policies.
Secondly, multiple instances of interfering small cells have been deployed at specific distances from the reference small cell in order to be aligned as much as possible with real case scenarios. We have considered this specific network model, as simple as it shows in regards to BS distribution, to focus on the main thesis objective which is the modeling of TDD and decoupling in a scenario that is close to real cases, and at the same time to avoid adding further complexity to the model itself. Instead, including any other BS distribution (stochastic for example) will bring significant additional complexity to our HetNet analysis. In this case, our work will be further away from reaching its objectives.
In this chapter, a geometric approach has been adopted to derive closed-form expressions for the interfering distances along with the location of the reference small cell user. This geometric approach was based on different methods, e.g. cells intersection method, randomly selected nodes in concentric circles method, etc. Based on the distances distribution, we have calculated the PDF and MGF of the interference and the signal of interest. In multiple small cells environment, a new type of interference to which we refer to as the co-tier interference has been modeled in addition to the cross-tier interference. Relying on the MGF results of both the interference and the signal of interest, we have derived closed-form expression for the spectral efficiency or what we refer to as capacity per unit bandwidth. Also, additional expressions have been derived for other performance metrics. e.g. the decoupling gain, power control and average reduction in power consumption. Moreover, the statistical model has been adapted to consider an unsynchronized TDD configuration across small cells, in addition to the initial synchronized TDD configuration.

Chapter 4

Performance Evaluation of TDD and Decoupling in 5G HetNets

4.1 Introduction

We evaluate under this chapter the system performance metrics, for which we have derived closed form expressions in Chapter 3. We define the system parameters and discuss the Monte-Carlo simulation results that are provided to validate the accuracy of the analytical model including 95% confidence intervals of disparity measures. Confidence intervals are derived for a sample mean, using the sample data values themselves. In this chapter, we denote by (Th.) the theoretical results and by (M.C.) the Monte-Carlo simulation results.

4.2 System Parameters

In this chapter, we consider analyzing the average capacity (C_{es}) of the reference small cell for each of the below listed scenarios. C_{es} is computed by adding the average users capacity in the small cell area (C_s) to the average users capacity in the expanded area (C_e). Uniformly distributed users are considered in both macro and small cells. The default system parameters are listed in Table 4.1. According to 3GPP standards, macro cell radius can be set from few kilometers up to 35 Km. In this model, we consider a macro cell radius $R = 1$ Km with a maximum BS transmission power $P_m = 43$ dBm (20 W) according to the 3GPP specifications in [118]. In this case, the power received at the macro cell edge will be around -85 dBm, which is considered as the minimum desired received signal level at the mobile user. The power received at the cell edge was calculated based on the path-loss expression in (3.1) or (3.2), leading to a path-loss constant $L_0 = 1.58 * 10^{-4}$. As for the small cell coverage, the radius can be typically set between 10 and 250 m. In this model, we consider a small cell radius $R_s = 200$ m with a maximum transmission power $P_s = 24$ dBm (0.25 W) according to the 3GPP specifications in [119]. Similarly to the macro cell case, the power received at the small cell edge will be around -83 dBm. The maximum UE transmission power is set to 23 dBm (0.22 W) according to [118].
Yet, in order to apply a sort of power control between macro cell users from one side and small cell users from the other side, we allow a slight difference between UE maximum transmission power in macro cell $P_{um} = 23.4$ dBm (0.22 W) and $P_{us} = 23$ dBm (0.2 W) in small cells. However, in Section 4.5.2 a dynamic uplink power control mechanism is considered instead. The latter is based on the open-loop power control strategy with a desired received signal level at the BS, $P_0 = 10^{-7}$ W (-40 dBm) [109].

4.2.1 TDD Frame Type

In this Chapter, we consider frame structures where all uplink/downlink combinations between the macro and small cells are taken into account, as shown in Fig. 4.1. In the sections that follow, both UL and DL throughputs will be evaluated and averaged over the period of the TDD frame defined in this figure.
It is important to note that, relying on the model developed in Chapter 3 and that encloses all possible inter-link interferences, any other TDD configuration with different length can be easily adopted and investigated.

Parameter	Value
Macro cell radius R	1000 m
Small cell radius R_s	200 m
Small cell offset factor R_e	300 m
Number of small cells N_s	$1 \leq N_s \leq 2$
Distance between the reference small cell and the macro cell d	600 m
Distance between the reference small cell and the interfering small cell d_{12}	800 m
Path-loss exponent γ	$2 \leq \gamma \leq 3$
Path-loss constant L_0	$1.58 * 10^{-4}$
Constant fading K	1
Carrier frequency	2.0 GHz
System bandwidth	20 MHz
Thermal noise power spectrum density	-174 dBm/Hz
Macro BS transmission power P_m	20 W
Small cell BS transmission power P_s	0.25 W
Macro user transmission power P_{um}	0.22 W
Small cell user transmission power P_{us}	0.2 W

Table 4.1: System parameters

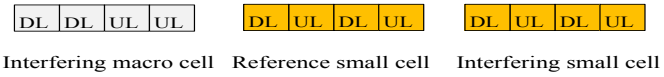

Figure 4.1: TDD frame structure in macro and small cells.

4.2.2 Constant Fading

In Fig. 4.2) and Fig. 4.3, we simulate exactly the same scenarios under a constant fading from one side and a random variable fading from the other side. Accordingly for the random variable fading, a log-normal shadowing and an exponential distribution with parameter $\lambda = 1$ as an approximation of the Rayleigh fading, were considered. We can conclude from these figures that we have obtained nearly the same throughput values in UL and DL and the same behavior as in the case of a constant composite fading; the decoupling strategy continues to prevail over the other association policies.

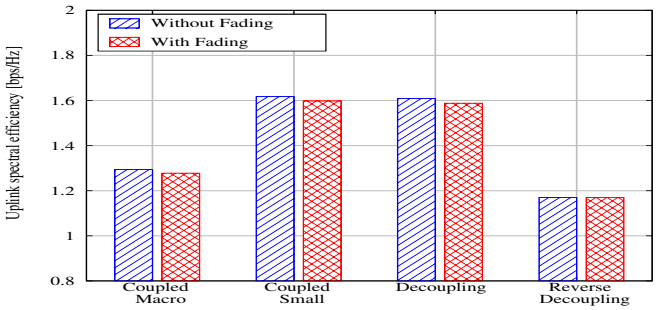

Figure 4.2: Uplink spectral efficiency with and without variable fading.

4.3 TDD HetNet Performance - Single Small Scenario

In order to first evaluate the system performance of a HetNet TDD based system in both uplink and downlink directions, we consider a HetNet with an offset factor $R_e = 0$. C_{es}, in this case, is equivalent to the average user capacity in the reference small cell (C_s).
Figure 4.4 captures the decrease in C_s by increasing the small cell radius. This is due to the fact that small cell users are in average closer to the macro BS and thus the interference from the macro BS and macro users will be

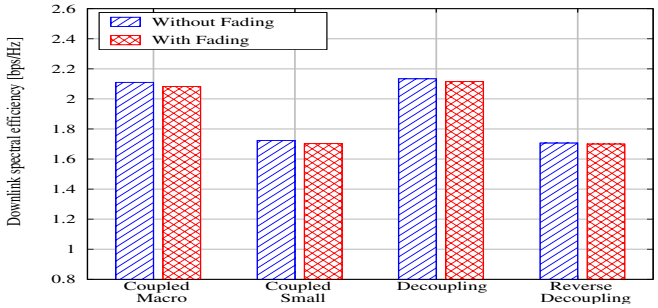

Figure 4.3: Downlink spectral efficiency with and without variable fading.

more significant. Moreover, we can observe that numerical results are in close agreement with the Monte-Carlo simulation.

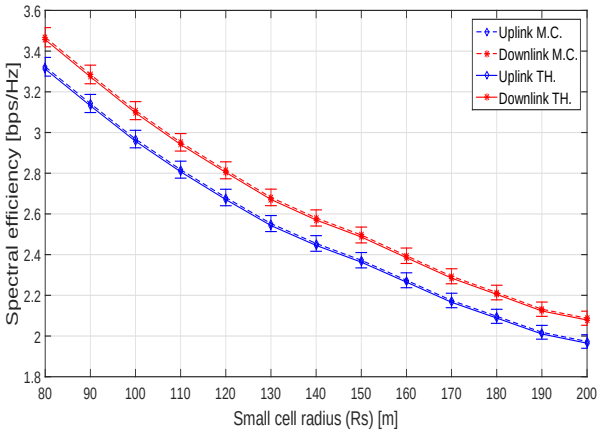

Figure 4.4: Capacity per unit bandwidth in the reference small cell as a function of small cell radius (R_s) with $N_s = 1$, $\gamma = 3$ and $d = 600$ m.

Figure 4.5 captures the increase in C_s when moving away the reference small cell from the macro cell. The interference, more specifically triggered by the macro BS, reduces when increasing the distance between the small cell and the macro cell. Figure 4.6 depicts C_s for different values of macro user uplink transmission power. Note

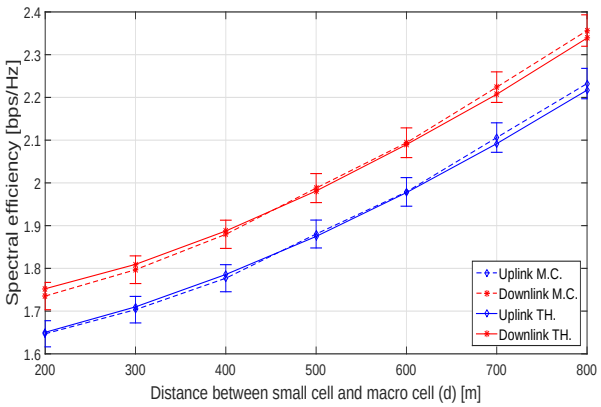

Figure 4.5: Capacity per unit bandwidth in the reference small cell as a function of the distance between the reference small cell and the macro cell (d) with $N_s = 1$, $\gamma = 3$ and $P_{um} = 0.22$ W.

that the increase of P_{um} value reduces the average small cell capacity and this is due to the increase of interference

triggered mainly by the macro users. Figure 4.7 investigates the effect of the path loss exponent in order to evaluate

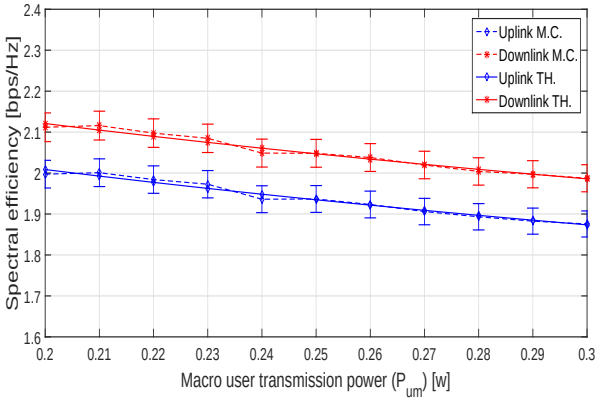

Figure 4.6: Capacity per unit bandwidth in the reference small cell as a function of the macro user transmission power (P_{um}) with $N_s = 1$, $\gamma = 3$ and $d = 600$ m.

the system performance under various propagation conditions and different environments. It can be observed that the increase in path loss exponent enhances the performance of the reference small cell users in uplink and downlink by mitigating the effect of the interference signal. From the aforementioned figures, it can be concluded that the

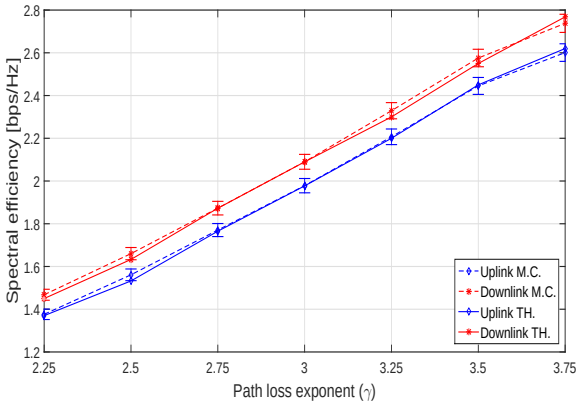

Figure 4.7: Capacity per unit bandwidth in the reference small cell as a function of the path loss exponent (γ) with $N_s = 1$, $d = 600$ m and $P_{um} = 0.22$ W.

derived capacity expression in (3.53) matches nearly perfectly Monte-Carlo simulation results.

4.3.1 Signal of Interest and Interference: Correlation Coefficient

Figures 4.8 and 4.9 show the correlation i.e. the statistical relationship between the signal of interest (S) and the interference (I) in the Up - Up and Down - Up scenarios respectively. Two scenarios are studied to compare the correlation coefficient among different scenarios from one side and to further justify our assumption about the dependency between S and I from the other side. Figure 4.8 shows a correlation of -0.002 and Fig. 4.9 shows a zero correlation. Therefore, it can be concluded that S and I are not statistically correlated and thus, they can be considered as two independent variables.

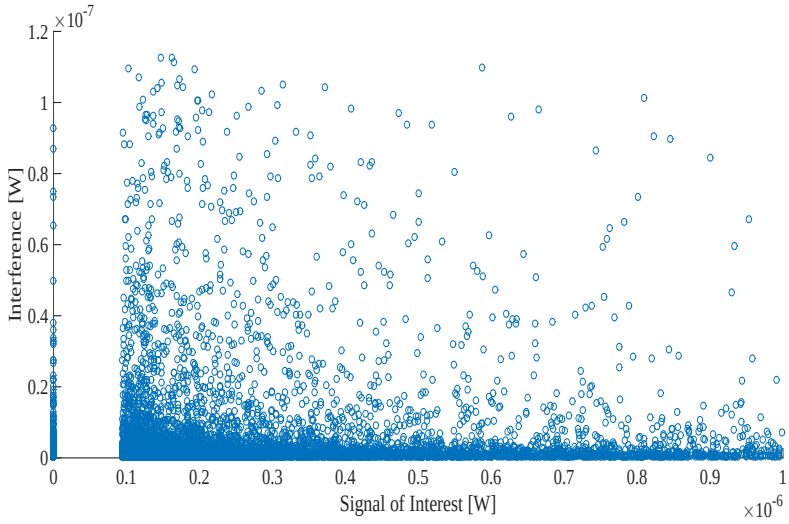

Figure 4.8: S and I correlation in the Up-Up scenario

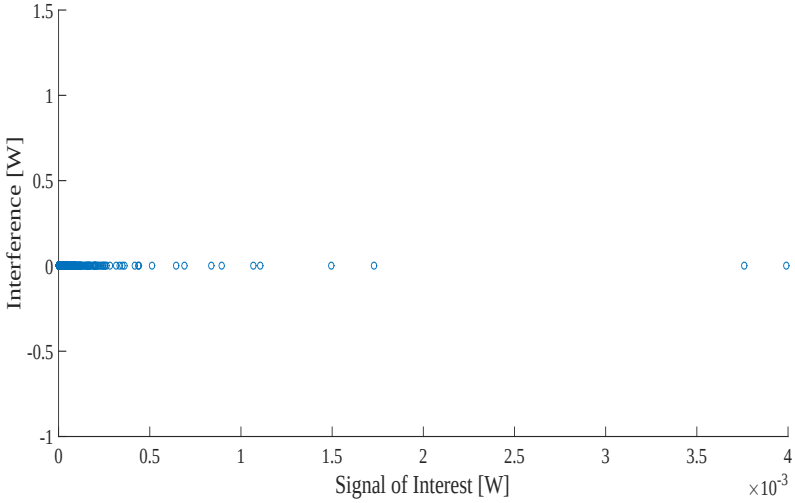

Figure 4.9: S and I correlation in the Down-Up scenario

4.3.2 Simulation vs Modeling: Execution Time

When evaluating the capacity expression in (3.53) over 4 TDD sub frames (Fig. 4.1), the execution time was found to be reduced by more than 50% compared to the time required to run 10 000 Monte-Carlo simulations over the same period. As we have mentioned in our model, we had recourse to the Laguerre polynomial in order to solve the capacity expression in (3.53). This expression will be then equal to the sum of n finite terms, where n may vary from 1 till infinity. Our purpose was to find the minimal value of n for which the series converges. Calculations were first done for n=4 and n=8 where we have retrieved a significant difference in the calculated values. Next, the calculations were done for n=8, 12, 16, 20, 24, 28, 32, 64, 80 and n= 100 until we found out that, with n=80 and n=100, the expressions converged nearly to the same value with a higher precision. Hence, we have chosen n=80 as the minimal value of n that gives us the more accurate and precise results.
Under this context, the required time to evaluate the capacity expression is found to be 0.55 sec for n=80. On the other hand, the computational time for running 10 000 Monte Carlo simulations is given by 1.13 sec. Note that the time to evaluate the capacity expressions and Monte-Carlo simulations depends on the type of processor, programming, and mathematical software package used. In this work, all capacity computations are conducted on a commonly laptop computer equipped with Intel(R) Core(TM)-i5 processor, 8 GB RAM, and using time functions in a standard mathematical software package, i.e., Matlab.

4.4 Impact of Decoupling Access Policy on TDD 5G HetNets - Single Small Cell Scenario

Our objective is to investigate analytically a TDD-based HetNet by applying various link association policies for a comprehensive performance comparison between DeUD and CoUD modes. Based on the statistical expressions derived for the interference and the desired signals in the previous chapter, the average UL/DL capacity of users in the small cell along with users in the expanded area will then computed separately. The main performance metric that is being measured, in both UL and DL, is the average capacity per unit bandwidth (C_{es}). It is calculated based on the average users capacity in the small cell area added to the average users capacity in the expanded area. Since the CM case represents the current system status before applying any change to the network configuration, our objective is to enhance the performance of the system in downlink and uplink by adopting three different association policies and comparing their performances in terms of spectral efficiency with the CM case.
Figure 4.10 depicts numerical values of C_{es} for each association strategy and in both UL/DL. We can conclude from this graph that the decoupling case shows an improvement in UL spectral efficiency (SE) around 1.65 bps/Hz in comparison with the CM case where the uplink SE is 1.35 bps/Hz. The same improvement in UL is observed for the coupled access with small cell case. The normal coverage area of the small cell, in this case (coupled with small cell), is expanded and the small cell users along with the users in the expanded area are now connected in UL and DL to the small cell BS. This situation is referred to as cell range expansion (CRE) technique. However and as expected, the coupled access with small cell case or what is called the CRE technique, leads to a degradation in downlink SE which is due mainly to the macro BS downlink interference affecting the users in the CRE region. This harmful downlink interference in the range expansion area is usually solved by applying the Almost Blank Subframe (ABS) technique [120]. This degradation can be easily observed in Fig. 4.10 where the downlink SE is reduced from 1.94 to 1.74 bps/Hz, whereas the decoupling case is showing a slight DL improvement from 1.94 to 1.96 bps/Hz.

Moving to the reverse decoupling case, we can notice a degradation in SE for both directions, from 1.35 to 1.23 bps/Hz in UL and from 1.94 to 1.78 bps/Hz in DL.
The aforementioned results indicate that the DeUD mode with decoupling access brings greater benefits in the uplink and maintains the same performance improvement in the downlink.

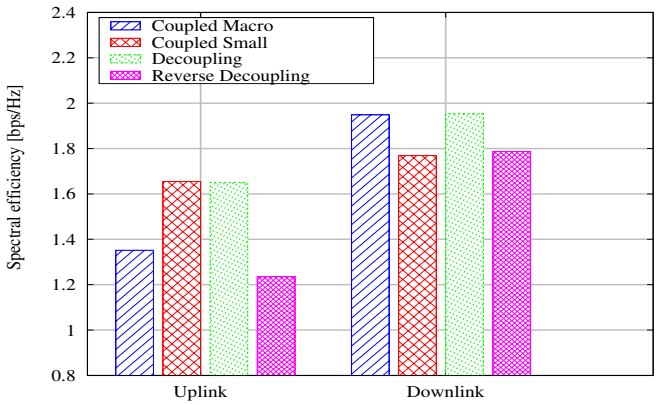

Figure 4.10: Capacity per unit bandwidth (C_{es}) in both UL/DL directions for various link association policies with $N_s = 1$, $\gamma = 3$ and $R_e = 300$ m.

Figures 4.11 and 4.12 show the uplink and downlink spectral efficiencies, for various association policies while varying R_e, the distance offset factor, between R_s and $R - d$. As expected, the decoupling case among all other cases, maintains a higher SE in uplink and downlink for all offset values. We can observe in Fig. 4.11 that the uplink SE, for the decoupling case, shows a considerable degradation for R_e values greater than 280 m, whereas the downlink SE, for the same case, shows a continuous improvement for all offset values as shown in Fig. 4.12. When increasing the offset value, the decoupled users attached to the macro cell in the downlink and to the small cell in the uplink, are now closer to the macro cell and further away from the small cell. Thus, the downlink received power from the macro BS will be effectively increased and the uplink received power by the small cell BS will be decreased. This explains the degradation in uplink SE and the improvement in downlink SE. Consequently, it is paramount to find out the trade-off between the uplink SE and the downlink SE which is in our case a threshold for R_e equal to 260

or 280 m. Last but not least, it can be concluded from Fig. 4.11 and Fig. 4.12, that Monte-Carlo simulation results match nearly perfectly the derived capacity expressions for various link association policies.

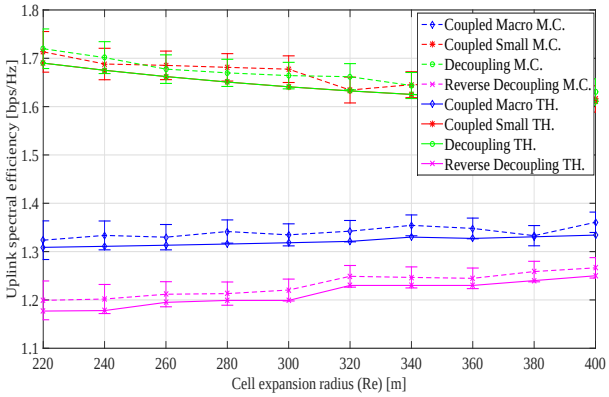

Figure 4.11: Comparison of the uplink spectral efficiency between CoUD and DeUD modes for various (R_e) offset factor with $N_s = 1$ and $\gamma = 3$.

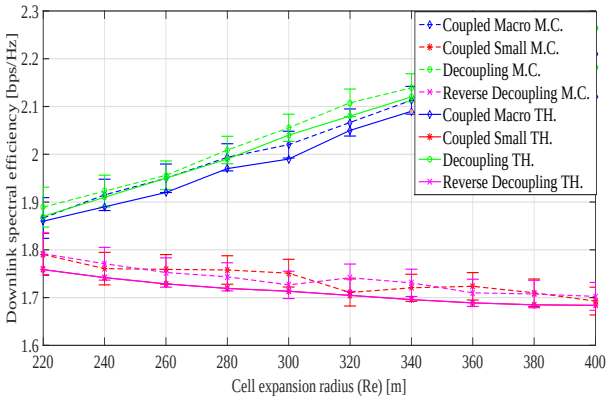

Figure 4.12: Comparison of the downlink spectral efficiency between CoUD and DeUD modes for various (R_e) offset factor with $N_s = 1$ and $\gamma = 3$.

4.5 Performance Evaluation of TDD and Decoupling - Multiple Small Cells Scenario

A new design parameter emerges when tackling a multiple small cells scenario. This parameter is the distance between small cells denoted by d_{12}. Deploying a new network configuration with randomly positioned interfering small cell implies 1000 iterations of Monte-Carlo simulations to obtain consistent and stable results. For each Monte-Carlo iteration, i.e. for each d_{12}, we generate uniformly distributed users in different cells for a large number of Monte-Carlo simulations (around 1000 iterations), to reach a total of 1 000 000 iterations.
In Fig. 4.13, we evaluate the average user capacity C_{es} in a multiple small cells environment for different association policies. As expected, we notice a decrease in UL and DL throughput values in comparison with the single small cell case (Fig. 4.10). With the increase in the number of interfering small cells, the interference level increases and thus, the average user throughput decreases for various association policies. Consequently and since the decoupling strategy prevails over the other policies, it will be more interesting to study the impact of the small cells distribution on the decoupling gain in a multiple small cells environment.
Figure 4.14 depicts the uplink decoupling gain as a function of the distance between the reference small cell and the interfering small cell (d_{12}). We introduce Monte-Carlo simulations to demonstrate the accuracy of the analytical

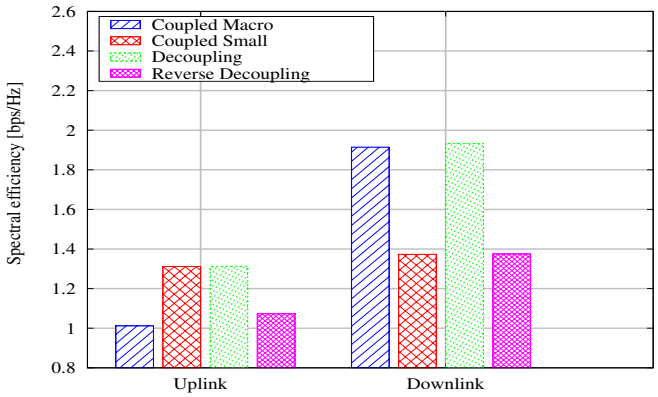

Figure 4.13: Capacity per unit bandwidth (C_{es}) in both UL/DL directions for various link association policies with multiple small cells deployment: $N_s = 2$, $\gamma = 3$, $R_e = 300$ m and $d_{12} = 800$ m.

expressions derived for the decoupling gain in the previous chapter. We can observe that keeping the interfering small cell far from the reference small cell for a given distance, increases the uplink decoupling gain. Exceeding this threshold, we can notice that the uplink gain maintains a constant value regardless the distance between small cells, i.e. no more gain in UL is realized throughput when moving away the interfering small cell for more than 1100 m from the reference small cell. To better understand this behavior, we benefit from the expressions derived in the previous section for different uplink scenarios (Down - Up and Up - Up), to plot the graph in Fig. 4.15. Since increasing the distance (d_{12}) has a minimal impact on the uplink gain in the Down - Up scenario, it is clearly shown that the behavior observed in Fig. 4.14 is provoked mainly by the Up - Up scenario. In the Up - Up scenario and when increasing the distance between small cells to more than 1100 m, the impact of the interfering small user I_i becomes almost negligible and thus, the major impact on the uplink throughput appears to be the interference experienced from the macro user I_m. This interference has a negative impact on the decoupling case in comparison with the CM case, because of the presence of a decoupled zone in the interfering small cell. The latter allows a closer area for the macro users toward the reference small cell and thus, a considerable interference with the uplink desired signal in that small cell. This will explain the steadiness of the uplink gain beyond a given distance (d_{12}).

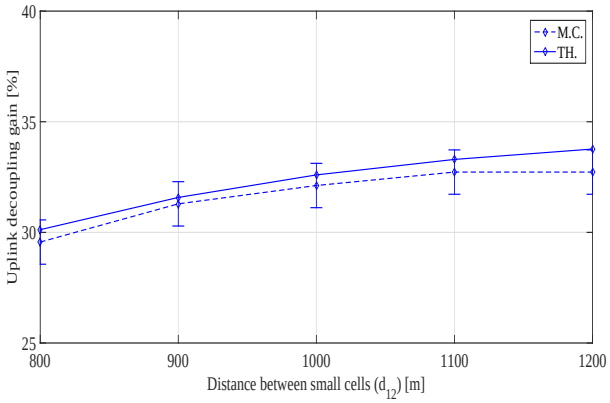

Figure 4.14: Uplink decoupling gain (η_{UL}) as a function of the distance between small cells (d_{12}) with $N_s = 2$, $\gamma = 3$ and $R_e = 300$ m.

Figure 4.16 depicts the downlink decoupling gain as a function of the distance between the reference small cell and the interfering small cell (d_{12}). It can be noticed that the downlink decoupling gain shows a slight downward trend when the distance d_{12} increases. Analyzing the two main downlink scenarios in Fig. 4.17, we found out that the main reason behind the downlink gain decrease is the interference experienced from the macro user at the small cell user in the Up - Down scenario. Similar to the uplink case, this interference has a negative impact on the decoupling case because of the presence of a decoupled zone in the interfering small cell. The latter allows a closer area for the macro users to interfere with the downlink desired signal at the small cell user. However, the fact that

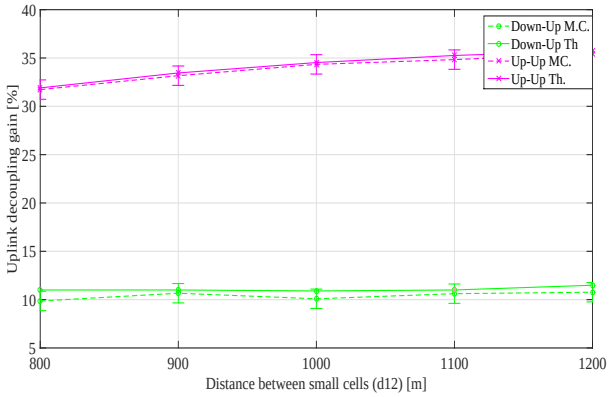

Figure 4.15: Uplink decoupling gain breakdown analysis: Down - Up and Up - Up scenarios with $N_s = 2$, $\gamma = 3$ and $R_e = 300$ m.

the decoupling case improves the uplink scenarios in the expanded area at the expense of the downlink scenarios, explains the steadiness of the uplink decoupling gain and the degradation of the downlink gain after a given value of d_{12}. This will explain as well the zero value of the downlink gain obtained in the Down - Down scenario ($\eta_{DL} = 0$).

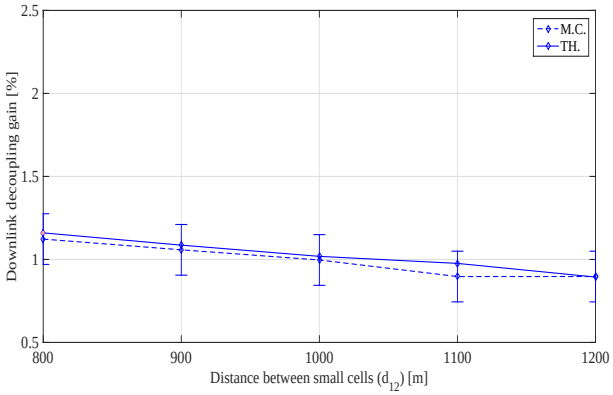

Figure 4.16: Downlink decoupling gain (η_{DL}) as a function of the distance between small cells (d_{12}) with $N_s = 2$, $\gamma = 3$ and $R_e = 300$ m.

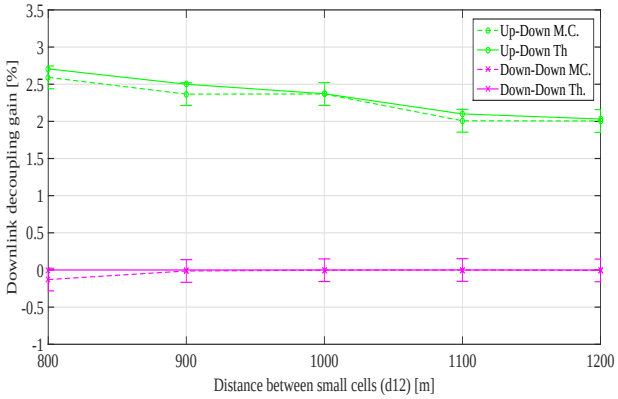

Figure 4.17: Downlink decoupling gain breakdown analysis: Up - Down and Down - Down scenarios with $N_s = 2$, $\gamma = 3$ and $R_e = 300$ m.

Furthermore, it would be interesting to address a joint optimization problem, i.e. to evaluate the uplink decoupling gain as a function of two variables: the small cell offset factor and the distance between small cells. While accounting for two small cell offset values ($R_e = 250$ m and $R_e = 300$ m), Fig. 4.18 highlights the gain obtained for d_{12} below 1100 m, the range where the uplink gain is achieving a significant improvement (Fig. 4.14). We can notice that the highest uplink decoupling gain (36.2 %) is achieved with $d_{12} = 1000$ m and $R_e = 250$ m. On the other hand, when increasing the offset value to e.g. $R_e = 300$ m, the decoupled zone in the interfering small cell becomes larger and macro users closer to the reference small cell and thus, the interference increases. Moreover, the uplink desired signal decreases because of the small cell users that are now transmitting to a farther cell. Consequently, the uplink gain decreases to 32.5 %.

To further elaborate on the joint optimization subject, Fig. 4.19 captures the system performance under all possible

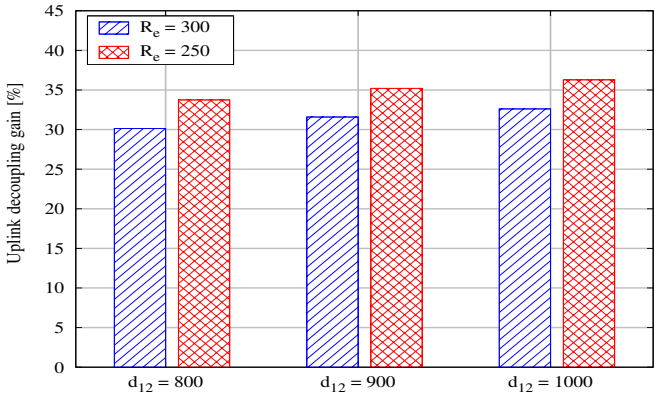

Figure 4.18: Uplink decoupling gain (η_{UL}) as a function of both the offset factor (R_e) and the distance between small cells (d_{12}) with $N_s = 2$ and $\gamma = 3$.

combinations between the small cell coverage (R_e) and small cell placement (d_{12}). Consequently, it is paramount to find the optimal solution which is in our case, a combination of a decoupling region with a radius R_e equal to 210 m and a small cell placement with a distance d_{12} equal to 1000 m.

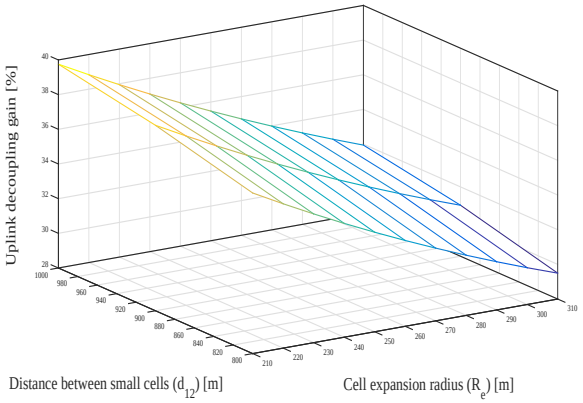

Figure 4.19: Uplink decoupling gain (η_{UL}) as a function of all possible (R_e, d_{12}) combinations with $N_s = 2$ and $\gamma = 3$.

4.5.1 Simulation vs Modeling: Execution Time in Multiple Small Cells Environment

The required time to analytically evaluate the decoupling gain expression in (3.93) is found to be 10 to 15 seconds, giving fairly accurate results with a higher precision ($n = 80$) adopted in the computation of Laguerre polynomial in (3.86). On the other hand, the computational time for running 1 000 000 Monte-Carlo simulations is given by 4 570 seconds which is significantly larger, when compared to the analytical expression evaluation time. Hence, there is a strong need for an analytical model as a replacement for the time consuming Monte-Carlo simulations, especially in multiple small cells environments.

4.5.2 Power Control and Reduction in Power Consumption

In order to investigate the impact of considering the power control in our model, we have introduced a power control mechanism with $P_0 = 10^{-7}$ W (-40 dBm) and P_{max} equal to 0.2 W for both macro and small cell users. Comparing Fig. 4.20 (with power control) to Fig. 4.13 (without power control), we can deduce that, considering power control (PC) will reduce uplink throughputs and increase downlink throughputs for various association policies. In uplink, considering the PC will reduce the uplink transmitted signal with a slight change in the interference signal; this will explain the decrease in throughput value. However, in downlink, the decrease in uplink transmitted signal will reduce the uplink to downlink interference and keep the same downlink signal; this will justify the increase in downlink throughput. Moreover, it can be concluded that the impact of decoupling remains the same when considering the power control mechanism; the decoupling technique continues to prove that it prevails over the other association policies. Figure 4.21 shows the reduction in uplink power consumption when implementing the

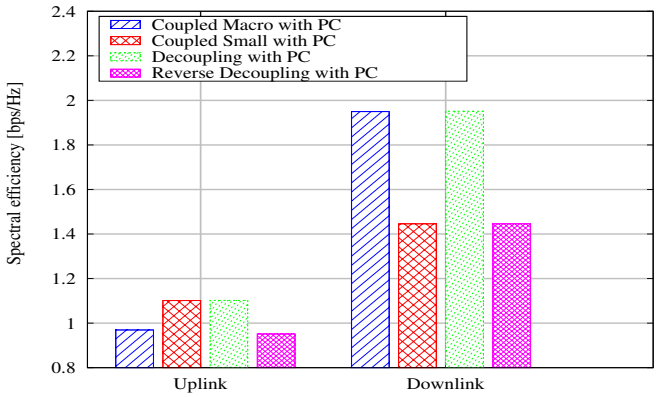

Figure 4.20: Spectral efficiency (C_{es}) in both UL/DL directions considering power control (PC) with $P_0 = 10^{-7}$ W (-40 dBm), $N_s = 2$, $\gamma = 3$, $R_e = 300$ m and $d_{12} = 800$ m.

power control mechanism with various association policies. It can be noticed that the coupled with macro cell policy captures the highest reduction in power consumption (PR = 61.7 %), from 0.26 W (without PC) to 0.16 W (with PC). With PC, the macro users that are close to their BS refrain from transmitting with P_{max}, instead they will be compensating the path loss with a transmitted power less than P_{max}. This is behind the remarkable uplink power reduction noticed in the coupled with macro case.

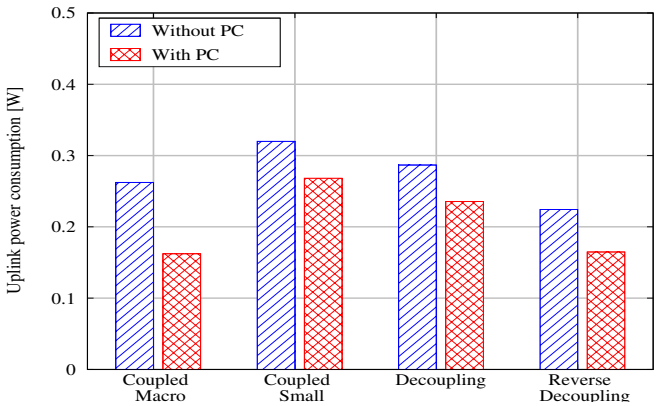

Figure 4.21: Uplink power consumption with PC and without PC with $P_0 = 10^{-7}$ W (-40 dBm), $N_s = 2$, $\gamma = 3$, $R_e = 300$ m and $d_{12} = 800$ m.

4.5.3 Unsynchronized TDD configuration

To investigate an unsynchronized case, we consider frame structures that cover all possible uplink/downlink combinations between the macro and the small cells, as shown in Fig. 4.22. In Fig. 4.23, a slight decrease in uplink

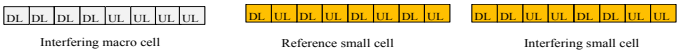

Figure 4.22: Unsynchronized TDD frame structure across small cells.

throughput can be noticed for different association policies when considering the unsynchronized TDD case. This is due mainly to the interference experienced from the interfering small cell downlink signal at the reference small cell uplink desired signal. This type of interference, referred to as Down - Up interference, exists and has a considerable effect in the case of an unsynchronized TDD configuration, more specifically in the case where the interfering small cell is operating in uplink and the reference small cell is operating in downlink. Moreover, it is interesting to note that,

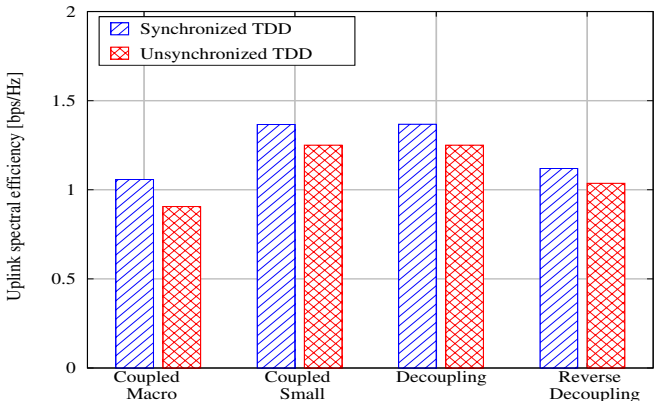

Figure 4.23: Comparison of the uplink spectral efficiency (C_{es}) between a synchronized and an unsynchronized TDD mode with $N_s = 2$, $\gamma = 3$, $R_e = 300$ m and $d_{12} = 800$ m.

due to the fact that the users in different small cells are not synchronized in downlink/uplink transmissions, users in the expanded areas of the interfering small cell and the reference small cell cannot be decoupled at the same time. Therefore, the decoupling zone at the interfering small cell is no more a second or an additional source of interference. This will explain the improvement brought to the uplink decoupling gain in the case of an unsynchronized TDD configuration as shown in Fig. 4.24.

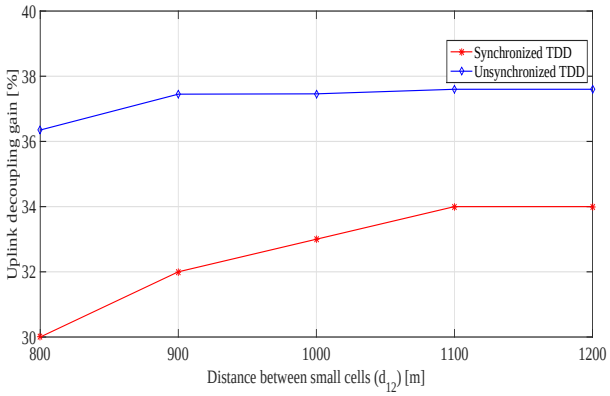

Figure 4.24: Comparison of the uplink decoupling gain (η_{UL}) between a synchronized and an unsynchronized TDD mode for various d_{12} values with $N_s = 2$, $\gamma = 3$ and $R_e = 300$ m.

4.6 Conclusion

Our proposed model provides a valuable tool to evaluate the system performance in terms of downlink/uplink average capacity, decoupling gains and other performance metrics. The provided numerical results will help in optimizing networks parameters and designing cellular network under various conditions.
In this chapter, we have first evaluated the system performance of a HetNet TDD based system in both uplink and downlink directions, taking into account all possible UL/DL TDD combinations between the macro cell and the small cell. The network consists of one macro cell and one small cell. For example, the system performance was evaluated when controlling the user transmit power using power control mechanism. Further, the effect of large path loss exponents proved to enhance the performances of small cell users.
Second, we have conducted both downlink and uplink performance comparison study for four various cell association rules in TDD HetNet, based on a geometric probability approach. The network also consists of one macro cell and one small cell. Two cases were considered with UL/DL coupled access and two others with decoupled access. We have observed that the decoupling case (part of DeUD mode) brings a higher downlink and uplink throughputs for various offset values and thus, improves the overall system performance when being combined with a dynamic TDD technology. However and as expected, the coupled access with small cell case, i.e. the CRE technique, leads to a degradation in downlink spectral efficiency due mainly to the macro BS downlink interference affecting the users in the CRE region. Also, we have found out that our modeled network can be further optimized when choosing a specific small cell offset as a trade-off between UL and DL spectral efficiencies.
Last but not least, we have analyzed, in a multiple small cells environment, the uplink and downlink decoupling gains as a function of both the small cell offset factor and the distance between small cells. We have realized that our modeled network can be further optimized by adopting the optimal combination of both the small cell offset factor and the distance between small cells. Identifying the location of the interfering small cell and the small cell offset factor will help in improving the gain that the decoupling mode can bring to a multiple small cells TDD HetNet. Considering a power control mechanism has reduced uplink throughputs and increased downlink throughputs for various association policies. Moreover, implementing the power control mechanism with various association policies has caused a reduction in mobile users' uplink power consumption, especially in the coupled with macro cell case. A slight decrease in uplink throughput has been noticed for different association policies when considering the unsynchronized TDD case. Also, an improvement in the uplink decoupling gain has been detected in the case of an unsynchronized TDD configuration.
However and in order to analytically model an environment relative to a real case scenario, the derived expressions in Chapter 3 must be updated to include the following: high number of small cells, multiple users, scheduling strategies, dynamic resource allocation algorithm, various channel models and load traffic disparity. Such an enhanced analytical model will incur huge computational complexity and any assumption made at this stage in the design parameters, aiming to reduce complexity will lead to non-realistic results. In this context and in order to overcome this limitation, we implement in the next chapter the decoupling and dynamic TDD techniques in a system level simulator, and we consider these techniques in the design of a joint optimization algorithm. This will allow as well to figure out the gain from an adaptive TDD and decoupling in a HetNet based system, according to time-variant traffic loads.

Chapter 5

Adaptive TDD and Decoupling in 5G HetNets: Simulation-Based Evaluation

5.1 Introduction

It is worth mentioning that the statistical models developed in chapters 3 and 4 play an imperative role in evaluating the system performance metrics such as spectral efficiency, decoupling gain and average power consumption. However, this model evaluates the average capacity of only one user and without addressing the traffic adaptation and dynamic resource allocation challenges. Moreover, it doesn't consider a variable fading in the propagation model. For this reason, we propose a 5G HetNet system level simulator where we can present the motivation and accurately assess the role of both decoupling and dynamic TDD techniques in the UL/DL optimization problem. In this chapter, we create appropriate simulation environment that is relative to real scenarios i.e. simulations where multiple small cells are deployed in a heavy loaded HetNet system and under various traffic loads. These simulation scenarios consider random users distribution with scheduling decisions in both the uplink and the downlink directions. Our objective is to prove that there is an optimal combination between the TDD scheme and the user association policy with respect to any change in the system, especially in the UL/DL traffic ratio. In this context, we consider one conventional UL/DL coupled user association policy and two types of decoupled UL/DL link association policies.

5.2 Network Model

We consider a two-tier heterogeneous cellular network consisting of one macro cell and multiple small cells as shown in Fig 5.1. We denote by N_s the number of small cells. In the coming sections, the radius of the macro cell and the small cell will be denoted by R and R_s, respectively. All users are uniformly distributed between the macro cell and the small cells. They are using a full buffer traffic model in UL as well as in DL. We define η, as the UL to DL traffic ratio between the users operating in UL and those operating in DL. The total number of active users equipment (UEs) is denoted by N_u.
As simulation setup, we consider the LTE-sim simulator [121] to which we have added customized features in order to be aligned with our system model. The added modules include, but not limited to, decoupling and dynamic TDD techniques. More details about the customization are available under Section 5.3.

5.2.1 UL/DL User Association Policies

Three different association policies have been implemented in this chapter; they can be dynamically selected as input parameters for the simulations that follow. In these simulations, we compare the conventional UL/DL coupled user association policy with two types of decoupled UL/DL link association policies as follows:

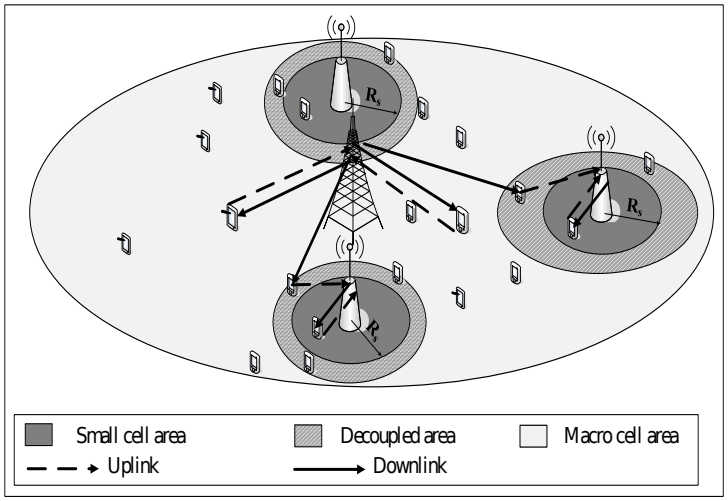

Figure 5.1: Illustration of the proposed system model.

- Cell association criteria in DL and UL is based on DL Reference Signal Received Power (RSRP) which is the conventional LTE user association policy. This case is referred to as **CoUD**.

- Cell association criteria in DL is based on DL Reference Signal Received Power (RSRP) whereas the criteria in UL is based on the uplink received power with cell selection offset in case of a small cell. A cell selection offset is added to the received power at the small cells to increase their coverage in UL and thus, to offload UL traffic from the macro cell. In this work, we consider an offset equal to 13 dB. This value was selected from the recent literature on decoupling ([96], [104] and [105]) having power based association criteria in UL with selected bias values. We have analyzed the derived expressions in the aforementioned articles in order to retrieve a common offset value which is 13 dB.
  This case is referred to as **DeUD_PO**.

- Cell association criteria in DL is based on DL Reference Signal Received Power (RSRP) whereas the criteria in UL is based on the path loss. This case is referred to as **DeUD_PL**.

5.2.2 Dynamic TDD Approach

In the 3GPP standard, dynamic TDD is supported by seven configurations with respect to different uplink and downlink traffic ratios [62]. As shown in Fig. 5.2, each radio frame consists of 10 subframes, and the UL/DL ratio is different for each TDD frame configuration. This enables either the macro cell or the small cells base stations to select different configurations according to the traffic variation. In this context, we define the following notations:

- m denotes the UL/DL TDD configuration in the macro cell.

- s denotes the UL/DL TDD configuration in all small cells.

- $T = (m, s)$ denotes the joint UL/DL TDD configuration in the system.

For example, we denote by (0,5) a joint TDD configuration between macro and small cells where 0 and 5 are the UL/DL TDD configurations adopted in the macro cell and the small cells respectively (see Fig. 5.2).

TDD UL-DL Configuration	DL-UL Switch-point periodicity	Subframe number									
		0	1	2	3	4	5	6	7	8	9
0	5 ms	D	S	U	U	U	D	S	U	U	U
1	5 ms	D	S	U	U	D	D	S	U	U	D
2	5 ms	D	S	U	D	D	D	S	U	D	D
3	10 ms	D	S	U	U	U	D	D	D	D	D
4	10 ms	D	S	U	U	D	D	D	D	D	D
5	10 ms	D	S	U	D	D	D	D	D	D	D
6	5 ms	D	S	U	U	U	D	S	U	U	D

Figure 5.2: Supported TDD configurations in 3GPP [62].

5.3 System Level Simulator for Next Generations HetNets

We propose a 5G HetNet system level simulator that supplements the existing LTE-Sim simulator [121]. The latter is an open source framework to simulate LTE networks including downlink and uplink scenarios at system level. More details about LTE-Sim are included in Appendix A. This combination allows for detailed simulation of both dynamic TDD and decoupling techniques and to study their impact in real case scenarios. All the add-ons and customization made on top of LTE-Sim simulator to answer our proposal requirements, are described in details under this section.

5.3.1 Selection of LTE-Sim Simulator

The most common simulators for mobile networks are Vienna [125], NS3 [126], SimuLTE [127], NetSim [123], OPNET [124] and LTE-Sim [121]. After a thorough research, a decision has been made to adopt the LTE-Sim simulator because it has the required tools to build a simulation platform for next generation 5G HetNets. The survey we have done on available system level simulators (Table 5.1) further justifies the selection of LTE-Sim:

1. LTE-Sim has been written in C++, using the object-oriented paradigm, as an event-driven simulator in order to ensure modularity, polymorphism, flexibility, and high performance.
2. LTE-Sim is an open source framework so it is easy to apply changes at the core or simulation level.
3. It is a system level simulator where we can manage HetNets which is essential in this thesis.
4. It includes basic downlink and uplink scenarios which is also the target of a thesis addressing a joint UL/DL optimization problem in HeNets.
5. It supports basic conventional TDD configurations. This part can be enhanced by allowing base stations to dynamically select different TDD configurations according to instant traffic loads.

Simulator	Duplex Mode	HetNets	Open Source
Vienna	FDD (DL direction)	✓	Commercial
NS3	FDD	✓	Open Source
SimuLTE, OMNeT++ & INET	FDD	✓	Open Source
NetSim	FDD	✓	Commercial
OPNET	TDD	✓ (Customized)	Commercial
LTE-Sim	TDD	✓	Open Source

Table 5.1: A survey of system level simulators.

5.3.2 System Level Simulator Framework

LTE-Sim is an event-driven simulator. Its main classes handle: (i) network devices, (ii) protocol stack entities, (iii) PHY layer, (iv) channel behavior, and (v) network topology. In order to implement all aspects related to our proposal, LTE-Sim has been upgraded by means of new classes and functionalities listed in the sections that follow.

5.3.3 LTE-Sim Customization and Add-Ons

In this section, we present a novel module developed for the simulation of both TDD and decoupling techniques with the LTE-Sim simulator. The main focus of this module is the implementation of customizable TDD configurations and various association policies. Figure 5.3 illustrates all changes applied on top of LTE-Sim Release 5 in a way to fit our proposal requirements.

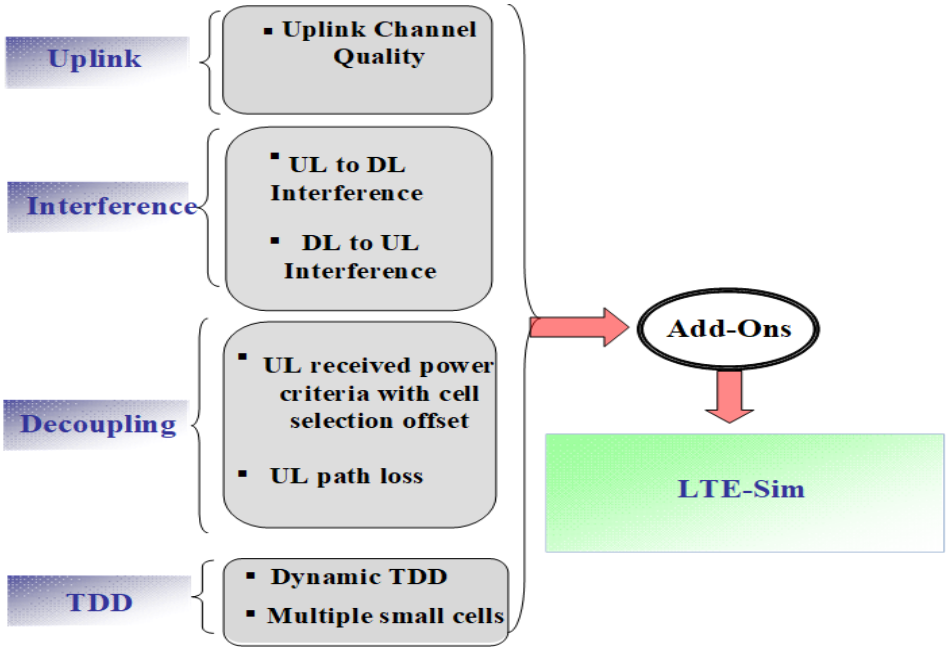

Figure 5.3: LTE-Sim add-ons

- Instead of using the CQI indicator for downlink and uplink scheduling, a new metric named uplink channel quality is implemented in the uplink scheduling.
- Updating the conventional TDD framework to include the dynamic TDD feature.
- Calculating the cross-link interference (UL to DL and DL to UL). This interference results from applying the dynamic TDD approach.
- Developing two types of decoupled UL/DL link association policies: one based on UL path loss and the other based on UL received power assisted with cell selection offset.
- Creating and configuring multiple instances of small cells in a HetNet dynamic TDD based system.

Fig. 5.4 gives the UML diagram of the classes we modified to ensure required customization. This diagram shows the modified functions /variables along with the added new functions/variables. The latter are highlighted in blue.
More details about the various classes and their interoperation are provided in the next sections and under Appendix A.3.

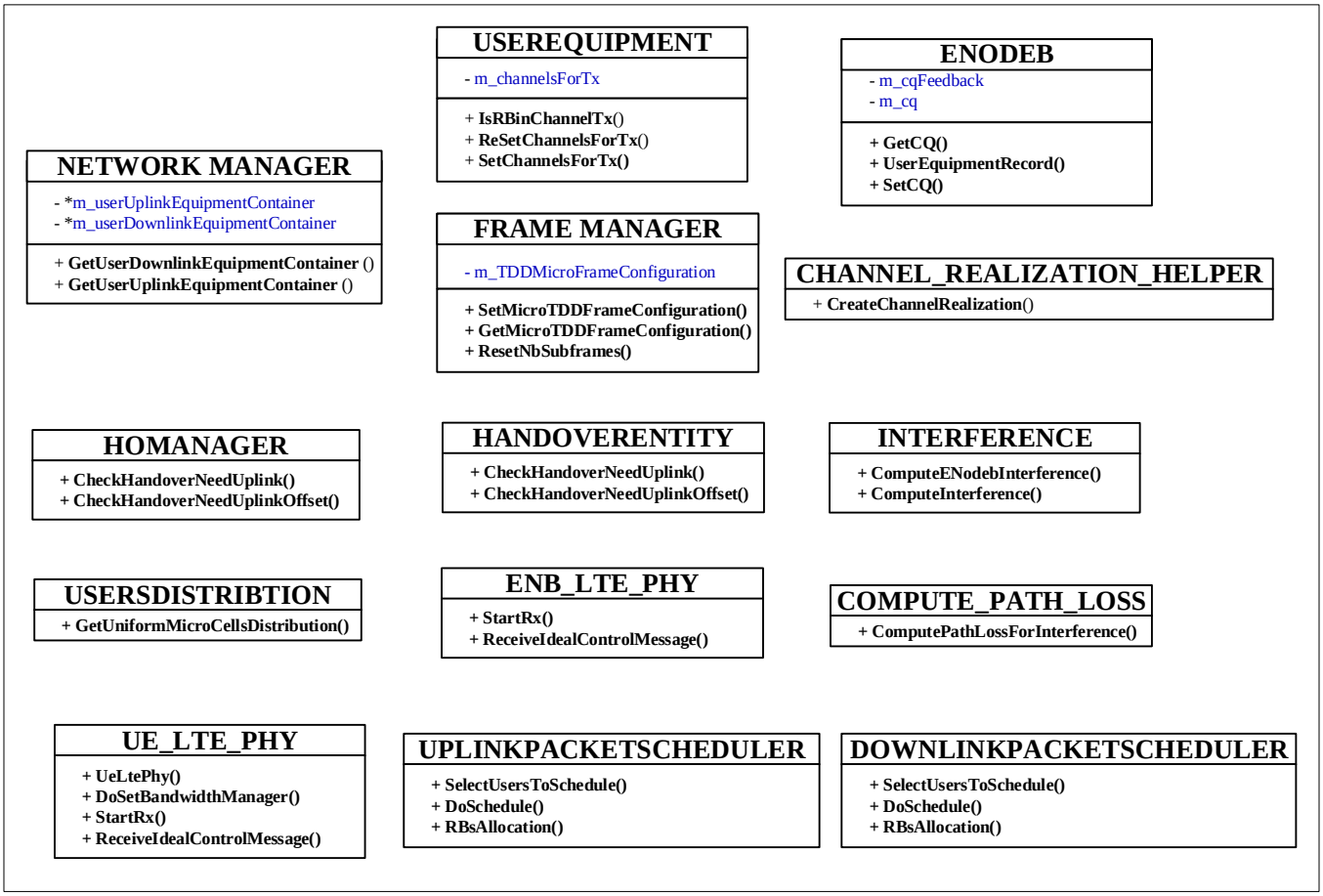

Figure 5.4: LTE-Sim: Updated class diagram

Uplink Channel Quality

The uplink scheduler in the current version of LTE-sim is very basic and still relying on downlink CQI feedback. This scheduler is not aligned with the real and correct uplink behavior in LTE environment. Under this context, we propose to consider an uplink scheduler based on the uplink channel quality and to include the uplink interference at each resource block.
The most crucial part in the uplink interference calculation at a resource block level is to get the number of allocated RBs per user from the scheduler, use this value to calculate during the transmission period the transmitted power and then calculate the interference per RB. In uplink, the interference occurs at the BS level and it is caused by mobiles that might be having different powers, transmitting from different locations, and having a transmission period based on the selected scheduling algorithm. In downlink, it is much easier to calculate the transmitted power per RB where the eNodeB is constantly transmitting on all RBs.
Taking an example where the allocated RBs for a micro user are highlighted in purple and the allocated RBs for a macro user are highlighted in green (figure 5.5). Calculating the uplink interference on RB_2 for the micro user will take into account the transmitted power of the macro user that is transmitting on the same RB_2. However, calculating the interference on RB_1 for the macro user will not consider the transmitted power of the micro user that is not transmitting on the same RB_1.

We describe in Appendix A.3 the changes applied at the source code level to optimize the uplink process.

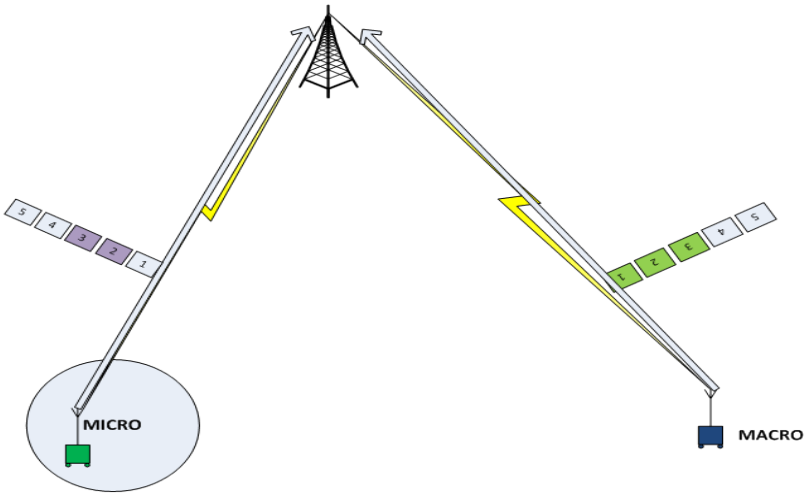

Figure 5.5: Uplink scheduling [resource block level]

Dynamic TDD

One important step toward the implementation of the dynamic TDD approach is to create a new TDD configuration variable for small cells (TDD_Smallcells), that is different from the macro cell configuration (TDD_Macrocell) as shown in Fig. 5.6. Also, this will require adding the function FrameManager::GetMicroSubFrameType (see Fig. 5.4)

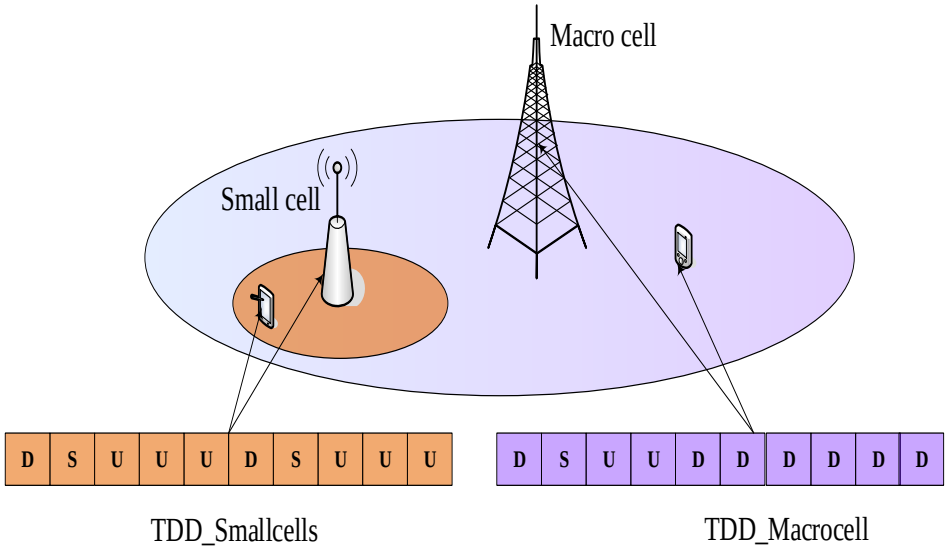

Figure 5.6: TDD configuration between macro and small cells.

and updating FrameManager::ResourceAllocation within the existing source code.

Cross-link Interference

Dynamic TDD enables flexible adjustments of uplink and downlink resources according to the instantaneous traffic load. However, it also brings new challenges in heterogeneous cellular networks because of the introduction of cross-link interference i.e., uplink to downlink interference and downlink to uplink interference. For example, a small cell can be operating in a specific direction while a macro cell might be operating in the opposite direction. This will induce an UL to DL or a DL to UL interference or what is called cross-link interference. Therefore, we first introduce the calculation of the UL to DL interference at the mobile user level with the Interference::ComputeInterference

function. Second, we introduce the calculation of the DL to UL interference at the base station level with the Interference::ComputeENodebInterference function (see Fig. 5.4).

Decoupling

In the initial version of LTE-Sim simulator, the user association criteria in DL and UL is based on DL Reference Signal Received Power (RSRP) which is the conventional LTE user association policy. However, since our proposal requires the implementation of the UL/DL decoupled access policy, we have added two different decoupling policies to the existing simulator, **DeUD_PO** and **DeUD_PL**:

A. DeUD_PO

A cell selection offset is added to the received power at the small cells to increase their coverage in UL and thus, to offload UL traffic from the macro cell. Under the scope of this work, we consider a new variable designating the offset or the bias value. This variable is set to 13 dB by default.
To implement this policy under the system level simulator, we create three new functions: NetworkManager::SelectTargetNodeUplinkOffset, HandoverEntity::CheckHandoverUplinkNeedOffset, and PowerBasedHoManager::CheckHandoverNeedUplinkOffset (see Fig. 5.4).

A. DeUD_PL

To implement this policy under the system level simulator, we create as well three new functions: NetworkManager::SelectTargetNodeUplink, HandoverEntity::CheckHandoverUplinkNeed, and PowerBasedHoManager::CheckHandoverNeedUplink (see Fig. 5.4).

Multiple Small Cells

The deployment of multiple small cells requires the development of a new method that will randomly distribute the small cells inside the macro cell region. The detailed method of creation of these small cells, along with their respective eNBs is available under Appendix A.3.

5.3.4 System Level Simulator Setup

For our simulation-based evaluation, we use the LTE-Sim [121] system level simulator to which we have added the enhancements previously described in Section 5.3.3.
For the selected scheduling algorithms, there are various scheduling methods that have been developed over time to enhance the process of data distribution. In this work, we shall be concentrating on two algorithms in particular: Round Robin as uplink scheduler and Proportional Fair as downlink scheduler. As for the selected propagation loss model, the large scale shadowing fading has been modeled through a log-normal distribution with 0 mean and a standard deviation of 8 dB. The penetration loss is set to default value of 10 dB. The fast fading is conceived for all the implemented propagation loss models by the Jakes model [122] for the Rayleigh fading, taking into account the user speed, the sub-carrier frequency, and a number of multiple paths uniformly chosen in the set [6, 8, 10, 12]. In our simulator, we consider the users in a constant position with zero speed. Figure 5.7 shows an example of multipath realizations when users speeds are equal to 0, 3, 30, and 120 km/h. As for the pathloss, the implemented models can be grouped under one expression that can be written as follows:

$$PL(dB) = A + 37.6 log_{10} r \ @ \ 2\text{GHz}, \tag{5.1}$$

where r is the distance between the transmitter and the receiver in kilometers and A is a constant that is set to 140.7 in urban areas, to 128.1 in suburban areas and to 100.54 in rural areas. In our simulation, small cells and macro cell are mapped to urban and suburban areas respectively.
The thermal noise per sub-channel is derived as follows:

$$\begin{aligned}\text{Thermal noise per sub-channel}(dB) = \text{Thermal noise density}(dB/Hz) + \\ 10 log_{10}(\text{Sub-channel bandwidth in Hz}) + \text{Noise figure}(dB).\end{aligned} \tag{5.2}$$

The simulation parameters in Table 5.2 have been considered so as to create the most appropriate simulation environment that is relative to real scenarios.

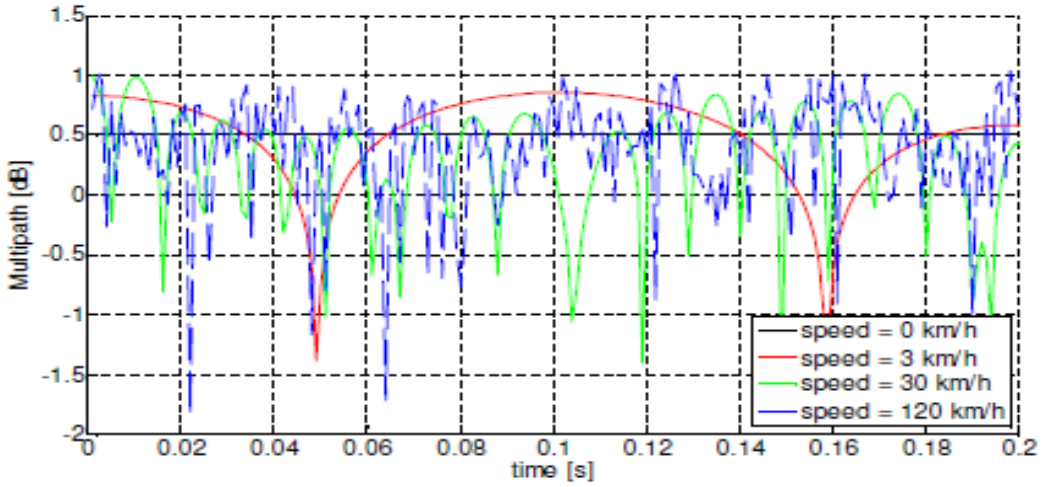

Figure 5.7: Fast fading realization

Parameter	**Value**
Macro cell radius (R)	1 Km
Small cell radius (R_s)	250 m
Min. distance between small cell and macro cell	50 m
Carrier frequency	2.0 GHz
Duplex mode	Dynamic TDD
TDD frame length	10 subframes
Sub-frame duration	1 ms
System bandwidth	20 MHz
Resource blocks or sub-channels	100
Max. macro BS transmit power	46 dBm
Max. small cell BS transmit power	30 dBm
Max. UE transmit power	23 dBm
Thermal noise power spectrum density	-174 dBm/Hz
Sub-channel bandwidth	180 KHz
Thermal noise per sub-channel	-148.95 dB
Noise figure	2.5 dB
User mobility model	Constant position, speed =0

Table 5.2: Simulation parameters

To note that on both downlink and uplink scenarios, only one flow per user was initiated, transmitting an infinite buffer application on top of UDP transport protocol. Resource allocation in each simulation is carried out over a period of 1 second (i.e. 100 LTE frames). In order to obtain accurate and stable results, simulation output values are averaged over 100 iterations. In the conducted simulations, we follow the procedure elaborated in Algorithm 1 to jointly implement a dynamic TDD based system with coupled/decoupled user association policies and to analyze the outcome resulting from this joint implementation. The algorithm starts by initializing the design parameters to their conventional values. The joint TDD configuration between macro and small cells is set to (0,0) and the association policy is set to CoUD. V captures any change in the system variables, e.g. traffic load. This change triggers a while loop till finding the optimal UL/DL average throughput (C_{opt}). At each step, the iteration changes at least one of the design parameter: m, s or the association policy. The calculated UL/DL total throughput resulting from this iteration is compared to the previous values of C_{opt}. The algorithm terminates by finding the optimal combination of TDD configuration and association policy that offers the highest (C_{opt}) throughput.

Algorithm 1 Adaptive TDD and coupled/decoupled user association policies

```
1: procedure SIMULATION PROCEDURE
2:     T=(m,s) ← Joint TDD configuration
3:     ua ← User association policy
4:     V ← System input variables
5:     C_opt ← UL and DL optimal average throughput
6:     Temp_opt ← UL and DL temporary optimal average throughput
7:     C_opt ← Calculate(ua,(m, s), V)
8:     while V changes do
9:         for m ← 0 to 6 do
10:            for s ← 0 to 6 do
11:                ua ← CoUD
12:                Temp_opt ← Calculate(ua,(m, s), V)
13:                if Temp_opt > C_opt then
14:                    C_opt ← Temp_opt.
15:                ua ← DeUD
16:                Temp_opt ← Calculate(ua,(m, s), V)
17:                if Temp_opt > C_opt then
18:                    C_opt ← Temp_opt.
```

5.3.5 Network Performance Metrics

In this chapter, several performance metrics are identified to be used as a means to evaluate and compare all simulation results. We present hereafter the definition and the motivation of each of these metrics.

A. Throughput

Throughput measures the network actual data transmission rate, which can vary wildly through different areas of a HetNet based system. While the network bandwidth measures the theoretical limit of data transfer, throughput tells how much data is actually being sent. Specifically, throughput measures the amount of data that is successfully being sent over a specific period or simulation time. In our simulator, we capture the total average system throughput in Mbps, including the macro cell and the small cells throughputs in both UL and DL directions.

B. Outage / Coverage Probability

A crucial aspect in the evaluation and planning of a wireless network is the effect of interference imposed on radio links. The probabilities that the throughput drops below and rises above a certain threshold are defined as outage probability and coverage probability, respectively. The outage/coverage probability is crucial in terms of benchmarking the average throughput of a randomly chosen user in the network, and serves as a fundamental metric for network performance analysis and optimization. In our simulator, we capture the average outage probability of the users associated to the macro cell from one side and those attached to the small cells from the other side.

C. Throughput Percentile

In 3GPP, the cell edge user throughput is defined as the 5^{th} percentile point of the CDF of users' average throughput per transmission, assuming that 95% of the users are expected to achieve a certain throughput per transmission regardless of their geographical location in the cell. If the optimization goal is to maximize the coverage, the 5^{th} percentile cell edge users should acquire an acceptable throughput. Similarly, the 50^{th} and 90^{th} percentile are defined as the 50^{th} and 90^{th} point of the CDF of the UE throughput respectively. They are measured to evaluate the users throughput inside a specific cell. In our simulator, we investigate the 5^{th}, 50^{th} and 90^{th} percentile uplink throughput for different association policies in comparison.

In order to evaluate the presented performance metrics and since the current version of the simulator provides

a sophisticated tracing functionality, we develop a new windows based application to analyze the LTE-Sim traces (Fig. 5.8), parse them and represent the calculated metrics under a graphical user interface.

```
TX INF_BUF ID 37 B 29 SIZE 1490 SRC 1 DST 33 T 0.102 0
TX INF_BUF ID 38 B 29 SIZE 1490 SRC 1 DST 33 T 0.102 0
TX INF_BUF ID 39 B 29 SIZE 283 SRC 1 DST 33 T 0.102 0
TX INF_BUF ID 40 B 1 SIZE 180 SRC 2 DST 5 T 0.102 0
TX INF_BUF ID 41 B 32 SIZE 762 SRC 2 DST 36 T 0.102 0
TX INF_BUF ID 42 B 35 SIZE 180 SRC 3 DST 39 T 0.102 0
TX INF_BUF ID 43 B 37 SIZE 680 SRC 3 DST 41 T 0.102 0
RX INF_BUF ID 31 B 4 SIZE 1490 SRC -1 DST 8 D 0.001 0
RX INF_BUF ID 32 B 4 SIZE 536 SRC -1 DST 8 D 0.001 0
RX INF_BUF ID 33 B 14 SIZE 120 SRC -1 DST 18 D 0.001 0
RX INF_BUF ID 34 B 19 SIZE 986 SRC -1 DST 23 D 0.001 0
RX INF_BUF ID 35 B 20 SIZE 212 SRC -1 DST 24 D 0.001 0
RX INF_BUF ID 36 B 27 SIZE 28 SRC -1 DST 31 D 0.001 0
RX INF_BUF ID 37 B 29 SIZE 1490 SRC -1 DST 33 D 0.001 0
RX INF_BUF ID 38 B 29 SIZE 1490 SRC -1 DST 33 D 0.001 0
RX INF_BUF ID 39 B 29 SIZE 283 SRC -1 DST 33 D 0.001 0
RX INF_BUF ID 40 B 1 SIZE 180 SRC -1 DST 5 D 0.001 0
RX INF_BUF ID 41 B 32 SIZE 762 SRC -1 DST 36 D 0.001 0
RX INF_BUF ID 42 B 35 SIZE 180 SRC -1 DST 39 D 0.001 0
RX INF_BUF ID 43 B 37 SIZE 680 SRC -1 DST 41 D 0.001 0
TX INF_BUF ID 44 B 3 SIZE 272 SRC 0 DST 7 T 0.103 0
TX INF_BUF ID 45 B 5 SIZE 148 SRC 0 DST 9 T 0.103 0
```

Figure 5.8: LTE-Sim traces example

5.4 Simulation Results

In this section, we evaluate first the performance of a HetNet system adopting the conventional TDD configuration (i.e. an UL/DL fixed configuration) with coupled/decoupled association policies. Then, we will follow the procedure in Algorithm 1 and assess the improvement brought by the joint implementation of dynamic TDD and UL/DL decoupled access to the system, in terms of UL and DL throughputs.

5.4.1 Coupled/Decoupled Association Policies in a Conventional TDD System

Figure 5.9 shows the evolution of UE average uplink throughput as a function of the number of small cells for various association criteria with T = (0,0). We notice that the decoupling case with path loss option (DeUD_PL) outperforms CoUD and DeUD_PO cases regardless of the number of deployed small cells. This is due to the fact that users are dispersed and not centralized in one area (cell edge area or cell center area). Moreover, it came to our attention that CoUD case tends to progress similarly to DeUD when the number of small cells significantly increases. This can be explained by the fact that, when increasing the number of small cells, the users in coupled mode are now in the range of small cells in terms of DL signal received power, without the need to refer to the UL path loss option.

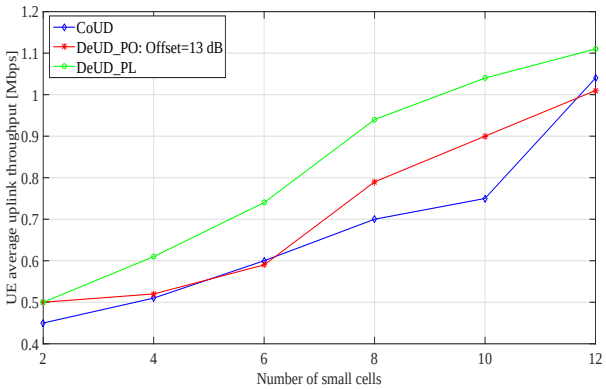

Figure 5.9: Comparison of the UE average uplink throughput between CoUD, DeUD_PO and DeUD_PL cases vs the number of small cells with $N_u = 100$, $\eta = 0$ dB and T = (0,0) (conventional TDD).

Figure 5.10 depicts the 5^{th} percentile uplink throughput in a conventional TDD HetNet under various small cells density. It can be observed that the DeUD_PL case prevails over the DeUD_PO case when deploying two to four small cells, however and after adding increasingly more small cells, we notice a drastic change in the behavior of both cases. The DeUD_PO case outperforms the DeUD_PL for dense small cells networks i.e. when number of deployed small cells is greater than four. This is due to the fact that, when adding more small cells, the cell edge users will be more subject to harmful interference from close macro users. Consequently, and in order to mitigate the UL interference caused by the macro users, the path loss association policy is no more able to do the job. Instead, applying the association policy that extends the small cell coverage by adding a specific bias i.e. the DeUD_PO policy will reduce the UL interference and thus, improve the 5^{th} percentile uplink throughput.

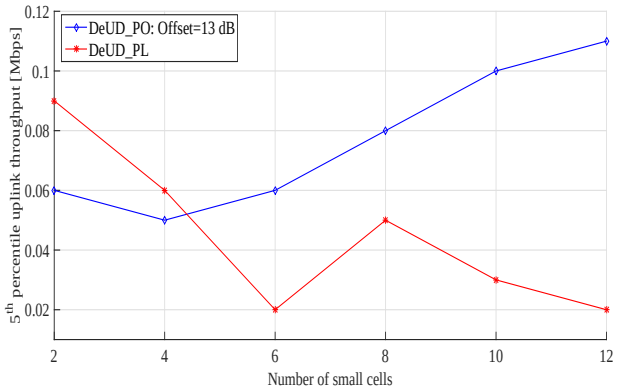

Figure 5.10: 5^{th} percentile uplink throughput comparison between DeUD_PO and DeUD_PL cases vs the number of small cells with $N_u = 100$, $\eta = 0$ dB and T = (0,0) (conventional TDD).

Figure 5.11 shows the 5^{th}, 50^{th} and 90^{th} percentile uplink throughput for the three association policies in a HetNet system with 12 small cells. We can observe that the 5^{th} percentile uplink throughput in the DeUD_PO case is increased by 37.5 % compared to the CoUD case and by more than 400 % compared to the DeUD_PL. The small cell expansion caused by the DeUD_PO plays an imperative role in decreasing the level of UL interference by attaching the macro users to the nearest small cell. This explains the improvement in 5^{th} percentile uplink throughput brought by the DeUD_PO case to the cell edge users. As for the 50^{th} percentile uplink throughput, we notice that the DeUD_PO case outperforms both the CoUD and DeUD_PL cases by 120 % and 41 % respectively. Note that the gains in the 5^{th} and 50^{th} percentile are resulting from the higher coverage of the small cells in the DeUD_PO case with an offset equal to 13 dB. Looking at the 90^{th} percentile UL throughput, we can see that the DeUD_PL case achieves the highest throughput which can be explained by the fact that small cells serve less users than the DeUD_PO case so these users get a higher throughput but at the expense of the 5^{th} and 50^{th} percentile users.

Figure 5.12 captures the average outage probability of the users associated to the macro cell from one side and those attached to the small cells from the other side. In this work, we define the outage probability in one cell as the percentage of users that fail to reach the minimum throughput demand (considered as equal to 250 Kbps) out of the total number of users attached to that cell. As expected, it can be noticed that the macro cell has a very high outage rate (more than 80 %) in the coupled CoUD case. This is basically due to the fact that the macro cell is very congested in the UL because of the adopted association policy that is based on the downlink received power. Hence, macro cell BS won't have enough resources to serve all of its associated users with a high throughput level. However, in the decoupled case, users are distributed more evenly between the macro and the small cells. This is reflected more obviously in the DeUD_PO case where the macro cell reaches an outage probability of 37 % and the small cells achieve an average outage rate of 40 %. In this case, macro users who used to suffer from low throughput are moved to the edge of the small cells, causing a state of evenness in terms of outage probability between macro cell and small cells.

Table 5.3 shows the average number of users per cell where we calculate the average for the macro cell and the small cells separately for a total number of 200 users for all cases. Note that we consider in this scenario a total of four randomly distributed small cells. This table shows how most of the users are connected to the macro cell and how the small cells are under-utilized in the conventional CoUD case. On the other hand, the users in the DeUD_PL

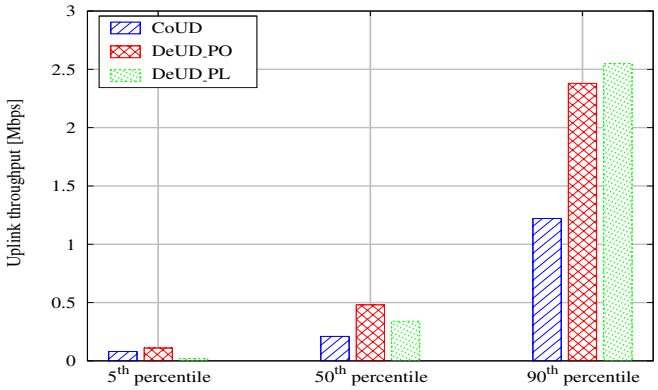

Figure 5.11: 5^{th}, 50^{th} and 90^{th} percentile uplink throughput comparison of CoUD, DeUD_PO and DeUD_PL cases with $N_u = 100$, $N_s = 12$, $\eta = 0$ dB and T = (0,0) (conventional TDD).

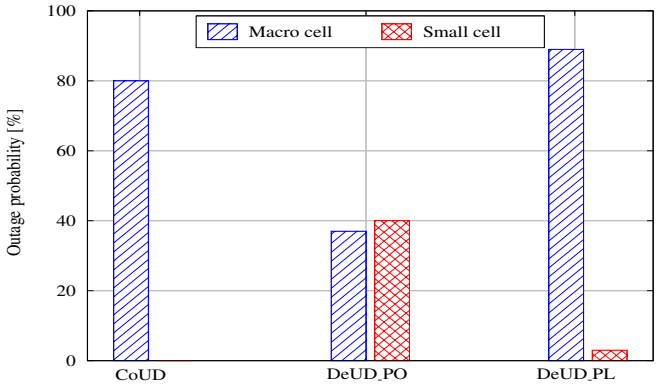

Figure 5.12: Outage probability in macro and small cells between CoUD, DeUD_PO and DeUD_PL cases with $N_u = 100$, $N_s = 4$, $\eta = 0$ dB and T = (0,0) (conventional TDD).

case are distributed in a more homogeneous way among the macro cell and the small cells, which ensures much more efficient resource utilization.

	Macro cell	**Small cell**
DeUD_PL	126	25
CoUD	146	5

Table 5.3: Average number of users per node (macro and small cells) for the CoUD and DeUD_PL cases.

Figure 5.13 shows the comparison between both CoUD and DeUD_PL cases under various small cell downlink transmitted powers. It can be observed that the DeUD_PL outperforms the CoUD case, in terms of total average UL throughput irrespective of the small cell downlink power. This is due mainly to the fact that the decoupling policy improves the average UL throughput of both macro and small cell users, whereas the coupled policy improves the UL throughput of small cell edge users. Increasing the DL signal received power will extend the small cell uplink coverage in the CoUD case where the UL association citeria is based on DL received power. This will offload the macro cell, mitigate the uplink interference experienced from the macro users at the small cell BS and thus, improve the small cell users uplink throughput. However, in the DeUD_PL case, the UL association criteria is based on the uplink path loss and thus, not affected by the change in the small cell transmit power. This will justify the steady value of the UL throughput shown in Fig. 5.13.

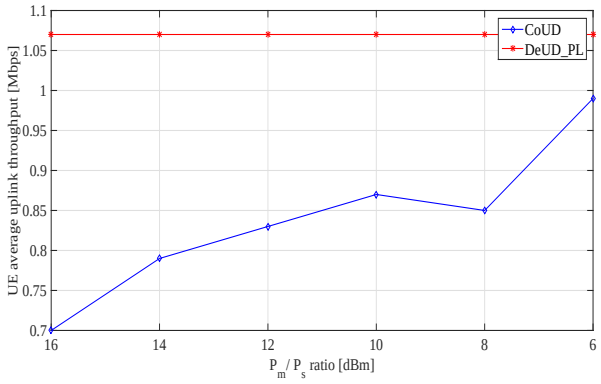

Figure 5.13: Comparison of the UE average uplink throughput between CoUD and DeUD_PL cases vs the small cell downlink transmit power with $N_u = 100$, $N_s = 10$, $\eta = 0$ dB and T = (0,0) (conventional TDD).

Figures 5.14 and 5.15 prove that a TDD configuration can perform better with the coupled access policy contrary to another TDD configuration that can be more effective with a decoupled policy. For example, T = (1,0) with CoUD in Fig. 5.14 and T = (1,5) with DeUD_PO in Fig.5.15. Hence, we conclude that there is a need for a joint optimization of decoupling and dynamic TDD techniques to further improve the system performance in terms of UL and DL spectral efficiencies. This optimization problem will be tackled in the simulation scenarios that follow.

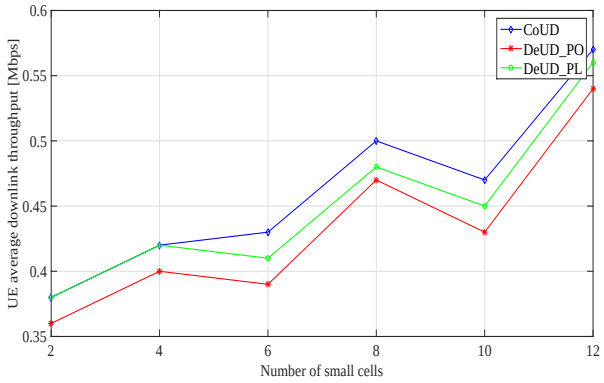

Figure 5.14: Comparison of the UE average downlink throughput between CoUD, DeUD_PO and DeUD_PL cases vs the number of small cells with $N_u = 100$, $\eta = 0$ dB and T = (1,0).

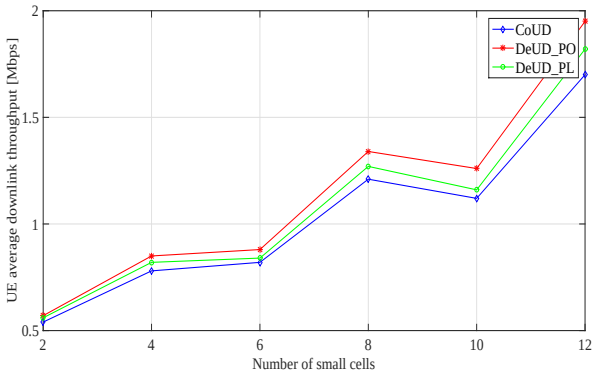

Figure 5.15: Comparison of the UE average downlink throughput between CoUD, DeUD_PO and DeUD_PL cases vs the number of small cells with $N_u = 100$, $\eta = 0$ dB and T = (1,5).

5.4.2 Joint Optimization of TDD and Coupled/Decoupled Association Policies

In Fig. 5.16, we show the performance of different schemes in different traffic load conditions. This figure investigates a joint UL and DL system throughput optimization between the following four schemes: 1) Conventional TDD, in which we consider the same synchronized TDD configuration between the macro cell and small cells (T = (0,0) in this case), along with the conventional CoUD association policy. 2) Conventional TDD with DeUD. We consider the DeUD_PL case as the association policy adopted in the next simulations to represent the decoupled access technique (DeUD). 3) Dynamic TDD, in which we consider unsynchronized and dynamic TDD configuration between the macro cell and the small cells that will vary according to UL/DL traffic demands. A conventional CoUD policy is considered in this case. 4) Dynamic TDD with DeUD, in which we consider a joint implementation of dynamic TDD with decoupled UL/DL user association. The purpose is to find the optimal scenario that will jointly improve the UL and DL throughputs in a HetNet TDD based system.

Figure 5.16 shows the performance for the case of four small cells. The number of users operating in UL and DL

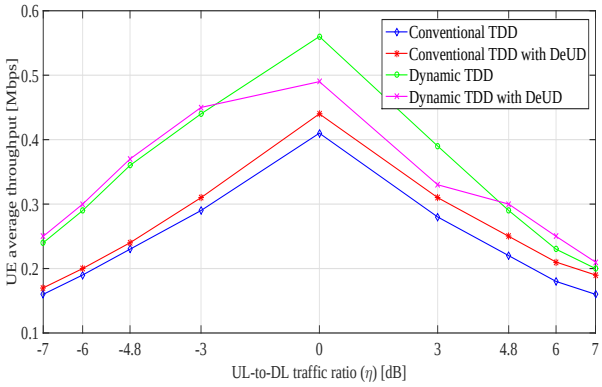

Figure 5.16: Uplink and downlink UE average throughput in different traffic load conditions with conventional TDD or dynamic TDD, with decoupling or without decoupling considering $N_s = 4$.

is varied by changing the UL to DL traffic ratio (η), expressed in dB. As an example, $\eta < 0$ means that the downlink traffic is greater than the uplink traffic, whereas $\eta > 0$ means the opposite. It can be noticed that increasing either the UL or DL traffic load degrades the performance of the different schemes. Comparing the first two schemes, we can observe that the conventional TDD with decoupling outperforms the conventional TDD with CoUD case. However, it is worth noting that the average gain achieved for $\eta > 0$ (around 16 %) is higher than the one reached for $\eta < 0$ (around 4 %). This is due mainly to the higher UL interference levels experienced when $\eta > 0$ and knowing that the main role of DeUD is to reduce that type of interference. It is obvious as well that the dynamic TDD scheme outperforms both conventional TDD schemes since as expected, adjusting the TDD configuration dynamically according to the instantaneous traffic load will improve the overall system performance. For example, when $\eta = 6$ dB i.e. the UL traffic is around four times the DL traffic, the system adjusts the TDD configuration to T = (3,3) by following the procedure in Algorithm 1 in a way to improve the system performance in terms of both UL and DL throughputs. However, for $\eta = -6$ dB i.e. the DL traffic is around four times the UL traffic, T is adjusted to (5,5). Moving to the fourth scheme, we can observe that implementing jointly both dynamic TDD and DeUD techniques will further improve the system performance, mainly in high load conditions for $\eta > 4.8$ dB and $\eta < -3$ dB. This can be explained by the fact that the DeUD is more effective while dealing with higher interference levels mostly experienced in high load conditions. Also, it can be concluded from this figure that during low traffic conditions, the dynamic TDD feature by dynamically adjusting the DL/UL resources can improve the overall system performance without having recourse to the decoupling policy.

Next, we investigate in Fig. 5.17 and Fig. 5.18 the benefits that the four schemes can bring to a dense HetNet with high number of deployed small cells. We can clearly see that, even in lightly loaded systems where $\eta = 0$ dB, the proposed algorithm i.e. the fourth scheme, also achieves high throughput gain in terms of UL and DL throughput. This gain significantly improves as the number of small cells increases.

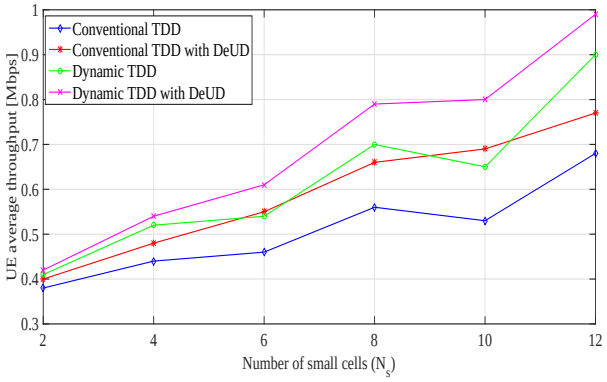

Figure 5.17: Uplink and downlink UE average throughput with conventional TDD or dynamic TDD, with decoupling or without decoupling vs number of small cells with $N_u = 100$ and $\eta = 0$ dB.

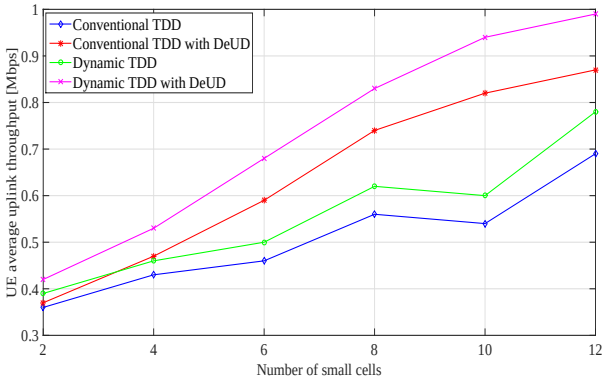

Figure 5.18: Uplink UE average throughput with conventional TDD or dynamic TDD, with decoupling or without decoupling vs number of small cells with $N_u = 100$ and $\eta = 0$ dB.

5.5 Conclusion

The focus in this chapter was to study and assess the gains that different association policies can bring to a dynamic TDD HetNet system in response to various traffic loads. We have presented simulation results based on a system level simulator under which additional modules have been developed to motivate our system model. We have created appropriate simulation environment that is relative to real scenarios, i.e. simulations where multiple small cells are deployed in a heavy loaded HetNet system and under various traffic loads. These simulations consider random users distribution with scheduling decisions in both the uplink and the downlink directions. We benefit from the system level simulator developed in this chapter to analyze the outcome of an adaptive TDD and decoupling policy compared to conventional HetNets. Relying on the proposed algorithm, we have shown the performance results of a joint dynamic TDD with coupled/decoupled user association policies in a dense HetNet deployment. The findings confirm that the DeUD_PO policy can achieve high gains in the 5^{th} and 50^{th} percentile throughput. However, DeUD_PL policy outperforms both CoUD and DeUD PO cases when comparing the average throughput per user, regardless of the number of deployed small cells.
Also, we have observed that the DeUD_PO policy causes a balance in the users' outage probability between macro cell and small cells, contrary to CoUD and DeUD_PL association policies. Additionally, we have realized that the DeUD_PL policy outperforms the CoUD case, in terms of total average UL throughput irrespective of the small cell downlink power. This is due mainly to the fact that the decoupling policy improves the average UL throughput of both macro and small cell users, whereas the coupled policy improves the UL throughput of small cell edge users.
Moreover, it is further observed that the proposed algorithm (Dynamic TDD with DeUD) yields significant performance improvements in UL and DL throughput compared to a number of conventional schemes, especially in

dense HetNet deployment and in highly loaded systems. Also, we have noticed that during low traffic conditions, the dynamic TDD feature, by dynamically adjusting the DL/UL resources, can improve the overall system performance without having recourse to the decoupling policy.

Chapter 6

Conclusion

In this chapter, we summarize the conclusions that we have drawn from this research, and we provide directions for future work.

6.1 Summary of Conclusions

This thesis addresses the challenge of integrating both TDD and uplink / downlink decoupling techniques into the same model as a first step and to integrate them into the same simulator as a second step.
Developing a statistical model for a given cellular system plays an imperative role in the design and analysis of that wireless cellular system. In our case, it offers a simple analysis tool to assess a given TDD/Decoupling-based HetNet deployment. The analytical formulas provide relevant insights about network performance without the need for time consuming Monte-Carlo Simulations. Our proposed tool is also useful for network designers who can use it to determine the range of deployment parameters given a target QoS.
Therefore, and in order to meet the first thesis objective and evaluate the system performance when implementing a dynamic TDD mechanism associated with uplink / downlink decoupling, we have developed a statistical and analytical framework that was segregated into three main sections:

- **TDD Statistical Model in a Single Small Cell Environment**: We have proposed an uplink and a downlink inter-cell interference model for a dynamic TDD HetNet system considering various distance distributions. We have considered a network consisting of one macro cell and one small cell. We have first derived an analytical expression for the distribution of the interfering distance considering all possible interference scenarios that could occur in TDD-based networks while taking into account the harmful impact of interference. Secondly, based on the latter result, we have derived the distribution and moment generating function (MGF) of the uplink and downlink inter-cell interference. Same has been applied to the location of the reference small cell user and thus, to the distribution of the desired signal. Finally, we have built on the derived expressions for interference and desired signal to analyze the average capacity of the reference cell in both uplink and downlink transmissions. The proposed model provides a valuable tool to evaluate the system performance in terms of downlink/uplink average capacity. The provided numerical results help in optimizing the design parameters under various conditions. For example, the system performance was evaluated when controlling the macro user transmission power. Further, the effect of large path loss exponents proved to enhance the performances of small cell users.
  Monte-Carlo simulation results have been provided to demonstrate the accuracy of the derived analytical expressions, including 95% confidence intervals of disparity measures. When evaluating the capacity expression over 4 TDD sub frames, the execution time was found to be reduced by more than 50% compared to the time required to run 10 000 Monte-Carlo simulations over the same period.

- **Modeling of Various Association Policies in a Single Small Cell Environment**: We have conducted both downlink and uplink performance comparison study for four various cell association rules in TDD HetNet, based on a geometric probability approach. The network was consisting of one macro cell and one small cell. Two cases were considered with UL/DL coupled access and two others with decoupled access. This section complements the previous one by modeling the decoupling technique on top of the TDD HetNet model. Taking

all possible TDD subframes combinations between the macro and small cells, four coupled and decoupled cell associations strategies have been investigated in details. This study provides more complete insights into the benefits of decoupling mode in different network deployments with multiple input requirements. We have observed that the decoupling case brings greater benefits in the uplink and maintains the same improvement in the downlink for various offset values and thus, improves the overall system performance when being combined with a dynamic TDD technology. The same improvement in UL has been observed for the coupled access with small cell case. However and as expected, we have noticed that the coupled access with small cell case, i.e. the CRE technique, leads to a degradation in downlink spectral efficiency due mainly to the macro BS downlink interference affecting the users in the CRE region. As for the reverse decoupling case, we have captured a degradation in spectral efficiency for both UL and DL directions. On another note, we have found out that our modeled network can be further optimized when choosing a specific small cell offset as a trade-off between UL and DL spectral efficiencies.

- **Joint Modeling of TDD and Decoupling in Multiple Small Cells Environment**: We have developed a joint TDD and DeUD statistical model with multiple small cells deployment. This study was based on a geometric probability approach and considered the modeling of both cross-tier and co-tier interferences, in addition to the average user spectral efficiency. The cross-tier interference is the interference incurred at one tier (reference small cell) arising from the other tier (macro cell), whereas the co-tier interference is the interference incurred at the reference small cell arising from other small cells. We have analyzed, in a multiple small cells environment, the uplink and downlink decoupling gains as a function of both the small cell offset factor and the distance between small cells. Uplink power control have been added as well to the developed model. This mechanism was based on the open-loop power control strategy standardized in 3GPP LTE. Moreover, the developed statistical model has been adapted to consider an unsynchronized TDD configuration across small cells, in addition to the initial synchronized TDD configuration. Monte-Carlo simulations results have been presented to validate the accuracy of this model. Confidence intervals are derived for a sample mean, using the sample data values themselves. In this case, the computational time for running 1 000 000 Monte-Carlo simulations was given by 4 570 seconds which is significantly larger, when compared to the analytical expression evaluation time. This explained the strong need for an analytical model as a replacement for the time consuming Monte-Carlo simulations, especially in multiple small cells environments.
  Regarding our findings, we have observed that the decoupling case brings higher uplink and downlink throughputs for various offset values. Furthermore, we have realized that our modeled network can be further optimized by adopting the optimal combination of both the small cell offset factor and the distance between small cells. Identifying the location of the small cell interferer and the small cell offset factor will help in improving the gain that the decoupling mode can bring to a multiple small cells TDD HetNet. Considering a power control mechanism has reduced uplink throughputs and increased downlink throughputs for various association policies. Moreover, implementing the power control mechanism with various association policies has caused a reduction in mobile users' uplink power consumption, especially in the coupled with macro cell case. A slight decrease in uplink throughput has been noticed for different association policies when considering the unsynchronized TDD case. Also, an improvement in the uplink decoupling gain has been detected in the case of an unsynchronized TDD configuration.

It is worth mentioning that the proposed model plays an imperative role in evaluating the system performance metrics such as spectral efficiency, decoupling gain and average power consumption. However, this model evaluates the average capacity of only one user and without addressing the traffic adaptation and dynamic resource allocation challenges. Also, it doesn't consider a variable slow and fast fading. Including these enhancements in our model will incur huge computational complexity and any assumption made at this stage in the design parameters, aiming to reduce model complexity will lead to non-realistic results. For this reason, we have implemented a 5G HetNet system level simulator that supplements an existing LTE simulator. By this implementation, we will be answering the second thesis objective and discovering the benefits of an adaptive TDD and decoupling compared to conventional HetNets. We have created appropriate simulation environment that is relative to real scenarios i.e. simulations where multiple small cells are deployed in a heavy loaded HetNet system and under various traffic loads. These simulation scenarios consider random users distribution with scheduling decisions in both the uplink and the downlink directions. Our objective was to prove that there is an optimal combination between both the macro cell and the small cells TDD configurations from one side and the decoupling association with its various parameters from the other side, and this with respect to any change in the system, especially in the UL/DL traffic ratio:

- **Adaptive TDD and Decoupling in 5G HetNets: Simulation-Based Evaluation**: We have presented simulation results based on a system level simulator under which additional modules have been developed to motivate our system model. Relying on the proposed algorithm, we have shown the performance results of a joint dynamic TDD with coupled/decoupled user association policies in a dense HetNet deployment. The implemented association policies are as follows:
  - Cell association criteria in DL and UL is based on DL Reference Signal Received Power (RSRP) which is the conventional LTE user association policy. This case is referred to as **CoUD**.
  - Cell association criteria in DL is based on DL Reference Signal Received Power (RSRP) whereas the criteria in UL is based on the uplink received power with cell selection offset in case of a small cell. This case is referred to as **DeUD_PO**.
  - Cell association criteria in DL is based on DL Reference Signal Received Power (RSRP) whereas the criteria in UL is based on the path loss. This case is referred to as **DeUD_PL**.

  The findings confirm that the DeUD_PO policy can achieve high gains in the 5^{th} and 50^{th} percentile throughput. However, DeUD_PL policy outperforms both CoUD and DeUD PO cases when comparing the average throughput per user, regardless of the number of deployed small cells. Also, we have observed that the DeUD_PO policy causes a balance in the users' outage probability between macro cell and small cells, contrary to CoUD and DeUD_PL association policies. Additionally, we have realized that the DeUD_PL policy outperforms the CoUD case, in terms of total average UL throughput irrespective of the small cell downlink power. This is due mainly to the fact that the decoupling policy improves the average UL throughput of both macro and small cell users, whereas the coupled policy improves the UL throughput of small cell edge users. Findings confirm as well, that in the conventional CoUD case, most of the users are connected to the macro cell and the small cells are under-utilized. On the other hand, the users in the DeUD_PL case appear to be distributed in a more homogeneous way among the macro cell and the small cells, which ensures much more efficient resource utilization.

  Moreover, it has been further observed that the proposed algorithm (Dynamic TDD with DeUD_PL) yields significant performance improvements in UL and DL throughput compared to a number of conventional schemes, especially in dense HetNet deployment and in highly loaded systems. This can be explained by the fact that the DeUD is more effective while dealing with higher interference levels mostly experienced in high load conditions. Also, we have noticed that during low traffic conditions, the dynamic TDD feature by dynamically adjusting the DL/UL resources can improve the overall system performance without adopting the decoupling policy.

6.2 Future Directions

We expose hereafter the future perspectives of the work in subsections 6.2.1, and 6.2.2, exposing short and long term perspectives respectively.

6.2.1 Short Term Perspectives

For short term perspectives, we propose to consider non-uniform users distribution including the case where the users can be present in the same place at the exact same time. Another possible extension is to consider various composite fading channel models in both macro and small cells and thus, incorporate new design parameters in the developed model. The derived expressions can be also considered to evaluate other important network performance metrics such as network outage and average user fairness, numerically. Moreover, a future work can focus on studying the network architectural and design changes that would enable the decoupling of UL and DL and which includes signaling and radio access protocols. This future work should outline the architectural changes required to facilitate the decoupled UL/DL. Based on a 3GPP architecture, several different degrees of decoupling were proposed which mainly differ in the rigor of decoupling and the chosen anchor points in the RAN/core. A solution can be with the centralized C-RAN technology that could be considered to gather all signaling information in UL and DL from different base stations, in a centralized cloud ready to be shared with users associated with different base stations.
Further, combining the decoupling approach with other emerging paradigms, such as COMP, mmWave, D2D and Massive MU-MIMO, would be interesting items for future work. For example, massive MIMO technique introduces

either diversity or spatial multiplexing gain, improving energy and spectral efficiencies, and deriving more power savings. As for the COMP technique, it is the key technique to improve the cell-edge throughput and/or system throughput in a HetNet based system.

6.2.2 Long Term Perspectives

As for long term perspectives, it is paramount to investigate the performance of the decoupling mode in 5G TDD systems with hybrid HetNet deployment, where mmWave small cells (for example) are supposed to be deployed as an overlay to traditional sub-6GHz macro cells. This inter-band connectivity in 5G networks between two different radio technologies (RAT) has been clearly described in 3GPP Release 16. As an example, a mobile user hosting a video streaming session which generally requires a high downlink throughput, will be associated in DL to a mmwave BS that offers a large bandwidth and thus a high throughput. However in UL, the mobile user suffering from a transmitted signal power limitation will be associated to a low frequency LTE BS to compensate and increase its uplink coverage.
Additionally, resorting to learning techniques to dynamically decide the best combination between the TDD scheme and the user association policy and this adapting to dynamic traffic load variations, would also be an interesting follow up work. Also, these learning algorithms should as well dynamically decide which procedure to adopt regarding the rate of deployment or change of each technique. For example, the association process for both UL and DL can be performed in a slower rate compared to the change in TDD reconfiguration rate.

Appendix A

A.1 About LTE-Sim

LTE-Sim is an open source framework to simulate LTE networks mainly developed by G. Piro and F.Capozzi [121] . It encompasses several aspects of LTE networks, including both the Evolved Universal Terrestrial Radio Access (E-UTRAN) and the Evolved Packet System (EPS). It supports single and multi-cell environments, QoS management, multi users environment, user mobility, handover procedures, and frequency reuse techniques. Three kinds of network nodes are modeled: user equipment (UE), evolved Node B (eNB) and Mobility Management Entity/Gateway (MME/GW). Four different traffic generators at the application layer have been implemented and the management of data radio bearer is supported. Finally, well-known scheduling strategies (such as Proportional Fair, Modified Largest Weighted Delay First, and Exponential Proportional Fair), AMC scheme, Channel Quality Indicator feedback, frequency reuse techniques, and models for physical layer have been developed.

A.2 Running LTE-Sim Simulator

Running LTE-Sim under windows was done following the below steps:

1. Install the Java JRE (1.7 or higher) from Oracle.

2. Install MinGW (0.5-beta - 20120426 - 1 or later). During the Select Components step, select "C++ Compiler" and "MSYS Basic System" for installation.

3. Download/Install Eclipse IDE for C++ Developers.

4. Create a new C++ Project.

5. Add "-static-libgcc -static-libstdc++" as Linker flags for the new project (Under the Project Properties, expand the C/C++ Build menu and click on Settings. Under the Tool Settings tab, expand the MinGW C++ Linker menu and click on Miscellaneous. Add the text to the Linker flags field.)

6. Download the LTE-Sim C++ open source project.

7. Copy/paste all files of LTE-Sim/src into the src folder of the newly created C++ project under Eclipse.

8. Run the project.

A.3 LTE-Sim Upgrade

In order to implement all aspects related to our proposal, we have upgraded LTE-Sim by means of new classes and functionalities listed below:

A.3.1 Uplink Channel Quality

The uplink process in LTE-Sim has been optimized by considering the below updates to the source code:

Add the uplink interference object to **EnbLtePhy::EnbLtePhy()** function:

```
Interference *interference = new Interference ();
SetInterference (interference);
```

Initialize a new variable under the structure **EnodeB:UserEquipmentRecord** called **std::vector int mcqFeedback** to store the uplink channel quality:

```
std::vector<int> m_cqFeedback;
void SetCQ (std::vector<int> cq);
std::vector<int> GetCQ (void) const;
```

Add **NetworkNode* src** parameter to **EnbLtePhy::StartRx** function. In this case, *src* parameter will be the UE (user equipment). Under this function, we will include the uplink interference and calculate the uplink channel quality per RB for each pair of (enb,Ue) as follows:

```
if (GetInterference() != NULL) {
   interference = GetInterference() - >
      ComputeENodebInterference((ENodeB * ) GetDevice(), chId);
} else {
   interference = 0;
}

noise_interference = 10. * log10(pow(10., NOISE / 10) + interference);
// dB

measuredSinr.push_back(power - noise_interference);

chId++;
}

AMCModule * amc = src - > GetProtocolStack() - > GetMacEntity() - > GetAmcModule();
std::vector < int > cqi = amc - > CreateCqiFeedbacks(measuredSinr);

UserEquipment * ue = (UserEquipment * ) src;
ENodeB * enb = (ENodeB * ) GetDevice();
ENodeB::UserEquipmentRecord * record = enb - >
   GetUserEquipmentRecord(ue - > GetIDNetworkNode());
if (record != NULL) {
   record - > SetCQ(cqi);
}
```

We create a new function named **Interference:ComputeENodebInterference** to include the uplink interference:

```
double Interference::ComputeENodebInterference(ENodeB * enb, int rb) {
   UserEquipment * ue;

   double interference = 0;

   std::vector < UserEquipment * > * ues = NetworkManager::Init() -
      > GetUserEquipmentContainer();
   std::vector < UserEquipment * > ::iterator it;

   for (it = ues - > begin(); it != ues - > end(); it++) {
      ue = ( * it);
```

```
      if (enb - > GetIDNetworkNode() != ue - > GetTargetNode() - > GetIDNetworkNode() &&
         enb - > GetPhy() - > GetBandwidthManager() - > GetUlOffsetBw() ==
         ue - > GetTargetNode() - > GetPhy() - > GetBandwidthManager() - > GetUlOffsetBw())

         if (ue - > GetChannelsForTx().size() > 0 && ue - > IsRBinChannelTx(rb))

      {
         double powerTXForSubBandwidth = 10 * log10(
            pow(10., (ue - > GetPhy() - > GetTxPower() - 30) / 10) /
            ue - > GetChannelsForTx().size());

         double nodeInterference_db = powerTXForSubBandwidth - 10 -
            ComputePathLossForInterference(enb, ue); // in dB
         double nodeInterference = pow(10, nodeInterference_db / 10);

         interference += nodeInterference;

      }
   }

   return interference;
}
```

Getting the channel quality value within the **UplinkPacketScheduler:: SelectUsersToSchedule** function:

```
user->m_transmittedData = 0;
user->m_channelContition  = record->GetCQ ();
```

Add the following variable **std::vector int mchannelsForTx** under **UserEquipment** class to store the allocated RBs for each user, calculated already by the uplink scheduler.

Add the below appropriate functions as members of the same class:

```
bool UserEquipment::IsRBinChannelTx(int rb) {
   for (std::vector < int > ::iterator it = m_channelsForTx.begin();
    it != m_channelsForTx.end(); it++) {
      int channel = ( * it);
      if (channel == rb) return true;
   }

   return false;
}

void UserEquipment::SetChannelsForTx(std::vector < int > channelsForTx) {
   m_channelsForTx.clear();
   m_channelsForTx = channelsForTx;
}

std::vector < int > UserEquipment::GetChannelsForTx(void) {
   return m_channelsForTx;
}
```

Modify **UeLtePhy::ReceiveIdealControlMessage** to set the allocated sub channels for each user:

```
NetworkManager::Init() - > GetUserEquipmentByID(node) -
   > SetChannelsForTx(m_channelsForTx);
```

Add a new function called **ResetChannelsForTx** to reset user RBs allocation on each subframe:

```
void UserEquipment::ReSetChannelsForTx() {
   m_channelsForTx.clear();
}
```

A.3.2 Dynamic TDD

This will require adding the function **FrameManager::GetMicroSubFrameType** and updating **FrameManager::ResourceAllocation** function, as per the below :

```
int FrameManager::GetMicroSubFrameType (int nbSubFrame)
{
  return TDDConfigurationMicro [GetMicroTDDFrameConfiguration ()][nbSubFrame-1];
}

void FrameManager::ResourceAllocation(void)
{ .....

 if (((record - > GetNodeType() == NetworkNode::TYPE_ENODEB) &&
     GetSubFrameType(GetNbSubframes()) == 0) ||
     ((record - > GetNodeType() == NetworkNode::TYPE_MICROENODEB) &&
     GetMicroSubFrameType(GetNbSubframes()) == 0)) {
   #
   ifdef FRAME_MANAGER_DEBUG
   std::cout << " FRAME_MANAGER_DEBUG: SubFrameType = "
   " SUBFRAME_FOR_DOWNLINK " << std::endl;#
   endif
   //record->DownlinkResourceBlokAllocation();
   Simulator::Init() - > Schedule(0.0, & ENodeB::DownlinkResourceBlokAllocation, record);
 } else if (((record - > GetNodeType() == NetworkNode::TYPE_ENODEB) &&
     GetSubFrameType(GetNbSubframes()) == 1) ||
     ((record - > GetNodeType() == NetworkNode::TYPE_MICROENODEB) &&
     GetMicroSubFrameType(GetNbSubframes()) == 1)) {
   #
   ifdef FRAME_MANAGER_DEBUG
   std::cout << " FRAME_MANAGER_DEBUG: SubFrameType = "
   " SUBFRAME_FOR_UPLINK " << std::endl;#
   endif
   //record->UplinkResourceBlockAllocation();
   Simulator::Init() - > Schedule(0.0, & ENodeB::UplinkResourceBlockAllocation, record);

}
```

A.3.3 Cross-link Interference

We first introduce the calculation of the UL to DL interference at the mobile user level with the **Interference::ComputeInterference** function as follows:

```
double Interference::ComputeInterference(UserEquipment * ue, int rb) {
  ENodeB * node;
  UserEquipment * ue1;
  ENodeB::UserEquipmentRecord * record;
  vector < ENodeB::UserEquipmentRecord * > ::iterator iter;
  double interference = 0;

  std::vector < ENodeB * > * eNBs = NetworkManager::Init() - > GetENodeBContainer();
  std::vector < ENodeB * > ::iterator it;
```

```
for (it = eNBs - > begin(); it != eNBs - > end(); it++) {
  node = ( * it);

  if (((node - > GetNodeType() == NetworkNode::TYPE_MICROENODEB) &&
      FrameManager::Init() - > GetMicroSubFrameType(FrameManager::Init() - > GetNbSubframes()) ==
      1) || ((node - > GetNodeType() == NetworkNode::TYPE_ENODEB) &&
      FrameManager::Init() - > GetSubFrameType(FrameManager::Init() - > GetNbSubframes()) ==
      1))

  // UL- DL interference
  {

    if (node - > GetIDNetworkNode() != ue - > GetTargetNode() - > GetIDNetworkNode() &&
      node - > GetPhy() - > GetBandwidthManager() - > GetUlOffsetBw() ==
      ue - > GetTargetNode() - > GetPhy() - > GetBandwidthManager() - > GetDlOffsetBw()) {

      for (iter = node - > GetUserEquipmentRecords() - > begin();
       iter != node - > GetUserEquipmentRecords() - > end(); iter++) {

        record = ( * iter);
        ue1 = record - > GetUE();

        if (ue1 - > GetChannelsForTx().size() > 0 && ue1 - > IsRBinChannelTx(rb))

        {

          double distance = ue1 - > GetMobilityModel() - > GetAbsolutePosition() - > GetDistance(
            ue - > GetMobilityModel() - > GetAbsolutePosition());

          if (distance != 0) {
            double powerTXForSubBandwidth = 10 * log10(
              pow(10., (ue1 - > GetPhy() - > GetTxPower() - 30) / 10) /
              ue1 - > GetChannelsForTx().size());

            double nodeInterference_db = powerTXForSubBandwidth - 10 -
              ComputePathLossForInterference(ue1, ue); // in dB
            double nodeInterference = pow(10, nodeInterference_db / 10);

            interference += nodeInterference;
          }
        }
      }
    }
  } else
    //  DL- DL interference

    if (node - > GetIDNetworkNode() != ue - > GetTargetNode() - > GetIDNetworkNode() &&
      node - > GetPhy() - > GetBandwidthManager() - > GetDlOffsetBw() ==
      ue - > GetTargetNode() - > GetPhy() - > GetBandwidthManager() - > GetDlOffsetBw()) {
      double powerTXForSubBandwidth = 10 * log10(
        pow(10., (node - > GetPhy() - > GetTxPower() - 30) / 10) /
        node - > GetPhy() - > GetBandwidthManager() - > GetDlSubChannels().size());

      double nodeInterference_db = powerTXForSubBandwidth - 10 -
        ComputePathLossForInterference(node, ue); // in dB
```

```
        double nodeInterference = pow(10, nodeInterference_db / 10);

        interference += nodeInterference;

      }

  }

  return interference;
}
```

Second, we introduce the calculation of the DL to UL interference at the base station level with the **Interference::ComputeENodebInterference** function as follows:

```
double Interference::ComputeENodebInterference(ENodeB * enb, int rb) {
    ENodeB * node;
    UserEquipment * ue1;
    ENodeB::UserEquipmentRecord * record;
    vector < ENodeB::UserEquipmentRecord * > ::iterator iter;
    double interference = 0;

    std::vector < ENodeB * > * eNBs = NetworkManager::Init() - > GetENodeBContainer();
    std::vector < ENodeB * > ::iterator it;

    for (it = eNBs - > begin(); it != eNBs - > end(); it++) {
      node = ( * it);

      if (((node - > GetNodeType() == NetworkNode::TYPE_MICROENODEB) &&
          FrameManager::Init() - > GetMicroSubFrameType(FrameManager::Init() - > GetNbSubframes()) ==
          1) || ((node - > GetNodeType() == NetworkNode::TYPE_ENODEB) &&
          FrameManager::Init() - > GetSubFrameType(FrameManager::Init() - > GetNbSubframes()) ==
          1))
      // UL-UL interference
      {

        if (node - > GetIDNetworkNode() != enb - > GetIDNetworkNode() &&
          node - > GetPhy() - > GetBandwidthManager() - > GetUlOffsetBw() ==
          enb - > GetPhy() - > GetBandwidthManager() - > GetUlOffsetBw()) {

          for (iter = node - > GetUserEquipmentRecords() - > begin();
          iter != node - > GetUserEquipmentRecords() - > end(); iter++) {

            record = ( * iter);
            ue1 = record - > GetUE();

            if (ue1 - > GetChannelsForTx().size() > 0 && ue1 - > IsRBinChannelTx(rb))

            {
              double powerTXForSubBandwidth = 10 * log10(
                pow(10., (ue1 - > GetPhy() - > GetTxPower() - 30) / 10) /
                ue1 - > GetChannelsForTx().size());

              double nodeInterference_db = powerTXForSubBandwidth - 10 -
                ComputePathLossForInterference(ue1, enb); // in dB
              double nodeInterference = pow(10, nodeInterference_db / 10);

              interference += nodeInterference;
```

```
          }

        }
      }
    } else
      // DL-UL interference

      if (node - > GetIDNetworkNode() != enb - > GetIDNetworkNode() &&
        node - > GetPhy() - > GetBandwidthManager() - > GetDlOffsetBw() ==
        enb - > GetPhy() - > GetBandwidthManager() - > GetUlOffsetBw()) {
        double powerTXForSubBandwidth = 10 * log10(
          pow(10., (node - > GetPhy() - > GetTxPower() - 30) / 10) /
          node - > GetPhy() - > GetBandwidthManager() - > GetDlSubChannels().size());

        double nodeInterference_db = powerTXForSubBandwidth - 10 -
          ComputePathLossForInterference(node, enb); // in dB
        double nodeInterference = pow(10, nodeInterference_db / 10);

        interference += nodeInterference;

      }

  }
```

A.3.4 Decoupling

To implement the DeUD_PO policy under the system level simulator, we create three new functions **NetworkManager::SelectTargetNodeUplinkOffset**, **HandoverEntity::CheckHandoverUplinkNeedOffset**, and **PowerBasedHoManager::CheckHandoverNeedUplinkOffset** as follows:

```
void NetworkManager::SelectTargetNodeUplinkOffset(UserEquipment * ue, double bias) {
  NetworkNode * targetNode = ue - > GetTargetNode();

  if (targetNode - > GetProtocolStack() - > GetRrcEntity() - >
    GetHandoverEntity() - > CheckHandoverUplinkNeedOffset(ue, bias)) {
    NetworkNode * newTagertNode =
      targetNode - > GetProtocolStack() - > GetRrcEntity() - >
      GetHandoverEntity() - > GetHoManager() - > m_target;

    ue - > SetTargetNode(newTagertNode);
  }
}

bool HandoverEntity::CheckHandoverUplinkNeedOffset(UserEquipment * ue, double bios) {
  return GetHoManager() - > CheckHandoverNeedUplinkOffset(ue, bios);
}

bool PowerBasedHoManager::CheckHandoverNeedUplinkOffset(UserEquipment * ue, double bias)
{
  NetworkNode * targetNode = ue - > GetTargetNode();

  double TXpower = 10 * log10(
    pow(10., (ue - > GetPhy() - > GetTxPower() - 30) / 10) /
    ue - > GetPhy() - > GetBandwidthManager() - > GetUlSubChannels().size());
  double pathLoss = ComputePathLossForInterference(ue, targetNode);
```

```
  double targetRXpower = TXpower - pathLoss;

  double RXpower;

  std::vector < ENodeB * > * listOfNodes = NetworkManager::Init() - > GetENodeBContainer();
  std::vector < ENodeB * > ::iterator it;
  for (it = listOfNodes - > begin(); it != listOfNodes - > end(); it++) {
    if (( * it) - > GetIDNetworkNode() != targetNode - > GetIDNetworkNode()) {

      NetworkNode * probableNewTargetNode = ( * it);

      TXpower = 10 * log10(
        pow(10., (ue - > GetPhy() - > GetTxPower() - 30) / 10) /
        ue - > GetPhy() - > GetBandwidthManager() - > GetUlSubChannels().size());
      pathLoss = ComputePathLossForInterference(ue, probableNewTargetNode);

      RXpower = TXpower - pathLoss;


      if (( * it) - > GetNodeType() == NetworkNode::TYPE_MICROENODEB) RXpower += bias;

      if (RXpower > targetRXpower) {
        if (NetworkManager::Init() - > CheckHandoverPermissions(probableNewTargetNode, ue)) {
          targetRXpower = RXpower;
          targetNode = probableNewTargetNode;
        }
      }
    }
  }

  if (ue - > GetTargetNode() - > GetIDNetworkNode() != targetNode - > GetIDNetworkNode()) {
    m_target = targetNode;
    return true;
  } else {
    return false;
  }
}
```

To implement the DeUD_PL policy under the system level simulator, we create as well three new functions **NetworkManager::SelectTargetNodeUplink**, **HandoverEntity::CheckHandoverUplinkNeed**, and **PowerBasedHoManager::CheckHandoverNeedUplink** as follows:

```
void NetworkManager::SelectTargetNodeUplink(UserEquipment * ue) {
  NetworkNode * targetNode = ue - > GetTargetNode();

  if (targetNode - > GetProtocolStack() - > GetRrcEntity() - >
    GetHandoverEntity() - > CheckHandoverUplinkNeed(ue)) {
    NetworkNode * newTagertNode =
      targetNode - > GetProtocolStack() - > GetRrcEntity() - >
      GetHandoverEntity() - > GetHoManager() - > m_target;

    ue - > SetTargetNode(newTagertNode);
  }
}

bool HandoverEntity::CheckHandoverUplinkNeed(UserEquipment * ue) {
```

```
  return GetHoManager() - > CheckHandoverNeedUplink(ue);
}

bool PowerBasedHoManager::CheckHandoverNeedUplink(UserEquipment * ue) {
  NetworkNode * targetNode = ue - > GetTargetNode();

  double targetpathloss = ComputePathLossForInterference(ue, targetNode);

  double pathloss;

  std::vector < ENodeB * > * listOfNodes = NetworkManager::Init() - > GetENodeBContainer();
  std::vector < ENodeB * > ::iterator it;
  for (it = listOfNodes - > begin(); it != listOfNodes - > end(); it++) {
    if (( * it) - > GetIDNetworkNode() != targetNode - > GetIDNetworkNode()) {

      NetworkNode * probableNewTargetNode = ( * it);

      pathloss = ComputePathLossForInterference(ue, probableNewTargetNode);

      if (pathloss < targetpathloss) {
        if (NetworkManager::Init() - > CheckHandoverPermissions(probableNewTargetNode, ue)) {
          targetpathloss = pathloss;

          targetNode = probableNewTargetNode;
        }
      }
    }
  }

  if (ue - > GetTargetNode() - > GetIDNetworkNode() != targetNode - > GetIDNetworkNode()) {
    m_target = targetNode;
    return true;
  } else {
    return false;
  }
}
```

A.3.5 Multiple Small Cells

To allow multiple small cells deployment, we create a new function that will randomly distribute the small cells inside the macro cell region. This function called **GetUniformMicroCellsDistribution** is created under **/src/utility/UsersDistribution.h**:

```
static vector < CartesianCoordinates * > *
  GetUniformMicroCellsDistribution(int idCell, int nbMicroCell, double microRadius) {
    NetworkManager * networkManager = NetworkManager::Init();
    vector < CartesianCoordinates * > * vectorOfCoordinates = new vector < CartesianCoordinates * > ;

    Cell * cell = networkManager - > GetCellByID(idCell);

    double radius = (cell - > GetRadius() * 1000) * 0.8;
    double maxRadius = radius - (microRadius * 1000);

    CartesianCoordinates * cellCoordinates = cell - > GetCellCenterPosition();
```

```
    double r;
    double angle;

    for (int i = 0; i < nbMicroCell; i++) {

      r = (double)(rand() % (int) maxRadius);

      angle = (double)(rand() % 360) * ((2 * 3.14) / 360);

      CartesianCoordinates * newCoordinates = GetCartesianCoordinatesFromPolar(r, angle);

      //Compute absoluteCoordinates
      newCoordinates - > SetCoordinateX(cellCoordinates - > GetCoordinateX() +
        newCoordinates - > GetCoordinateX());
      newCoordinates - > SetCoordinateY(cellCoordinates - > GetCoordinateY() +
        newCoordinates - > GetCoordinateY());

      vectorOfCoordinates - > push_back(newCoordinates);
    }

    return vectorOfCoordinates;
  }
```

The creation of these small cells and their respective eNBs will be as follows:

```
// Creation of small cells

 for (idCell = 1; idCell <= nbMicroCells; idCell++) {

   vector < CartesianCoordinates * > * positions = GetUniformMicroCellsDistribution(0,
     nbMicroCells, microRadius);

   Cell * microCell = networkManager - > CreateCell(idCell, microRadius, 0.01,
     positions - > at(idCell - 1) - > GetCoordinateX(),
     positions - > at(idCell - 1) - > GetCoordinateY());

   cells - > push_back(microCell);

   std::cout << "Created MicroCell ID " << microCell - > GetIdCell() <<
     " position " << microCell - > GetCellCenterPosition() - > GetCoordinateX() <<
     " " << microCell - > GetCellCenterPosition() - > GetCoordinateY() << std::endl;

 }

// Creation of small cells eNBs

for (int i = 0; i < nbMicroCells; i++) {
  ENodeB * MicroEnb = networkManager - > CreateEnodeb(idEnb + 1 + i,
    cells - > at(idEnb + 1 + i),
    cells - > at(idEnb + 1 + i) - > GetCellCenterPosition() - > GetCoordinateX(),
    cells - > at(idEnb + 1 + i) - > GetCellCenterPosition() - > GetCoordinateY(),
    dlChannels - > at(i + 1), ulChannels - > at(i + 1), spectrum);

  MicroEnb - > GetPhy() - > SetTxPower(30);
  MicroEnb - > SetNodeType(NetworkNode::TYPE_MICROENODEB);
  MicroEnb - > SetDLScheduler(ENodeB::DLScheduler_TYPE_PROPORTIONAL_FAIR);
```

```
  MicroEnb - > SetULScheduler(ENodeB::ULScheduler_TYPE_ROUNDROBIN);
  std::cout << "Created MicroEnb" << " ID " << MicroEnb - > GetIDNetworkNode() <<
    " cell " << MicroEnb - > GetCell() - > GetIdCell() <<
    " Power " << MicroEnb - > GetPhy() - > GetTxPower() <<
    " position " << MicroEnb - > GetMobilityModel() - > GetAbsolutePosition() - > GetCoordinateX() <<
    " " << MicroEnb - > GetMobilityModel() - > GetAbsolutePosition() - > GetCoordinateY() <<
    " channels " << MicroEnb - > GetPhy() - > GetDlChannel() - > GetChannelId() <<
    MicroEnb - > GetPhy() - > GetUlChannel() - > GetChannelId() << std::endl;
}
```

Publications

Conferences

[128] B. Lahad, M. Ibrahim, S. Lahoud, K. Khawam and S. Martin,“A Statistical Model for Uplink/Downlink Intercell Interference and Cell Capacity in TDD HetNets," *2018 IEEE International Conference on Communications (ICC)*, Kansas City, MO, USA, 2018, pp. 1-6

[129] B. Lahad, M. Ibrahim, S. Lahoud, K. Khawam and S. Martin,“Analytical Evaluation of Decoupled Uplink and Downlink Access in TDD 5G HetNets," *2018 IEEE 29th Annual International Symposium on Personal, Indoor and Mobile Radio Communications (PIMRC)*, Bologna, Italy, 2018, pp. 1-7.

[131] B. Lahad, M. Ibrahim, S. Lahoud, K. Khawam and S. Martin,“Uplink/Downlink Decoupled Access with Dynamic TDD in 5G HetNets," *2020 IEEE International conference on Wireless Communications and Mobile Computing (IWCMC)*, Limassol, Cyprus, 2020, pp. 1-6.

Journal in IEEE Transactions on Mobile Computing

[130] B. Lahad, M. Ibrahim, S. Lahoud, K. Khawam and S. Martin,“Joint Modeling of TDD and Decoupled Uplink/Downlink Access in 5G HetNets with Multiple Small Cells Deployment," *Accepted in IEEE Transactions on Mobile Computing*, 2020.

Bibliography

[1] Cisco Visual Networking Index : Global Mobile Data Traffic Forecast Update, 2016–2021, Cisco, February 2017.

[2] “Radio frequency (RF) system scenario (release 10)," 3GPP TS 36.211, Jun. 2012.

[3] “Further enhancements to LTE Time Division Duplex (TDD) for Downlink-Uplink (DL-UL) interference management and traffic adaptation ," 3GPP TR 36.828, Jun. 2012.

[4] J. G. Andrews, “Seven ways that HetNets are a cellular paradigm shift," *IEEE Commun. Mag.*, vol. 51, no. 3, pp. 136-144, Mar. 2013.

[5] F. Boccardi, R.W. Heath, A. Lozano, T.L. Marzetta, and P. Popovski, “Five Disruptive Technology Directions for 5G," *IEEE Communications Magazine*, Vol. 52. No. 2, 2014, pp. 74-80.

[6] S.Brueck, “Heterogeneous networks in LTE-Advanced, 8th International Symposium on Wireless Communication Systems,” *Aachen*, pp. 171–175, 2011.

[7] C.E. Shannon. A mathematical theory of communication. Bell system Tech. J. 27, July and October 1948.

[8] Erik Dahlman, Stefan Parkvall, and Johan Skold. 4G: LTE/LTE-advanced for Mobile Broadband. Academic Press, 2011.

[9] A. S. Marcano and H. L. Christiansen, “Impact of NOMA on Network Capacity Dimensioning for 5G HetNets," *in IEEE Access*, vol. 6, pp. 13587-13603, 2018.

[10] P. Wang, J. Xiao, and L. P, “Comparison of Orthogonal and Non-Orthogonal Approaches to Future Wireless Cellular Systems," *IEEE Veh. Technol. Conf.*, vol. 1, no. 3, pp. 4–11, 2006.

[11] D. Ni, L. Hao, Q. T. Tran and X. Qian, “Power Allocation for Downlink NOMA Heterogeneous Networks," *in IEEE Access*, vol. 6, pp. 26742-26752, 2018.

[12] Y. Saito, Y. Kishiyama, A. Benjebbour, T. Nakamura, A. Li, and K. Higuchi, “Non-orthogonal multiple access (NOMA) for cellular future radio access," *in Proc. IEEE 77th Veh. Technol. Conf. (VTC-Spring*), Jun. 2013, pp. 1-5.

[13] Z. Ding, M. Peng, and H. V. Poor, “Cooperative non-orthogonal multiple access in 5G systems," *IEEE Commun. Lett.*, vol. 19, no. 8, pp. 1462-1465, Aug. 2015.

[14] K. Higuchi and A. Benjebbour, “Non-orthogonal multiple access (NOMA) with successive interference cancellation for future radio access," *IEICE Trans. Commun.*, vol. 98, no. 3, pp. 403-414, 2015.

[15] L. Dai, B. Wang, Y. Yuan, S. Han, C.-L. I, and Z. Wang, “Non-orthogonal multiple access for 5G: Solutions, challenges, opportunities, and future research trends," *IEEE Commun. Mag.*, vol. 53, no. 9, pp. 74-81, Sep. 2015.

[16] Y. Saito, Y. Kishiyama, A. Benjebbour, T. Nakamura, A. Li, and K. Higuchi, “Non-orthogonal multiple access (NOMA) for cellular future radio access," *IEEE Veh. Technol. Conf.*, pp. 0–4, 2013.

[17] Z. Ding et al., “Application of Non-orthogonal Multiple Access in LTE and 5G Networks," *IEEE Commun. Mag.*, vol. 55, no. 2, pp. 185–191, 2017.

[18] Y. Yuan et al., “Non-Orthogonal Transmission Technology in LTE Evolution," *IEEE Commun. Mag.*, vol. 54, no. 7, pp. 68–74, 2016.

[19] S. M. Riazul Islam, N. Avazov, O. A. Dobre, and K.-S. Kwak, “Power-Domain Non-Orthogonal Multiple Access (NOMA) in 5G Systems: Potentials and Challenges," *IEEE Commun. Surv. Tutorials*, vol. 19, no. 2, 2017.

[20] A. Benjebbour, Y. Saito, Y. Kishiyama, A. Li, A. Harada, and T. Nakamura, “Concept and practical considerations of non-orthogonal multiple access (NOMA) for future radio access," *in Proc. Int. Symp. Intell. Signal Process. Commun. Syst. (ISPACS)*, Nov. 2013, pp. 770-774.

[21] Z. Ding, Z. Yang, P. Fan, and H. V. Poor, “On the performance of non- orthogonal multiple access in 5G systems with randomly deployed users," *IEEE Signal Process. Lett.*, vol. 21, no. 12, pp. 1501-1505, Dec. 2014.

[22] Z. Yang, Z. Ding, P. Fan, and N. Al-Dhahir, “A general power allo- cation scheme to guarantee quality of service in downlink and uplink NOMA systems," *IEEE Trans. Wireless Commun.*, vol. 15, no. 11, pp. 7244-7257, Nov. 2016.

[23] S. Timotheou and I. Krikidis, “Fairness for non-orthogonal multiple access in 5G systems," *IEEE Signal Process. Lett.*, vol. 22, no. 10, pp. 1647-1651, Oct. 2015.

[24] J. Choi, “Power allocation for max-sum rate and max-min rate proportional fairness in NOMA," *IEEE Commun. Lett.*, vol. 20, no. 10, pp. 2055-2058, Oct. 2016.

[25] Interworking and JOINt Design of an Open Access and Backhaul Network Architecture for Small Cells based on Cloud networks, IJOIN, 2012, https://cordis.europa.eu/project/rcn/105819/factsheet/fr.

[26] Mobile Cloud Networking project, MCN, 2013, http://mobile-cloud-networking.eu/site/.

[27] “Special articles on 5G technologies toward 2020 deployment," *Technical Journal*, vol. 17, no. 4, 2016.

[28] C. Li, J. Zhang, J. G. Andrews and K. B. Letaief, “Success Probability and Area Spectral Efficiency in Multiuser MIMO HetNets," *in IEEE Transactions on Communications*, vol. 64, no. 4, pp. 1544-1556, April 2016.

[29] F. Rusek et al., “Scaling up MIMO: Opportunities and challenges with very large arrays," *IEEE Signal Process. Mag.*, vol. 30, no. 1, pp. 40–60, Jan. 2013.

[30] Y. Kim et al., “Full dimensionMIMO (FD-MIMO): The next evolution of MIMO in LTE systems," *IEEE Wireless Commun.*, vol. 21, no. 2, pp. 26–33, Apr. 2014.

[31] H. S. Dhillon, M. Kountouris, and J. G. Andrews, “Downlink MIMO HetNets: Modeling, ordering results and performance analysis," *IEEE Trans. Wireless Commun.*, vol. 12, no. 10, pp. 5208–5222, Oct. 2013.

[32] A. K. Gupta, H. S. Dhillon, S. Vishwanath, and J. G. Andrews, “Downlink multi-antenna heterogeneous cellular network with load balancing," *IEEE Trans. Commun.*, vol. 62, no. 11, pp. 4052–4067, Nov. 2014.

[33] V. Chandrasekhar, M. Kountouris, and J. G. Andrews, “Coverage in multi-antenna two-tier networks," *IEEE Trans. Wireless Commun.*, vol. 8, no. 10, pp. 5314–5327, Oct. 2009.

[34] A. Adhikary, H. Dhillon, and G. Caire, “Massive-MIMO meets HetNet: Interference coordination through spatial blanking," *IEEE J. Sel. Areas Commun.*, vol. 33, no. 6, pp. 1171–1186, Jun. 2015.

[35] R. Heath, M. Kountouris, and T. Bai, “Modeling heterogeneous network interference using poisson point processes," *IEEE Trans. Signal Process.*, vol. 61, no. 16, pp. 4114–4126, Aug. 2013.

[36] Nokia Siemens Networks, Nokia, “Aspects of Pico Node Range Extension", 3GPP TSG RAN WG1 Meeting 61. R1-103824. [(accessed on 20 March 2019)];2010 Available online: http://goo.gl/XDKXI.

[37] E. Dahlman, S. Parkvall, and J. Skold. 4G: LTE/LTE-advanced for mobile broadband. Academic Press, 2013.

[38] H. Elshaer, F. Boccardi, M. Dohler, and R. Irmer, “Downlink and uplink decoupling: a disruptive architectural design for 5G networks," *in GLOBECOM14. IEEE*, 2014, pp. 1798-1803.

[39] E. Liotou et al., “Shaping QoE in the 5G ecosystem," *2015 Seventh International Workshop on Quality of Multimedia Experience (QoMEX)*, 2015, pp. 1-6.

[40] 3GPP TR 36.819, “Coordinated multi-point operation for LTE physical layer aspects," *V.11.1.0*, December 2011.

[41] A. He, D. Liu, Y. Chen and T. Zhang, “Stochastic geometry analysis of energy efficiency in HetNets with combined CoMP and BS sleeping," *2014 IEEE 25th Annual International Symposium on Personal, Indoor, and Mobile Radio Communication (PIMRC)*, Washington, DC, 2014, pp. 1798-1802.

[42] Tao Han and N. Ansari. On greening cellular networks via multicell cooperation. IEEE Commun. Mag., 20(1):82–89, 2013.

[43] G. Cili, H. Yanikomeroglu, and F.R. Yu. Cell switch off technique combined with coordinated multi-point (comp) transmission for energy efficiency in beyond-lte cellular networks. In IEEE Int. Conf. Commun. (ICC), pages 5931–5935. IEEE, 2012.

[44] H. ElSawy, E. Hossain, and M. Haenggi. Stochastic geometry for modeling, analysis, and design of multi-tier and cognitive cellular wireless networks: A survey. IEEE Commun. Surveys & Tutorials, 15(3):996–1019, 2013.

[45] J.G. Andrews, F. Baccelli, and R.K. Ganti. A tractable approach to coverage and rate in cellular networks. IEEE Trans. Commun., 59(11):3122–3134, 2011.

[46] H.S. Dhillon, R.K. Ganti, F. Baccelli, and J.G. Andrews. Modeling and analysis of k-tier downlink heterogeneous cellular networks. IEEE J. Sel. Areas Commun, 30(3):550–560, 2012.

[47] K. M. S. Huq, S. Mumtaz, J. Bachmatiuk, J. Rodriguez, X. Wang and R. L. Aguiar, “Green HetNet CoMP: Energy Efficiency Analysis and Optimization," *in IEEE Transactions on Vehicular Technology*, vol. 64, no. 10, pp. 4670-4683, Oct. 201

[48] 3GPP. Coordinated Multi-Point Operation for LTE Physical Layer Aspects. TS 36.819, 3rd Generation Partnership Project (3GPP), September 2012.

[49] 3GPP. LTE Radio Access Network (RAN) Enhancements for Diverse Data Applications. TR 36.822, 3rd Generation Partnership Project (3GPP), September 2012.

[50] 3GPP. Technical Specification Group Radio Access Network; Evolved Universal Terrestrial Radio Access (E-UTRA) and Evolved Universal Terrestrial Radio Access Network (E-UTRAN); Overall description; Stage 2 (Release 11). TS 36.300, 3rd Generation Partnership Project (3GPP), September 2012.

[51] 3GPP. Study on Small Cell Enhancements for E-UTRA and E-UTRAN; Higher Layer Aspects. TR 36.842, 3rd Generation Partnership Project (3GPP), September 2014.

[52] F. Boccardi, J. Andrews, H. Elshaer, M. Dohler, S. Parkvall, P. Popovski, and S. Singh, “Why to decouple the uplink and downlink in cellular networks and how to do it," *arXiv preprint arXiv:1503.06746*, 2015.

[53] H. A. Mustafa, M. Z. Shakir, Y. A. Sambo, K. A. Qaraqe, M. A. Imran and E. Serpedin,“Spectral efficiency improvements in HetNets by exploiting device-to-device communications," *2014 IEEE Globecom Workshops (GC Wkshps)*, Austin, TX, 2014, pp. 857-862

[54] Astely, D., Dahlman, E., Fodor, G., Parkvall, S. and Sachs, J. (2013) LTE Release 12 and Beyond Accepted from Open Call. IEEE Communications Magazine, 51, 154-160. https://doi.org/10.1109/MCOM.2013.6553692

[55] K. Doppler, M. Rinne, C. Wijting, C. Ribeiro, and K. Hugl, “Device-to-device communication as an underlay to LTE-advanced networks," *in IEEE Mag. Communs.*, vol. 27, no. 12, pp. 42–49, Dec. 2009.

[56] P. Janis, C.-H. Yu, K. Doppler, C. B. Ribeiro, C. Wijting, K. Hugl, O. Tirkkonen, and V. Koivunen,“Device-todevice communication underlying cellular communications systems," *in Intl. Jour. Commun., Network and System Sciences*, vol. 2, no. 3, pp. 169–178, 2009.

[57] S. Hakola, T. Chen, J. Lehtomäki, and T. Koskela, “Device-to-device (D2D) communication in cellular network - performance analysis of optimum and practical communication mode selection," *pp. 1–6*, Apr. 2010.

[58] Lin, X., Andrews, J.G., Ghosh, A. and Ratasuk, R. (2014) An Overview of 3GPP Device-to-Device Proximity Services. IEEE Communications Magazine, 52, 40-48. https://doi.org/10.1109/MCOM.2014.6807945

[59] Omran, A., BenMimoune, A. and Kadoch, M. (2017) Mobility Management for D4D in HetNet. 2017 IEEE 30th Canadian Conference on Electrical and Computer Engineering, Windsor, Canada, 30 April-3 May 2017, 1-5. https://doi.org/10.1109/CCECE.2017.7946632

[60] Huq, K.M.S., Mumtaz, S., Rodriguez, J., Marques, P., Okyere, B. and Frascolla, V. (2017) Enhanced C-RAN Using D2D Network. IEEE Communications Magazine, 55, 100-107. https://doi.org/10.1109/MCOM.2017.1600497CM

[61] S. Guo, X. Hou and H. Wang, “Dynamic TDD and interference management towards 5G,"*2018 IEEE Wireless Communications and Networking Conference (WCNC)*, 2018, pp. 1-6.

[62] “Radio frequency (RF) system scenario (release 10)," 3GPP TS 36.211, Jun. 2012.

[63] 3GPP, TR36.828 (v11.4.0), “Further enhancements to LTE TDD for DL-UL interference management and traffic adaptation”, Jun. 2012.

[64] S. Sesia, I. Touk, and M. Baker, LTE - The UMTS Long Term Evolution: From Theory to Practice, John Wiley & Sons, Ltd, 2009.

[65] K. Smiljkovikj, H. Elshaer, P. Popovski, F. Boccardi, M. Dohler, L. Gavrilovska, and R. Irmer, “Capacity analysis of decoupled down- link and uplink access in 5G heterogeneous systems," *arXiv preprint arXiv:1410.7270*, 2014.

[66] X. Liu, R. Li, K. Luo, and T. Jiang, “Downlink and uplink decoupling in heterogeneous networks for 5G and beyond," *J. Commun. Inf. Netw.*, vol. 3, no. 2, pp. 1–13, 2018.

[67] N. H. M. Adnan, I. M. Rafiqul and A. H. M. Z. Alam, “Massive MIMO for Fifth Generation (5G): Opportunities and Challenges," *2016 International Conference on Computer and Communication Engineering (ICCCE)*, 2016, pp. 47-52.

[68] C. Seker, M. T. Güneser and T. Ozturk, “A Review of Millimeter Wave Communication for 5G," *2018 2nd International Symposium on Multidisciplinary Studies and Innovative Technologies (ISMSIT)*, 2018, pp. 1-5.

[69] Huawei has showcased its ability to improve 5G coverage, capacity, and user experience by carrying uplink data via 4G LTE bands and downlink data on 5G bands, 2017 Nov [accessed 2021 Aug 26]. https://www.zdnet.com/article/huawei-demos-5g-uplink-downlink-decoupling-tech/.

[70] Huawei ’s “5G UL & DL Decoupling" Receives 2019 GSMA Award for Best Mobile Technology Breakthrough, 2019 Feb [accessed 2021 Aug 26]. https://www.huawei.com/en/press-events/news/2019/2/huawei-5g-ul-dl-decoupling-awarded.

[71] “NR; User Equipment (UE) radio transmission and reception; Part 3: Range 1 and Range 2 Interworking operation with other radios (release 16)," 3GPP TS 38.101-3, Jan. 2020.

[72] “NR; User Equipment (UE) radio transmission and reception; Part 2: Range 2 Standalone (release 16)," 3GPP TS 38.101-2, Jan. 2020.

[73] “NR; User Equipment (UE) radio transmission and reception; Part 1: Range 1 Standalone (release 16)," 3GPP TS 38.101-1, Jan. 2020.

[74] Developing mmWave mobile radio interface, 2017 Aug. https://www.ericsson.com/en/blog/2017/8/developing-mmwave-mobile-radio-interface.

[75] K. W. Sung, H. Haas, and S. McLaughlin, “A semi-analytical PDF of downlink SINR for femtocell networks," *EURASIP J. Wireless Commun. and Networking*, Jan. 2010.

[76] S. Plass, X. G. Doukopoulos, and R. Legouable, “Investigations on link-level inter-cell interference in OFDMA systems," *in Proc. 2006 IEEE Symposium on Communications and Vehicular Technology*, pp. 49-52.

[77] X. Yang and A. O. Fapojuwo, “Analysis of heterogeneous cellular network with hexagonal tessellated macrocells and randomly positioned small cells," *IEEE WCNC*, 2016.

[78] M. Taranetz and M. Rupp, “A circular interference model for wireless cellular networks," *International Wireless Communications and Mobile Computing Conference*, 2014.

[79] C. Seol and K. Cheun, “A Statistical Inter-cell Interference Model for Downlink Cellular OFDMA Networks under Log-normal Shadowing and Multipath Rayleigh Fading," *IEEE Transactions on Communications*, vol. 57, no. 10, pp. 3069–3077, October 2009.

[80] C. Seol, K. Cheun, and S. Hong, “A Statistical Inter-cell Interference Model for Downlink Cellular OFDMA Networks under Log-normal Shadowing with Ricean Fading," *IEEE Communications Letters*, vol. 14, no. 11, pp. 1011–1013, November 2010.

[81] S. Elayoubi, B. Haddada, and B. Fourestie, “Performance evaluation of frequency planning schemes in OFDMA based networks," *IEEE Trans.Wireless Commun.*, vol. 7, no. 5, pp. 1623-1633, May 2008.

[82] R. Kwan and C. Leung, “On collision probabilities in frequency-domain scheduling for LTE cellular networks," *IEEE Commun. Lett.*, vol. 15, no. 9, pp. 965- 967, Sep. 2011.

[83] I. Viering, A. Klein, M. Ivrlac, M. Castaneda, and J. A. Nossek, “On uplink intercell interference in a cellular system," *in Proc. 2006 IEEE International Conference on Communications*, pp. 2095-2100.

[84] M. Ding, D. Lopez-Perez, G. Mao, and Z. Lin, “DNA-GA: A new approach of network performance analysis," *Proc. IEEE ICC 2016*,arXiv:1512.05429 [cs.IT], to be published.

[85] H. Tabassum, Z. Dawy, E. Hossain, and M. S Alouini, “A framework for uplink intercell interference modeling with channel-based scheduling," *IEEE Trans. Wireless Commun.*, vol. 12, no. 1, pp. 206-217, Jan. 2013.

[86] H. Tabassum, Z. Dawy, E. Hossain, and M. S Alouini, “Interference statistics and capacity analysis for uplink transmission in two-tier small cell networks: A geometric probability approach," *IEEE Trans. Wireless Commun.*, vol. 13, no. 7, pp. 3837-3852, Jul. 2014.

[87] Ahmad El-Hajj, Naeem Akl, Bilal Hammoud, and Zaher Dawy, “On interference modeling for the analysis of uplink/downlink interactions in TDD-OFDMA networks," *2015 International Wireless Communications and Mobile Computing Conference (IWCMC)*, pp. 497-502, 2015.

[88] F. Boccardi, J. Andrews, H. Elshaer, M. Dohler, S. Parkvall, P. Popovski, and S. Singh, “Why to decouple the uplink and downlink in cellular networks and how to do it," *arXiv preprint arXiv:1503.06746*, 2015.

[89] H. Elshaer, F. Boccardi, M. Dohler, and R. Irmer, “Downlink and uplink decoupling: a disruptive architectural design for 5G networks," *in GLOBECOM’14. IEEE*, 2014, pp. 1798-1803.

[90] “Load & backhaul aware decoupled downlink/uplink access in 5G systems," *arXiv preprint arXiv:1410.6680*, 2014.

[91] Qualcomm, “Range expansion for efficient support of heterogeneous networks," *3GPP TSG-RAN WG1 R1-083813*, 2008.

[92] K. Smiljkovikj, H. Elshaer, P. Popovski, F. Boccardi, M. Dohler, L. Gavrilovska, and R. Irmer, “Capacity analysis of decoupled down- link and uplink access in 5G heterogeneous systems," *arXiv preprint arXiv:1410.7270*, 2014.

[93] K. Smiljkovikj, P. Popovski, and L. Gavrilovska, “Analysis of the decoupled access for downlink and uplink in wireless heterogeneous networks," *Wireless Communications Letters, IEEE*, vol. 4, no. 2, pp. 173-176, 2015.

[94] H. ElSawy, E. Hossain, and M. Haenggi, “Stochastic Geometry for Modeling, Analysis, and Design of Multi-Tier and Cognitive Cellular Wireless Networks: A Survey," *IEEE Comm. Surveys & Tutorials*, Vol.15, No. 3, 2013

[95] W. Nie, L. Zhang, and G. Fang, “Uplink Performance Improvement by Decoupling Uplink/Downlink Access in HetNets," *IEEE Transactions on Vehicular Technology, IEEE*, vol. 66, no. 8, pp. 6862-6876, 2017.

[96] H. E. Shaer, M. N. Kulkarni, F. Boccardi, J. G. Andrews, and M. Dohler, “Downlink and Uplink Cell Association in Sub-6GHz and Millimeter Wave 5G Heterogeneous Networks," *Globecom Workshops (GC Wkshps)*, 2016 IEEE.

[97] Ahmad El-Hajj, Naeem Akl, Bilal Hammoud, and Zaher Dawy, “On interference modeling for the analysis of uplink/downlink interactions in TDD-OFDMA networks," *2015 International Wireless Communications and Mobile Computing Conference (IWCMC)*, pp. 497-502, 2015.

[98] H. Mehrpouyan, M. Matthaiou, R. Wang, G. K. Karagiannidis, and Y. Hua, “Hybrid millimeter-wave systems: A novel paradigm for HetNets," *IEEE Commun. Mag.*, vol. 53, no. 1, pp. 216-221, Jan. 2015.

[99] H. Elshaer, F. Boccardi, M. Dohler, and R. Irmer, “Downlink and uplink decoupling: a disruptive architectural design for 5G networks," *in GLOBECOM'14. IEEE*, 2014, pp. 1798-1803.

[100] “Load & backhaul aware decoupled downlink/uplink access in 5G systems," *arXiv preprint arXiv:1410.6680*, 2014.

[101] Qualcomm, “Range expansion for efficient support of heterogeneous networks," *3GPP TSG-RAN WG1 R1-083813*, 2008.

[102] M. S. ElBamby, M. Bennis, and M. Latva-aho, “UL/DL decoupled user association in dynamic TDD small cell networks," *in 2015 International Symposium on Wireless Communication Systems (ISWCS)*, Aug 2015, pp. 456–460.

[103] B. Lahad, M. Ibrahim, S. Lahoud, K. Khawam and S. Martin,“A Statistical Model for Uplink/Downlink Intercell Interference and Cell Capacity in TDD HetNets," *2018 IEEE International Conference on Communications (ICC)*, 2018, pp. 1-6.

[104] Q. Liao, D. Aziz, and S. Stanczak, “Dynamic joint uplink and downlink optimization for uplink and downlink decoupling-enabled 5G heterogeneous networks," *arXiv preprint*, 2016. [Online]. Available: http://arxiv.org/abs/1607.05459 13dB

[105] S. Singh, X. Zhang and J. G. Andrews, “Joint Rate and SINR Coverage Analysis for Decoupled Uplink-Downlink Biased Cell Associations in HetNets," *in IEEE Transactions on Wireless Communications*, vol. 14, no. 10, pp. 5360-5373, Oct. 2015.

[106] 3GPP, Tech. Specif. Group Radio Access Networks; Radio Frequency (RF) system scenarios (Release 9), 3GPP TS 25.942.

[107] 3GPP, Tech. Specif. Group Radio Access Network; Evolved Universal Terrestrial Radio Access (E-UTRA) and Evolved Universal Terrestrial Radio Access Network (E-UTRAN); Radio Frequency (RF) system scenarios (Release 10), 3GPP TS 36.942.

[108] 3GPP TS 36.213, v11.3.0, “Evolved Universal Terrestrial Radio Access (E-UTRA); Physical layer procedures," Jun. 2013.

[109] 3GPP TS 36.213, v11.3.0, “Evolved Universal Terrestrial Radio Access (E-UTRA); Physical layer procedures," Jun. 2013.

[110] Weisstein, Eric W. "Circle-Circle Intersection." From MathWorld–A Wolfram Web Resource. https://mathworld.wolfram.com/Circle-CircleIntersection.html.

[111] “Chain Rule in Leibniz Notation," *oregonstate.edu.*, Retrieved 2019-07-28.

[112] K. A. Hamdi, “A useful lemma for capacity analysis of fading interference channels," *IEEE Trans. Commun.*, vol. 58, no. 2, pp. 411-416, Feb. 2010.

[113] Mathar, R. (2013). GAUSS-LAGUERRE AND GAUSS-HERMITE QUADRATURE ON 64, 96 AND 128 NODES. viXra.

[114] Philip Rabinowitz and George Weiss, Tables of abscissas and weights for numerical evaluation of integrals of the form $\int_0^\infty e^{-x} x^n f(x) dx$, Math. Comp. 13 (1959), 285–294. MR 0107992.

[115] D. Fairthorne, “The distances between random points in two concentric circles," *Biometrika*, vol. 51, no. 1/2, pp. 275-277, Jun. 1964.

[116] Nokia Siemens Networks, Nokia, “Aspects of Pico Node Range Extension", 3GPP TSG RAN WG1 Meeting 61. R1-103824. [(accessed on 20 March 2019)];2010 Available online: http://goo.gl/XDKXI.

[117] B. Lahad, M. Ibrahim, S. Lahoud, K. Khawam and S. Martin,“Analytical Evaluation of Decoupled Uplink and Downlink Access in TDD 5G HetNets," *2018 IEEE 29th Annual International Symposium on Personal, Indoor and Mobile Radio Communications (PIMRC)*, Bologna, Italy, 2018, pp. 1-7.

[118] 3GPP, TR25.951 (v10.0.0), “Technical Specification Group Radio Access Network; Evolved Universal Terrestrial Radio Access (E-UTRA); Radio Frequency (RF) system scenarios (Release 10)”, Dec. 2010.

[119] 3GPP, TR25.951 (v10.0.0), “ Technical Specification Group Radio Access Network; FDD Base Station (BS) classification (Release 10)”, Apr. 2011.

[120] “3GPP TS 136.300, Evolved Universal Terrestrial Radio Access (EUTRA) and Evolved Universal Terrestrial Radio Access Network (EUTRAN); Overall description; Stage 2 (Release 10),” 2011.

[121] G. Piro, L. A. Grieco, G. Boggia, F. Capozzi, and P. Camarda,“Simulating LTE Cellular Systems: An Open-Source Framework,"*IEEE Trans. Veh. Technol.*, vol. 60, no. 2, pp. 498-513, Feb. 2011.

[122] J. W. C, *Microwave Mobile Communications New York. Wiley. 1975*.

[123] M. Lord and D. Memmi, “NetSim: a Simulation and Visualization Software for Information Network Modeling," *in e-Technologies, International MCETECH Conference*, pp. 167-177, 2008.

[124] X. Chang,“Network simulations with OPNET," *in Proc. 31st Conf. Winter Simulation: Simulation—A Bridge to the Future Volume 1, WSC’99*, New York, 1999, pp. 307–314.

[125] M. Rupp, S. Schwarz, and M. Taranetz,“*The Vienna LTE-Advanced Simulators: Up and Downlink, Link and System Level Simulation,*" Springer, 2016.

[126] G. F. Riley and T. R. Henderson, “The ns-3 Network Simulator," *in Modeling and Tools for Network Simulation, Berlin, Heidelberg: Springer Berlin Heidelberg*, 2010, pp. 15–34.

[127] A. Virdis, G. Stea, and G. Nardini,“Simulating LTE/LTE-Advanced Networks with SimuLTE," *in Simulation and Modeling Methodologies, Technologies and Applications*, 2015, pp. 83–105.

[128] B. Lahad, M. Ibrahim, S. Lahoud, K. Khawam and S. Martin,“A Statistical Model for Uplink/Downlink Intercell Interference and Cell Capacity in TDD HetNets," *2018 IEEE International Conference on Communications (ICC)*,Kansas City, MO, USA, 2018, pp. 1-6.

[129] B. Lahad, M. Ibrahim, S. Lahoud, K. Khawam and S. Martin,“Analytical Evaluation of Decoupled Uplink and Downlink Access in TDD 5G HetNets," *2018 IEEE 29th Annual International Symposium on Personal, Indoor and Mobile Radio Communications (PIMRC)*, Bologna, Italy, 2018, pp. 1-7.

[130] B. Lahad, M. Ibrahim, S. Lahoud, K. Khawam and S. Martin,“Joint Modeling of TDD and Decoupled Uplink/Downlink Access in 5G HetNets with Multiple Small Cells Deployment," *in IEEE Transactions on Mobile Computing*, 2020.

[131] B. Lahad, M. Ibrahim, S. Lahoud, K. Khawam and S. Martin,“Uplink/Downlink Decoupled Access with Dynamic TDD in 5G HetNets," *2020 International conference on Wireless Communications and Mobile Computing (IWCMC)*, Limassol, Cyprus, 2020, pp. 1-6.

université PARIS-SACLAY
ÉCOLE DOCTORALE
Sciences et technologies de l'information et de la communication (STIC)

Titre: Allocation conjointe des ressources radio sur les voies descendante et montante dans les réseaux 5G hétérogènes

Mots clés: Communications sans fil, Réseaux hétérogènes, 5G, TDD dynamique, Découplage uplink/downlink, Association d'utilisateurs

Résumé: La croissance rapide du trafic de données sans fil et des services intensifs en bande passante (voix sur IP, streaming vidéo, live streaming, etc.) nécessite de trouver des solutions viables pour améliorer la qualité de service et maximiser les performances du réseau. Pour s'adapter à ces applications intensives en bande passante, les réseaux cellulaires hétérogènes (HetNets) ont été introduits dans le 3GPP comme l'une des principales caractéristiques pour répondre à ces exigences avancées. Les opérateurs ont adopté des solutions HetNet pour décharger le trafic d'une station de base macro (BS) vers une petite cellule BS. Maintenant, en raison de la différence de charges de trafic de liaison montante (UL) et de liaison descendante (DL) attendues dans les prochaines générations HetNets, il devient essentiel d'ajuster dynamiquement les ressources UL/DL. Pour soutenir cette nouvelle approche, le duplexage temporel (TDD) dynamique a été proposé. Néanmoins, l'importance d'UL se pose avec l'évolution des réseaux sociaux et des solutions cloud. Par conséquent, il est très intéressant d'introduire de nouvelles techniques qui atténuent les interférences de l'UL, améliorent les débits UL et DL et permettent également une meilleure utilisation des ressources radio en fournissant un équilibrage de charge adéquat entre UL et DL. Une telle caractéristique supplémentaire est le découplage accès UL/DL. Afin d'aborder les défis susmentionnés, un changement impératif des HetNets classiques aux HetNets de nouvelle génération (5G) émerge dans le but d'améliorer globalement la performance du système.

Dans notre travail, nous développons d'abord un modèle TDD dans HetNets. Dans ce modèle, nous dérivons des expressions analytiques pour la distribution de l'emplacement du brouilleur considérant tous les scénarios d'interférences possibles qui pourraient se produire dans les réseaux basés sur TDD, tout en tenant compte de l'impact nocif de cette interférence. Basé sur ce dernier résultat, nous dérivons la fonction de distribution et de génération de moment (MGF) de l'interférence intercellulaire montante et descendante considérant un réseau composé d'une macrocellule et d'une petite cellule. Nous nous appuyons sur les expressions dérivées pour analyser la capacité moyenne de la cellule de référence dans les transmissions en liaison montante et en liaison descendante.

Deuxièmement, nous développons un modèle statistique conjoint TDD/découplage pour mettre en évidence les avantages que le mode d'accès de découplage peut apporter à un système basé sur HetNet TDD, en termes d'efficacité spectrale UL et DL. Cette étude était basée sur une approche de probabilité géométrique. L'introduction du mode de découplage nécessite une analyse approfondie de l'étude de comparaison avec le mode d'accès couplé UL/DL conventionnel. Par conséquent, nous dérivons les statistiques du signal d'interférence et du signal d'intérêt des deux modes, puis analysons leur impact sur le performance du système.

Ce travail a été étendu pour inclure le déploiement de plusieurs petites cellules, où des aperçus supplémentaires sur les avantages du mode de découplage sont fournies en termes de gains de découplage UL et DL. Nous nous appuyons sur les expressions de capacité dérivées dans le mode couplé et le mode découplé pour calculer le gain de découplage et ainsi identifier l'emplacement de la petite cellule interférente, où le mode découplé maintient un gain plus élevé à la fois en DL et en UL. Suite à la mise en œuvre du modèle développé, il est démontré que le cas de découplage apporte de plus grands avantages dans la liaison montante et maintient la même amélioration dans la liaison descendante pour diverses valeurs de décalage et, ainsi, améliore les performances globales du système lorsqu'il est associé avec une technologie TDD dynamique.

D'un autre côté, l'évaluation des avantages d'un TDD adaptatif et du découplage dans un système basé sur HetNet en fonction des charges de trafic variant dans le temps, nécessite de trouver un simulateur de niveau système où nous pouvons présenter le motif derrière l' adoption de découplage et de TDD dynamique et évaluer avec précision le rôle de ces techniques dans le problème d'optimisation UL / DL. Nous créons un environnement de simulation approprié qui est relatif à des scénarios réels, c'est-à-dire des simulations où plusieurs petites cellules sont déployées dans un système HetNet lourdement chargé et sous diverses charges de trafic. Ces scénarios de simulation prennent en compte la distribution aléatoire des utilisateurs avec des décisions d'allocation de ressources dans les directions montante et descendante. À partir des scénarios de simulation mise en œuvre, il est observé que l'algorithme adaptatif proposé (TDD dynamique avec stratégies de découplage) apporte des améliorations de performances significatives dans le débit UL et DL par rapport à un certain nombre de schémas conventionnels, principalement dans le déploiement HetNet dense et dans les systèmes fortement chargés.

Title: Joint Uplink/Downlink Radio Resource Allocation in 5G HetNets

Keywords: Wireless Communications, HetNets, 5G, Dynamic TDD, Uplink/Downlink Decoupling, User Association

Abstract: The rapid growth in wireless data traffic and bandwidth intensive services (voice over IP, video streaming, live streaming, etc.) necessitates finding viable solutions to improve service quality and maximize the network performance. To accommodate these bandwidth intensive applications, heterogeneous cellular networks (HetNets) were introduced in 3GPP as one of the main features to meet these advanced requirements. Operators have adopted HetNet solutions to offload traffic from a macro base station (BS) to a small cell BS. Yet, because of the difference in uplink (UL) and downlink (DL) traffic loads expected in the next HetNets generation, it becomes essential to dynamically adjust UL/DL resources. To support this new approach, dynamic time-division duplexing (TDD) has been proposed. Nevertheless, the importance of UL arises along with the evolution of social networking and cloud solutions. Therefore, it is of great interest to introduce novel techniques that mitigate UL interferences, improve UL and DL throughputs and allow as well, a better use of radio resources by providing adequate load balancing among UL and DL. Such an additional feature is the decoupled UL/DL access. In order to address the aforementioned challenges, an important shift from classical HetNets to next-generation HetNets (5G) is emerging in the aim of improving overall system performance.

In our work, we first develop a TDD model in HetNets. Under this model,we derive analytical expressions for the distribution of the interferer location considering all possible interference scenarios that could occur in TDD-based networks, while taking into account the harmful impact of interference. Based on the latter result, we derive the distribution and moment generating function (MGF) of the uplink and downlink inter-cell interference considering a network consisting of one macro cell and one small cell. We build on the derived expressions to analyze the average capacity of the reference cell in both uplink and downlink transmissions.

Second, we develop a joint TDD/decoupling statistical model to highlight the benefits that the decoupling access mode can bring to a HetNet TDD based system, in terms of UL and DL spectral efficiencies and throughputs. This study was based on a geometric probability approach. Introducing the decoupling mode necessitates a thorough comparison study with the conventional coupled UL/DL access mode. Therefore, we derive the statistics of the interference signal and the signal of interest of both modes and then analyze their impact on the system performance.

This work was extended to include multiple small cells deployment, where more insight into the benefits of decoupling mode is provided in terms of UL and DL decoupling gains. We build on the derived capacity expressions in the coupled and decoupled modes to calculate the decoupling gain and thus, identify the location of the interferer small cell where the decoupled mode maintains a higher gain in both DL and UL. Further to the implementation of the developed model, it is shown that the decoupling case brings greater benefits in the uplink and maintains the same improvement in the downlink for various offset values and thus, improves the overall system performance when being combined with a dynamic TDD technology.

On the other hand, evaluating the benefits of an adaptive TDD and decoupling in a HetNet based system according to time-variant traffic loads, necessitates finding a system level simulator where we can present the motivation and accurately assess the role of both decoupling and dynamic TDD techniques in the UL/DL optimization problem. We create appropriate simulation environment that is relative to real scenarios i.e. simulations where multiple small cells are deployed in a heavy loaded HetNet system and under various traffic loads. These simulation scenarios consider random users distribution with scheduling decisions in both the uplink and the downlink directions. From the applied simulation scenarios, it is observed that the proposed adaptive algorithm (dynamic TDD with decoupling policies) yields significant performance improvements in UL and DL throughput compared to a number of conventional schemes, mainly in dense HetNet deployment and in highly loaded systems.

Université Paris-Saclay
Espace Technologique / Immeuble Discovery
Route de l'Orme aux Merisiers RD 128 / 91190 Saint-Aubin, France